U.S. DEPARTMENT OF COMMERCE
National Technical Information Service
PB-298 465

Chemical Aspects of Afterburner Systems

Battelle Columbus Labs, OH

Prepared for

Industrial Environmental Research Lab, Research Triangle Park, NC

Apr 79

United States
Environmental Protection
Agency

Industrial Environmental Research
Laboratory
Research Triangle Park NC 27711

EPA-600/7-79-096
April 1979

PB 298465

EPA

Chemical Aspects of Afterburner Systems

Interagency Energy/Environment R&D Program Report

REPRODUCED BY
NATIONAL TECHNICAL
INFORMATION SERVICE
U. S. DEPARTMENT OF COMMERCE
SPRINGFIELD, VA. 22161

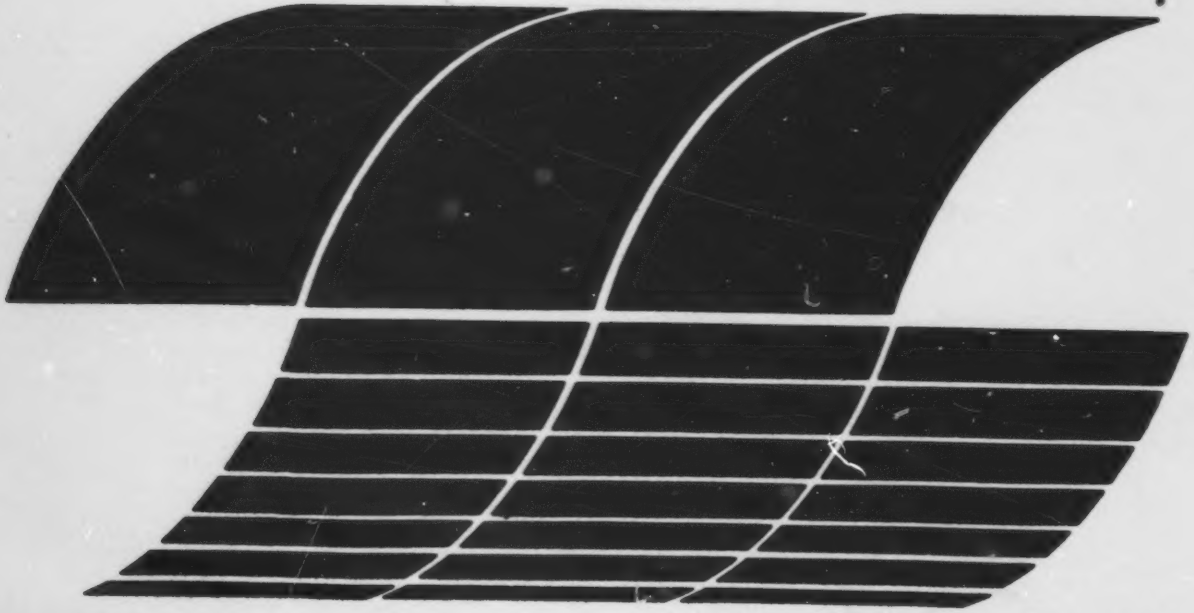

RESEARCH REPORTING SERIES

Research reports of the Office of Research and Development, U.S. Environmental Protection Agency, have been grouped into nine series. These nine broad categories were established to facilitate further development and application of environmental technology. Elimination of traditional grouping was consciously planned to foster technology transfer and a maximum interface in related fields. The nine series are:

1. Environmental Health Effects Research
2. Environmental Protection Technology
3. Ecological Research
4. Environmental Monitoring
5. Socioeconomic Environmental Studies
6. Scientific and Technical Assessment Reports (STAR)
7. Interagency Energy-Environment Research and Development
8. "Special" Reports
9. Miscellaneous Reports

This report has been assigned to the INTERAGENCY ENERGY-ENVIRONMENT RESEARCH AND DEVELOPMENT series. Reports in this series result from the effort funded under the 17-agency Federal Energy/Environment Research and Development Program. These studies relate to EPA's mission to protect the public health and welfare from adverse effects of pollutants associated with energy systems. The goal of the Program is to assure the rapid development of domestic energy supplies in an environmentally-compatible manner by providing the necessary environmental data and control technology. Investigations include analyses of the transport of energy-related pollutants and their health and ecological effects; assessments of, and development of, control technologies for energy systems; and integrated assessments of a wide-range of energy-related environmental issues.

EPA REVIEW NOTICE

This report has been reviewed by the participating Federal Agencies, and approved for publication. Approval does not signify that the contents necessarily reflect the views and policies of the Government, nor does mention of trade names or commercial products constitute endorsement or recommendation for use.

This document is available to the public through the National Technical Information Service, Springfield, Virginia 22161.

TECHNICAL REPORT DATA

(Please read Instructions on the reverse before completing)

1. REPORT NO. EPA-600/7-79-096	2.	3. RECIPIENT'S ACCESSION NO. PB298465
4. TITLE AND SUBTITLE Chemical Aspects of Afterburner Systems		5. REPORT DATE April 1979
		6. PERFORMING ORGANIZATION CODE
7. AUTHOR(S) R. H. Barnes, M. J. Saxton, R. E. Barrett, and A. Levy		8. PERFORMING ORGANIZATION REPORT NO.
9. PERFORMING ORGANIZATION NAME AND ADDRESS Battelle Columbus Laboratories 505 King Avenue Columbus, Ohio 43201		10. PROGRAM ELEMENT NO. 1NE829
		11. CONTRACT/GRANT NO. 68-02-2629
12. SPONSORING AGENCY NAME AND ADDRESS EPA, Office of Research and Development Industrial Environmental Research Laboratory Research Triangle Park, NC 27711		13. TYPE OF REPORT AND PERIOD COVERED Final; 3/77 - 3/79
		14. SPONSORING AGENCY CODE EPA/600/13

15. SUPPLEMENTARY NOTES IERL-RTP project officer is John H. Wasser, MD-65, 919/541-2476.

16. ABSTRACT

The report reviews the chemistry and reaction kinetics of oxidation and pyrolysis reaction that occur in afterburners (or fume incinerators) that are used to destroy organic pollutants in air or gas streams. Chemical kinetic rate data are compiled for both complex and global reaction mechanisms of interest for the design and analysis of afterburner systems. Direct-flame, thermal and catalytic afterburner systems are covered. Details are also given on techniques for estimating chemical rate data when experimental data are unavailable. Appropriate equations are given for calculating the chemical performance characteristics of afterburner systems, and recommendations are made for using chemical rate data for the analysis of afterburner systems.

17. KEY WORDS AND DOCUMENT ANALYSIS

a. DESCRIPTORS		b. IDENTIFIERS/OPEN ENDED TERMS	c. COSATI Field/Group	
Pollution	Oxidation	Pollution Control	13B	07B, 07C
Afterburners	Pyrolysis	Stationary Sources	21J	
Fumes	Organic Compounds	Chemical Rate Data		
Incinerators	Catalysis			
Chemical Properties			07D	
Kinetics			20K	

18. DISTRIBUTION STATEMENT Unlimited	19. SECURITY CLASS *(This Report)* Unclassified	21. NO. OF PAGES 118
	20. SECURITY CLASS *(This page)* Unclassified	22. PRICE PCA06/MF A01

EPA Form 2220-1 (9-73)

EPA-600/7-79-096
April 1979

Chemical Aspects of Afterburner Systems

by

R.H. Barnes, M.J. Saxton,
R.E. Barrett, and A. Levy

Battelle Columbus Laboratories
505 King Avenue
Columbus, Ohio 43201

Contract No. 68-02-2629
Program Element No. INE829

EPA Project Officer: John H. Wasser

Industrial Environmental Research Laboratory
Office of Energy, Minerals, and Industry
Research Triangle Park, NC 27711

Prepared for

U.S. ENVIRONMENTAL PROTECTION AGENCY
Office of Research and Development
Washington, DC 20460

ABSTRACT

This report reviews the chemistry and reaction kinetics of oxidation and pyrolysis reaction that occur in afterburners or fume incinerators that are used to destroy organic pollutants in air or gas streams. Chemical kinetic rate data are compiled for both complex and global reaction mechanisms of interest for the design and analysis of afterburner systems. Direct-flame, thermal and catalytic afterburner systems are covered. Details are also given on techniques for estimating chemical rate data when experimental data are unavailable.

Appropriate equations are given for calculating the chemical performance characteristics of afterburner systems, and recommendations are made for using chemical rate data for the analysis of afterburner systems.

The contents of this report are intended to be included in an afterburner standard practices manual which is to be prepared for EPA as part of this program. Other chapters in this manual will be concerned with mass-transfer effects and the use of the chemical data presented here for the detailed design and evaluation of practical afterburners.

TABLE OF CONTENTS

Page

ABSTRACT ii

TABLE OF CONTENTS iii

LIST OF FIGURES iv

LIST OF TABLES v

ACKNOWLEDGMENTS viii

INTRODUCTION 1

CHEMICAL ASPECTS OF AFTERBURNER SYSTEMS 4

- Oxidation Chemistry of Afterburner Systems 5
  - Chemical Kinetics 9
  - Rate Data Compilations 17
- Homogeneous Oxidation Reactions 19
  - Homogeneous Oxidation Rate Data 19
  - Afterburner Calculations 35
- Catalytic Oxidation Reaction 38
  - Catalytic Oxidation Rate Data 43
  - Afterburner Calculation 55

ESTIMATION PROCEDURES FOR CHEMICAL KINETIC RATE DATA 59

- Reaction Rate Theory 59
  - Unimolecular Reactions 60
  - Bimolecular Reactions 61
- Estimation Procedures 63
  - Theoretical Procedures 63
- Procedures for Rapid Estimation of Kinetic Data 69

SUMMARY AND CONCLUSIONS 69

REFERENCES 71

APPENDIX A A-1

APPENDIX B B-1

APPENDIX C C-1

LIST OF FIGURES

Page

Figure 1. Schematic of Typical Afterburner 4

Figure 2. Summary of Principal Chemical Reactions Involved in Hydrocarbon Oxidation 6

Figure 3. Major Reactions Involved in the Oxidation of Methane 7

Figure 4. Reaction Steps in Benzene Oxidation Through Hydroquinone as an Intermediate 8

Figure 5. Dependence of Activation Energy Upon Bond Strength of Weakest C–H Bond 25

Figure 6. Activation Energy for C_2H_4 Oxidation from 1000 to 1315°K 27

Figure 7. Arrhenius Plots Showing Temperature Dependence in Catalytic Oxidation of Methane 46

Figure 8. Plots of the Logarithm of Frequency Factor, A, as a Function of Activation Energy for Metal Oxides and Metals Supported on Alumina 46

Figure 9. Comparison of Catalytic Combustion of C_1 to C_3 Hydrocarbons 50

Figure 10. Arrhenius Plots of k_r from Naphthalene, Toluene, Benzene, and *o*-Xylene 52

Figure 11. Arrhenius Plots of k_a from Naphthalene, Toluene, Benzene, and *o*-Xylene 52

Figure 12. Arrhenius Plots for Oxidation Over NiO 57

Figure A-1. Effect of Added Oxygen on the Pyrolysis of Ethylene. Reaction Time: Homogeneous, 0.19 sec; Stainless Steel Surface, 0.18 sec. Surface-to-Volume Ratio, 0.7 cm^{-1}. 0.4% O_2 Is Roughly 1:1 O_2-to-Hydrocarbon Ratio A-4

Figure A-2. Percent Propane Converted to Products. Homogeneous Reaction Time $\simeq$ 0.22 sec. Variation in Temperature in °C Is Used to Attain Varying Product Conversions A-4

Figure A-3. Percent Propane Converted to Products. Conversions Varied with Temperature in °C; Oxidized Stainless Steel Surface; Surface-to-Volume Ratio, 0.7 cm^{-1}; Reaction Time $\simeq$ 0.22 sec A-5

Figure A-4. Product Distribution Along Reactor Length A-5

Figure A-5. Product Distribution Along Reactor Length A-6

LIST OF FIGURES
(Continued)

Page

Figure A-6. Arrhenius Plot for Assumed First- and Second-Order Reaction A-7

Figure A-7. Comparison of Decomposition Rates for Propane and Butane at Atmospheric Pressure A-7

Figure A-8. Percent Isobutane Converted to Products. Conversions Varied with Temperature in °C. Homogeneous; Reaction Time $\simeq 0.22$ sec A-8

Figure A-9. Percent Isobutane Converted to Products. Conversions Varied with Temperature in °C; Oxidized Stainless Steel Surface Present; Surface-to-Volume Ratio, 0.7 cm^{-1}; Reaction Time $\simeq 0.22$ sec A-8

Figure A-10. Kinetic Rate Data for Disappearance of Light Hydrocarbons by Thermal Pyrolysis A-10

Figure A-11. Reaction Velocity Constants for Heavy Hydrocarbons Relative to n-C_5H_{12} A-11

LIST OF TABLES

Page

Table 1. Comparison of Temperatures Required to Oxidize Various Compounds to CO_2 and H_2O 5

Table 2. Methane Oxidation Reaction Kinetics 8

Table 3. Activation Energies of Some Elementary Processes 10

Table 4. Conversion Factors for Reaction Rate Constants 11

Table 5. Typical Activation Energies and Frequency Factors 12

Table 6. Reaction Frequency Factors 13

Table 7. Effective Collision Diameters 14

Table 8. Differential and Integrated Forms for Simple-Order Reactions 15

Table 9. Properties of Afterburner Catalysts and Correlations for Mass Transport Coefficients 17

Table 10. Sources of Reaction Rate Data for Afterburners 18

Table 11. Literature Sources of Chemical Kinetic Rate Data 19

Table 12. Global Rate Constants for CH_4 Oxidation to CO 20

Table 13. General Overall Mechanism for Complete Oxidation of Hydrocarbons 21

LIST OF TABLES
(Continued)

Page

Table 14. Hydrocarbon Oxidation Kinetics for JP-5 Fuel (C_8H_{18}) 23
Table 15. Rate Constants for Oxidation of Miscellaneous Organic Compounds 23
Table 16. Rate Constants Measured in Thermal Afterburner System 24
Table 17. Activation Energies (kcal/mole) for Combustion in Air 24
Table 18. Activation Energies for Hydrocarbon-Oxygen Flames 25
Table 19. Ethylene Oxidation Mechanism 26
Table 20. Acetylene Oxidation Mechanism 27
Table 21. Global Rate Data for the Oxidation of Aromatics 28
Table 22. Global Rate Constants for CO Oxidation 29
Table 23. Hydrogen-Oxygen Reaction Mechanism 30
Table 24. Reaction Scheme for Combustion of Hydrogen and Oxygen 30
Table 25. Reaction Rate Constants for Combustion of Hydrogen and Oxygen 31
Table 26. High-Temperature Mechanism for Formaldehyde Oxidation 32
Table 27. Rate Constants for Simple Mechanism for Acetaldehyde Oxidation 32
Table 28. Reaction Mechanism and Kinetic Data 33
Table 29. Reaction Mechanism and Rate Constants for the Oxidation of Acetaldehyde 34
Table 30. Methanol Oxidation Mechanism 35
Table 31. Integrated Rate Expressions for Surface Catalyzed Oxidation 44
Table 32. Rate Constants for Catalysts for the Oxidation of Methane 47
Table 33. Temperatures for Complete Oxidation of Hydrocarbons 48
Table 34. Rate Parameters for Catalytic Oxidation of Methane 49
Table 35. Empirical Reaction Rate Parameters 50
Table 36. Summary of Reaction Rate Models Tested 51
Table 37. Rate Constants for Model 1 53
Table 38. Reaction Rate Parameters for the Catalytic Oxidation of Benzo(α) Pyrene 54
Table 39. Reaction Rate Parameters for Catalytic Oxidation of CO and Propylene 55
Table 40. Kinetic Parameters Over Co_3O_4 56
Table 41. Specific Rates Over Co_3O_4 56

LIST OF TABLES
(Continued)

Page

Table 42. Kinetic Parameters of Oxidations Over Supported Co_3O_4 Catalysts .. 57
Table 43. Specific Rates Over Support Co_3O_4 Catalysts ... 58
Table 44. Kinetic Parameters for Hydrocarbon Oxidation Over NiO(I) ... 59
Table 45. Intrinsic Activation Energies for Bimolecular Reactions ... 62
Table 46. Additive Volume Increments for Estimating Molar Volumes at the Normal Boiling Point ... 65
Table 47. Conventional Basic Values and Decrements for the Calculation of Bond Strengths ... 68
Table 48. Upper Limits for δ in Tolman's Three-Body-Collision Equation ... 68
Table A-1. Kinetic Rate Data for Disappearance of Light Hydrocarbons by Thermal Pyrolysis ... A-9
Table A-2. Kinetic Parameters for the Pyrolysis of Simple Alcohols and Mercaptans . A-9
Table B-1. Reaction Mechanism and Rate Parameters for NO Formation ... B-2
Table B-2. Kinetic Mechanism for Nitric Oxide Formation ... B-4
Table B-3. Rate Constants for N_2–O_2 Reactions ... B-4
Table C-1. Physical and Combustion Properties of Selected Organic Vapors in Air ... C-1
Table C-2. Electron Affinities ... C-4
Table C-3. The Contributions of Different End Groups to Activation Energies ... C-4
Table C-4. Procedure for Calculating Hard-Sphere Collision Parameters ... C-5
Table C-5. Parameters for Lennard-Jones Potential ... C-5
Table C-6. Lennard-Jones Potential Transport Integral $\Omega^{(2,2)*}$ ... C-6
Table C-7. Values of α for Calculating Activation Energies from Bond Strengths C-7
Table C-8. Dissociation Energies, D, of Some Molecules and Radicals ... C-9
Table C-9. Dissociation Energies of Bonds ... C-10
Table C-10. Dissociation Energies of Bonds in Kcal ... C-12

ACKNOWLEDGMENTS

The authors would like to thank Robert W. Coutant of Battelle and Gerald L. Brewer and Steven D. Olsen of the Air Correction Division of UOP, Inc. for reviewing the manuscript and their helpful suggestions. Also acknowledged is the helpful guidance of John H. Wasser who served as EPA Contract Officer.

1

CHEMICAL KINETICS OF FUME AFTERBURNER SYSTEMS

**R. H. Barnes, M. J. Saxton, R. E. Barrett,
and A. Levy**

INTRODUCTION

The purpose of this study was to review the chemical kinetics of afterburners or fume incinerators which are used for the destruction of organic vapors in effluent waste streams from industrial processes. This study is part of a program sponsored by EPA to develop standard practices for designing afterburners for different applications, and to perform an environmental assessment of afterburners. The information assembled here on the chemical kinetics is intended to provide data required for the predictive modeling and design of practical afterburner systems.

Afterburners are usually fairly simple combustors employed to destroy (by oxidation) waste fumes. The waste fumes to be destroyed come from a wide variety of sources such as paint drying, baking ovens, coffee roasters, solvent degreasers, asphalt processes, etc.

The elevated temperature required to promote the oxidation reactions may come from combustion of organic components of the waste stream, or, more generally, from the firing of an auxiliary fuel. The source of oxygen may be the waste stream or air, generally supplied via the auxiliary fuel burner. In principle, if combustion of the auxiliary fuel and oxidation of organics in the waste stream are complete, a noxious or environmentally unacceptable organic vapor is converted completely to CO_2 and H_2O.

Unfortunately, it is not quite this simple in practice. Frequently combustion is incomplete and undesirable partially oxidized species can be generated. Products of incomplete combustion may include such species as CO, the odoriferous aldehydes, ketones, and organic acids, soot, and other organics, possibly including the polynuclear organic materials. It is always possible to overdesign an afterburner system to insure more complete oxidation of organics; however, excessive overdesign is not desirable in an age of increasing fuel costs.

Mainly because of the fuel situation, there is strong interest in eliminating the use of afterburners wherever possible by modifying processes or by recovering the organics for further use; however, it does appear certain that afterburners will still be required for many applications. When an afterburner is required it is imperative that it be energy efficient while reducing effluent concentrations to the required limits. Once developed, good design procedures should provide a rationale for designing more effective systems in addition to serving as a basis for comparing contemplated afterburner systems with other alternatives.

Generally afterburners are classified into three categories.

- Direct flame
- Thermal
- Catalytic

Direct flame and thermal afterburners are similar. The basic difference is that the direct-flame afterburners provide for destruction of the organic vapors by passing a high percentage of the vapors directly through a flame. The thermal afterburner provides for exposure of the organic vapors to a high-temperature oxidizing atmosphere for a sufficient time so that the necessary oxidation reactions can occur. Temperatures in the range from 1200 to 1500°F (650 to 815°C) are generally required for successful operation of direct flame and thermal devices. Hydrocarbon levels can usually be satisfactorily reduced at temperatures below about 1400°F (760°C), but higher temperatures may be required to simultaneously oxidize the CO. The catalytic devices, which incorporate a catalytic surface to accelerate the oxidation reactions, generally operate at lower temperatures, in the range from about 700 to 900°F (370 to 480°C), and require less auxiliary fuel. However, catalytic units generally are more expensive and require more maintenance than the other two types of afterburners.

From a chemical viewpoint, two main types of reactions occur in afterburner systems: oxidation and pyrolysis reactions. In the case of the direct-flame and thermal afterburners, these reactions occur mainly in the gas phase with some influence from surface effects. With the catalytic devices, however, the reactions take place on the surface of the catalyst. In general, the detailed mechanisms for the oxidation and pyrolysis of even the simplest organic compounds are not completely understood, but it is well established that the reactions occur in many complicated sequential and concurrent steps involving a multitude of intermediate species.

It is the intention of this study not to delve into the detailed mechanisms of any reactions, but to review available information and put it in a form that can be used conveniently for the analysis and design of afterburner systems. For this purpose, reaction rates are best expressed in terms of overall or global reaction rates with corresponding distributions of reaction products. Data are correlated for different classes of organic compounds so that when information is unavailable for specific compounds, it may be possible to use correlations to estimate required rate constants and their accuracy. A part of this report also presents procedures for estimating rate constants using considerations based on kinetic theory and the statistical mechanics of chemical reaction rate theory. Using either the assembled data and/or the estimation procedures, it should be possible to obtain fairly reliable estimates of rate data for the practical design and evaluation of afterburner systems.

A comprehensive design model of an afterburner must take into account both the chemical and the mass-transport rates of the processes. In most afterburner systems, mixing controls the overall process with the chemistry playing a minor role. Knowledge of an approximate chemical rate constant can often be useful in establishing those cases where the chemical kinetics are not important and can be ignored in design consideration. On the other hand, when chemical rates are important, practical rate data are necessary to determine temperatures and residence times required to effectively oxidize specific compounds.

The operation of an afterburner can be described by three characteristic times which are defined below.

(1) **Chemical time**. For a first-order reaction the chemical time is defined by $\tau_c = 1/k$, where k is the rate constant. For reactions of other orders, the rate constant must be multiplied by the appropriate average concentrations.

(2) **Mixing time**. The mixing time can be estimated as $\tau_d = L^2/D$, where L is the length of the reaction zone in the afterburner, and D is the effective diffusion coefficient.

(3) **Residence time**. The residence time is $\tau_r = L/V$ where V is the average gas velocity.

The ratio of the chemical time to the residence time is the reciprocal of the first Damköhler group:

$$\frac{\tau_c}{\tau_r} = \frac{1}{N_{Da(I)}} = \frac{V}{kL}$$

and the ratio of the diffusion time to the residence time is the Peclet number (N_{Pe}) for mass transfer

$$\frac{\tau_d}{\tau_r} = \frac{VL}{D} = N_{pe} \quad .$$

These ratios characterize the performance of the afterburner. If they are too small, the chemistry is rate controlling; if they are too large, mixing is controlling. The reciprocal Damköhler number can be obtained from the global reaction rates given in this report. The Peclet number can be found from the Reynolds and Schmidt numbers using the graphical relationships in Levenspiel and Bischoff.(154)

Much of the oxidation and oxidative-pyrolysis data in the literature have been obtained in flames or laboratory combustion systems in such a way that many intermediates such as CO, H_2, and aldehydes are formed, and complete conversion to CO_2 and H_2O does not occur. In applying global rate data to afterburner design problems, it may be convenient to conceptually divide the combustion process into more than one stage. In the first stage, for example, the primary combustion reactions would be taken into account with subsequent stages being employed to extend the combustion of the partially oxidized species to the desired level of oxidation. As an illustration of this approach, the global oxidation data for a specific hydrocarbon might be based on a specific yield of CO. To reduce the level of CO further, an additional stage of combustion would then be incorporated into the design considerations to further oxidize the CO to CO_2. Calculations for this latter stage would be based on global kinetics for the oxidation of CO.

The next section of this report discusses the chemical aspects of afterburner systems. This is followed by a review of chemical kinetic data which is organized under the following headings:

- Homogeneous oxidation of hydrocarbons
- Catalytic oxidation of hydrocarbons

This section is then followed by a section on procedures for estimating chemical kinetic rate data where experimental data are lacking. A final summary and conclusions section describes how the results presented in this report can be used to provide practical rate data for use in designing afterburner systems. Appendices are also included on the kinetics of the pyrolysis of hydrocarbons and the kinetics of pollutant formation reactions.

CHEMICAL ASPECTS OF AFTERBURNER SYSTEMS

Conceptually, afterburners can be considered as being divided into 3 sections: an auxiliary fuel combustion section, a fume and combustion product mixing section, and an oxidation (or reaction) section. This afterburner concept is illustrated in Figure 1. Physically, the afterburners sections shown in Figure 1 may be merged and all the processes may occur in one chamber.

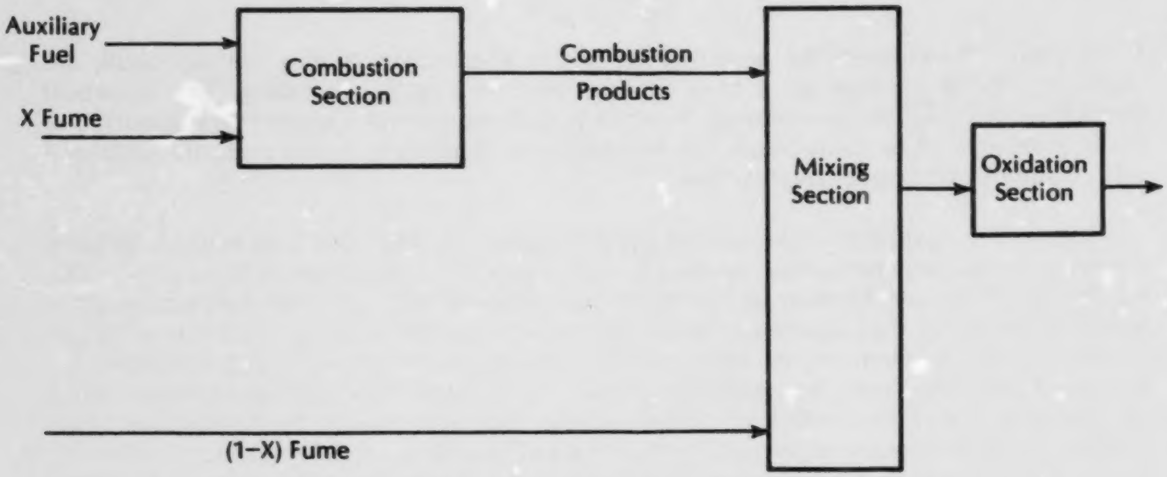

FIGURE 1. SCHEMATIC OF TYPICAL AFTERBURNER

In the combustion section, an auxiliary fuel is fired to supply the heat to warm the fume to a temperature that will promote oxidation of the organic vapors. Usually, a portion of the fume stream supplies the oxygen. (Part of the fume stream must be bypassed or the fuel/air mixture will be too lean to sustain combustion.) Both gaseous and liquid fuels are used to fire afterburners. Gaseous fuels have the advantage of permitting firing in multiple-jet (or distributed) burners. Oil combustion has the disadvantage of producing sulfur oxides (from sulfur in the oil) and normally produces higher nitrogen oxides emissions.

The mixing section is designed to provide intimate mixing between the combustion products (from combustion of the auxiliary fuel) and the remaining fume gases. To insure good mixing it is necessary to provide high velocity gas flow to produce turbulence. Gas velocities in afterburners range from 25 to 50 feet per second. Ideally, the temperature profile at the outlet of the mixing section would be flat. In thermal-type afterburners, the following temperatures are often used as guidelines:

Odor control: 900–1350°F

To oxidized hydrocarbons: 900–1200°F

To oxidized carbon monoxide: 1200–1450°F.

The oxidation section provides time for the organic vapors in the bypassed fume to be oxidized. Oxidation sections typically have length-to-diameter ratios of 2 to 3. Depending on the type of pollutant, residence times ranging from 0.2 to 1.0 seconds are required for thermal units. The residence time in most practical afterburner systems is dictated primarily by chemical kinetic considerations.

Catalytic afterburners provide a catalytic surface to promote oxidation for organic vapors. Consequently, catalytic afterburners operate at lower temperatures than the thermal types and require less fuel. The preheat temperature for catalytic devices varies with gas composition and type of contaminant to be oxidized, but is generally in the range from 650 to 1100°F, lower than the 1200 to 1500°F of most thermal afterburners.

A comparison of temperatures required in thermal and catalytic afterburners to convert various compounds to CO_2 and H_2O vapor is given in Table 1.

Catalysts in afterburners typically consist of either a metal mesh, ceramic honeycomb, or a ceramic matrix with a surface deposit of finely divided platinum or platinum family metals. In industrial processes, 10 to 100 ft^3 of catalyst bed are used per 1000 scfm of gas flow. In afterburners, however, the requirement is in the range of 1 to 2 ft^3 per 1000 scfm. Catalytic afterburners have the disadvantage that performance efficiency deteriorates as the unit is used, and require periodic replacement of the catalytic material.

TABLE 1. COMPARISON OF TEMPERATURES REQUIRED TO OXIDIZE VARIOUS COMPOUNDS TO CO_2 AND H_2O(1)

Compound	Ignition Temperature, °F	
	Thermal	Catalytic
Benzene	1076	575
Toluene	1026	575
Xylene	925	575
Ethanol	738	575
MIBK	858	660
MED	960	660
Methane	1170	932
Carbon Monoxide	1128	500
Hydrogen	1065	250
Propane	898	500

OXIDATION CHEMISTRY OF AFTERBURNER SYSTEMS

Hydrocarbons in the gas phase react very slowly with oxygen at temperatures below 200°C, however, as the temperature is increased a variety of oxygen-containing compounds begin to form. As the temperature is increased further, CO and H_2O are formed as major products and compounds such as CO_2, H_2O_2, and CH_2O begin to appear. In the range from 300 to 400°C a faint light often appears. This may be followed by one or more blue flames that successively traverse the reaction vessel. At yet higher temperatures, 500°C or above, explosive reactions can occur. Detailed information on the homogeneous combustion of hydrocarbons can be found in References (2) through (5).

Hydrocarbon combustion at lower temperatures is usually initiated by the reaction

$$RH + O_2 \rightarrow R\cdot + HO_2 \quad .$$

With hydrocarbons, this reaction is endothermic by about 45 to 50 kcal/mole. In the case of aldehydes, the reaction is 35 to 40 kcal/mole endothermic, and the activation energy is slightly greater. The hydrocarbon radical, R·, can react with oxygen and go through a wide variety of reactions and intermediates such as depicted by Bradley(3) as shown in Figure 2. As can be seen in this figure incomplete combustion can lead to the formation of many oxygenated compounds. In contrast, thermal-cracking or pyrolytic reactions are known to contribute significantly to hydrocarbon combustion reactions at high temperatures.

Methane, the simplest of the hydrocarbons, when oxidized at low temperatures (<550°C) is affected by the surface of the reaction vessel, the surface-to-volume ratio, and the presence of inert gases. A phenomenological reaction scheme for methane oxidation at low temperatures is shown in Figure 3. Methane combustion at high temperatures involves mainly taking into account the oxidation of CO to CO_2 by the reaction

$$OH + CO \rightarrow H + CO_2 \quad .$$

At high temperatures the oxidation of the CO by this reaction competes for the OH resulting in retardation of the CH_4 reaction. At high temperatures pyrolytic reactions also become important. With methane and all other hydrocarbons, the primary initiation step at high temperatures is the pyrolysis of the hydrocarbon to give alkyl radicals. A detailed mechanism for the oxidation of methane is given in Table 2.

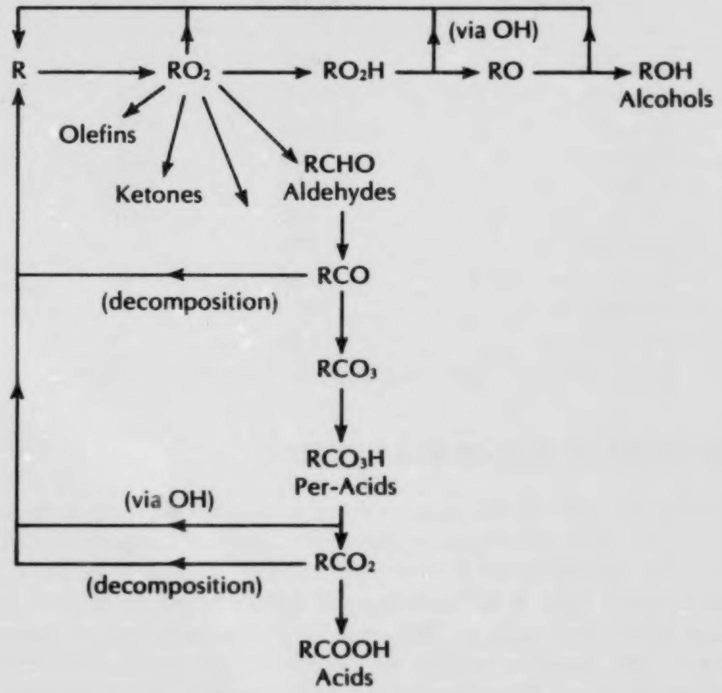

FIGURE 2. SUMMARY OF PRINCIPAL CHEMICAL REACTIONS INVOLVED IN HYDROCARBON OXIDATION(3)

$$\begin{array}{rcl} CH_4 + O_2 & \rightarrow & CH_3 + HO_2 \end{array} \quad \text{chain initiation}$$

$$\left.\begin{array}{rcl} CH_3 + O_2 & \rightarrow & CH_2 + OH \\ OH + CH_4 & \rightarrow & H_2O + CH_3 \\ OH + CH_2O & \rightarrow & H_2O + CHO \end{array}\right\} \text{chain propagation}$$

$$\begin{array}{rcl} CH_2 + O_2 & \rightarrow & HO_2 + HCO \end{array} \quad \text{chain branching}$$

$$\left.\begin{array}{rcl} HCO + O_2 & \rightarrow & CO + HO_2 \\ HO_2 + CH_4 & \rightarrow & H_2O_2 + CH_3 \\ HO_2 + CH_2O & \rightarrow & H_2O_2 + HCO \end{array}\right\} \text{chain propagation}$$

$$\left.\begin{array}{rcl} OH & \rightarrow & \text{wall} \\ CH_2O & \rightarrow & \text{wall} \end{array}\right\} \text{chain termination}$$

FIGURE 3. MAJOR REACTIONS INVOLVED IN THE OXIDATION OF METHANE(5)

For the oxidation of saturated hydrocarbons above methane, the mechanism of oxidation is further complicated by the greater instability of the higher alkyl radicals and the wide range of intermediates that are produced. Below about 400°C, the intermediates are comprised largely of aldehydes and methanol, while at higher temperatures the olefins become important. A review of cool flame information for the oxidation of C_2 to C_{13} hydrocarbons has been reported by Cechaux and Delfosse.(160,161)

When unsaturated hydrocarbons are oxidized, addition of oxygen to the double bond is more likely to occur. The initial adduct is generally unstable and can decompose rapidly to different intermediates of which the aldehydes are probably the most important

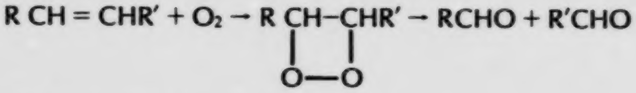

$$R\,CH = CHR' + O_2 \rightarrow R\,\underset{O-O}{CH-CHR'} \rightarrow RCHO + R'CHO$$

The aldehydes can then be further oxidized.

The oxidation of aromatic hydrocarbons in general has not really been investigated extensively. The major steps in the mechanism for benzene oxidation are thought to be

$$C_6H_6 + O_2 \rightarrow C_6H_5 + HO_2$$
$$C_6H_5 + O_2 \rightarrow C_6H_5O_2$$
$$C_6H_5O_2 + C_6H_6 \rightarrow C_6H_5O + C_6H_5 + OH$$
$$C_6H_5O + C_6H_6 \rightarrow C_6H_5OH + C_6H_5$$

The phenol, C_6H_5OH, which forms in high yields because of its great stability is further oxidized to $C_6H_4(OH)_2$, which is in turn oxidized according to the scheme shown in Figure 4. The products on the right in the figure can then be oxidized further. Oxidation of the acetylene generally occurs through a series of chain reactions with formaldehyde and formic acid as intermediates. The high-temperature oxidation of acetylene is also complicated by the tendency of acetylene to polymerize. A short review of the oxidation of aromatic compounds can be found in an article by Santoro and Glassman.(162)

TABLE 2. METHANE OXIDATION REACTION KINETICS[6]

Reaction	Forward Rate Constant[a]	Forward Rate Constant at 2000°K	Reverse Rate Constant at 2000°K
$CH_4 + M \rightarrow CH_3 + H + M$	$3.32 \times 10^{-7} \exp(-44500/T)$	$7.2 + 10^{-17}$	3.05×10^{-31}
$CH_4 + OH \rightarrow CH_3 + H_2O$	$9.96 \times 10^{-10} \exp(-6290/T)$	4.3×10^{-11}	1.74×10^{-13}
$CH_4 + H \rightarrow CH_3 + H_2$	$3.72 \times 10^{-20} T^3 \exp(-4400/T)$	3.3×10^{-11}	1.34×10^{-12}
$CH_4 + O \rightarrow CH_3 + OH$	$3.49 \times 10^{-11} \exp(-4560/T)$	3.6×10^{-12}	1.1×10^{-13}
$CH_3 + O \rightarrow CH_2O + H$	1.66×10^{-10}	1.66×10^{-10}	8.8×10^{-17}
$CH_3 + O_2 \rightarrow CH_2O + OH$	3.32×10^{-14}	3.32×10^{-14}	7.2×10^{-20}
$CH_2O + O \rightarrow CHO + OH$	$8.30 \times 10^{-11} \exp(-2300/T)$	2.63×10^{-11}	1.5×10^{-14}
$CH_2O + OH \rightarrow CHO + H_2O$	$8.97 \times 10^{-10} \exp(-3170/T)$	1.84×10^{-10}	1.42×10^{-14}
$CH_2O + H \rightarrow CHO + H_2$	$2.24 \times 10^{-11} \exp(-1890/T)$	8.7×10^{-12}	7.0×10^{-15}
$CH_2O + M \rightarrow CHO + H + M$	$6.64 \times 10^{-12} \exp(-18500/T)$	6.38×10^{-16}	5.4×10^{-32}
$CHO + O \rightarrow CO + OH$	1.66×10^{-10}	1.66×10^{-10}	1.9×10^{-19}
$CHO + OH \rightarrow CO + H_2O$	1.66×10^{-10}	1.66×10^{-10}	2.1×10^{-20}
$CHO + H \rightarrow CO + H_2$	3.32×10^{-10}	3.32×10^{-10}	4.6×10^{-19}
$CHO + M \rightarrow CO + H + M$	$8.30 \times 10^{-12} \exp(-9570/T)$	7.0×10^{-14}	1.0×10^{-35}
$CO + OH \rightarrow CO_2 + H$	$6.64 \times 10^{-12} \exp(-4030/T)$	8.9×10^{-13}	3.8×10^{-13}
$H_2 + OH \rightarrow H + H_2O$	$4.82 \times 10^{-10} \exp(-5530/T)$	3.0×10^{-11}	3.0×10^{-12}
$H_2 + O \rightarrow H + OH$	$5.31 \times 10^{-10} \exp(-7540/T)$	1.2×10^{-11}	1.1×10^{-11}
$H + O_2 \rightarrow O + OH$	$3.65 \times 10^{-10} \exp(-8450/T)$	5.34×10^{-12}	2.3×10^{-11}
$H + OH + Ar \rightarrow H_2O + Ar$	$2.31 \times 10^{-26} T^{-2}$	5.8×10^{-33}	5.14×10^{-21}
$H + OH + H_2O \rightarrow H_2O + H_2O$	$3.86 \times 10^{-25} T^{-2}$	9.65×10^{-32}	8.56×10^{-20}
$H + HO_2 \rightarrow OH + OH$	$4.15 \times 10^{-10} \exp(-950/T)$	2.58×10^{-10}	1.0×10^{-15}
$H + O_2 + M \rightarrow HO_2 + M$	$4.13 \times 10^{-33} \exp(500/T)$	5.32×10^{-33}	3.6×10^{-14}
$OH + OH \rightarrow H_2O + O$	$9.13 \times 10^{-11} \exp(-3520/T)$	1.57×10^{-11}	2.0×10^{-12}

[a] Units: No. Particles, cm^3, sec, °K.

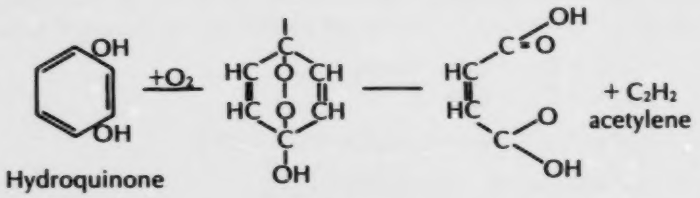

FIGURE 4. REACTION STEPS IN BENZENE OXIDATION THROUGH HYDROQUINONE AS AN INTERMEDIATE

Solid surfaces can affect combustion in two ways. One is in terms of quenching which can lead to the formution of oxygenated organic compounds such as the aldehydes which are undesirable in afterburner applications. The other involves catalytic effects. Catalytic oxidation is the basis of the catalytic-type afterburner.

Catalytic oxidation falls into two categories: selective oxidation and complete oxidation. Only complete oxidation is of interest for afterburners since the main objective is complete conversion of organics to CO_2 and H_2O vapor. In general detailed mechanisms for catalytic oxidation reactions are not known.

Chemical Kinetics

Hydrocarbon oxidation reactions can be represented by the chemical equation

$$C_aH_b + \left(a + \frac{b}{4}\right) O_2 = aCO_2 + \frac{b}{2}H_2O$$

where C_aH_b is any hydrocarbon.* This equation is often called an overall or global reaction. A global expression shows only the net result of a reaction and neglects the many complicated reaction steps that lead from initial reactants to the final products. Global reactions are readily adaptable and useful for the kinetic analysis and engineering design of afterburner systems.

There are many gas-phase and surface catalyzed oxidation reactions for which single global expressions can be used successfully as a basis for calculating reaction rates. However, in the case of the homogeneous gas-phase oxidation of paraffinic hydrocarbons, the use of a quasi-global approach has been required for treating reaction kinetics. The quasi-global approach is based on the reaction

$$C_aH_b + \frac{a}{2}O_2 \rightarrow aCO + \frac{b}{2}H_2$$

with subsequent oxidation of CO and H_2 leading to the final combustion products CO_2 and H_2O. The H_2 oxidation is quite rapid compared to CO oxidation for which global rate expressions are available. Thus, in this case, the overall gas-phase oxidation kinetics would be represented by a series combination of two fairly simple reactions. In considering heterogeneous reactions on catalytic surfaces, in addition to the chemical kinetics, mass-transport processes must also be taken into account.

In general, both the homogeneous gas-phase and catalytic reactions involving the destruction of organics or hydrocarbons in afterburner systems can be represented by the chemical equation

$$\alpha F + \beta O_2 \rightarrow \text{Products}$$

where F denotes the hydrocarbon fuel and α and β are stoichiometric factors. The chemical reaction rate for the disappearance of the hydrocarbon can be written as

$$\frac{1}{\alpha}\frac{dn_F}{dt} = -kn_F^{\alpha}\, n_{O_2}^{\beta}$$

---

*Substituted hydrocarbons containing atoms such as O, N, S, Cl, etc., can be taken into account by appropriate modifications to the above equation.

where k is the reaction-rate constant and n the species concentrations. This is basically a bimolecular reaction of order $\alpha + \beta$. Care must be taken to observe how the rate constant is defined. Sometimes αk is defined as the rate constant. For most afterburner applications, the reaction expression, to a good approximation, can be reduced either to second order where both α and β are taken as unity, or to first order in n_F. The first-order approximation applies when the O_2 is in large excess, which is usually the case with afterburner systems. In this case, n_{O_2} raised to the appropriate power β is treated as a constant.

The reaction-rate constant k generally is written in one of two forms. The Arrhenius form is

$$k = A\, e^{-E_A/RT}$$

where E_A is the Arrhenius activation energy, A is the frequency factor, T is temperature, and R is the gas constant. Arrhenius activation energies for typical hydrocarbons are given in Table 3. A more elaborate expression, sometimes used, assumes the form

$$k = B\, T^m\, e^{-E_B/RT}$$

where the value of m ranges usually from −1 to 4. This latter expression is often referred to as the modified Arrhenius equation. In most cases the influence of the exponential is so much greater than the T^m term that the relationship essentially reduces to an Arrhenius-type expression. The relationships between the different reaction rate parameters can be expressed by the two equations(8)

$$A = B\, T^m\, e^m$$

and

$$E_A = E_B + mRT \quad .$$

TABLE 3. ACTIVATION ENERGIES OF SOME ELEMENTARY PROCESSES(7)

Reaction	E_A, kcal/mole
$CH_4 \rightarrow CH_3 + H$	102
$C_2H_6 \rightarrow 2CH_3$	84
$C_3H_8 \rightarrow CH_3 + C_2H_5$	84
$n\text{-}C_4H_{10} \rightarrow 2C_5H_5$	84
$CH_3 + CH_4 \rightarrow CH_4 + CH_3$	14.7
$CH_3 + C_2H_6 \rightarrow CH_4 + C_2H_5$	10.4
$CH_3 + C_3H_8 \rightarrow CH_4 + C_3H_7$	5.5
$CH_3 + C_4H_{10} \rightarrow CH_4 + C_4H_9$	5.5
$C_2H_5 \rightarrow C_2H_4 + H$	39
$C_3H_7 \rightarrow C_2H_4 + CH_3$	18
$C_4H_9 \rightarrow C_2H_4 + C_2H_5$	22
$H + CH_4 \rightarrow CH_3 + H_2$	11–13
$H + C_2H_6 \rightarrow C_2H_5 + H_2$	9
$H + C_3H_8 \rightarrow C_3H_7 + H_2$	9
$H + C_4H_{10} \rightarrow C_4H_9 + H_2$	9

Rate constants have the dimensions of inverse time in seconds multiplied by concentration raised to the power $(1-\nu)$ where ν is the overall reaction order. The most common concentration units are moles/liter, moles/cm^3, and molecules/cm^3. In terms of these last units, a first-order rate constant would have dimensions of reciprocal seconds while a second-order rate constant has dimensions of cm^3/molecule-sec. Reactions with nonintegral overall order have rate concentrations with concentration units raised to nonintegral powers. Common conversion factors for second- and third-order reactions are given in Table 4.

Homogeneous Reaction Rates. Bimolecular reactions have frequency factors, A, which lie in the range from 10^8 to 10^{12} liter/mole-sec and Arrhenius activation energies, E_A, that range from 0 to 70 kcal. Some specific values of E_A and A are listed in Table 5, while Table 6 presents values of A for various types of typical reactions.

It is sometimes helpful in understanding reaction rate constants to consider the collision-theory approximation for a bimolecular rate constant where the rate constant can be expressed as

$$k = p\, Z\, e^{-E_0/k_B T}$$

where Z is the hard sphere collision frequency, p the steric factor and E_0 the energy threshold for the reaction. The collision frequency can be found from simple kinetic theory to be

$$Z = \left(\frac{8\pi k_B T}{\mu}\right)^{1/2} \sigma_{AB}^2, \text{ cm}^3\text{/molecule-sec}$$

TABLE 4. CONVERSION FACTORS FOR REACTION RATE CONSTANTS

Second-Order Reactions

	A		
B	cm^3/mole-sec	liter/mole-sec	cm^3/molecule-sec
cm^3/mole-sec	1	10^3	6.023×10^{23}
liter/mole-sec	10^{-3}	1	6.023×10^{20}
cm^3/molecule-sec	1.66×10^{-24}	1.66×10^{-21}	1

Third-Order Reactions

	A		
B	cm^6/mole^2-sec	liter/mole^2-sec	cm^6/molecule^2-sec
cm^6/mole^2-sec	1	10^6	3.628×10^{47}
liter/mole^2-sec	10^{-6}	1	3.628×10^{41}
cm^6/molecule^2-sec	2.76×10^{-48}	2.76×10^{-42}	1

To convert a rate constant from units A to units B, multiple A by the conversion factor found vertically below A in the horizontal row B.

TABLE 5. TYPICAL ACTIVATION ENERGIES AND FREQUENCY FACTORS[9]

Reaction	Activation Energy, kcal/g-mole	Frequency Factor
First-order gaseous decompositions:		sec^{-1}
Nitrogen tetroxide	13.9	8.0×10^{14}
Ethyl chlorocarbonate	29.1	9.2×10^{8}
Ethyl peroxide	31.5	5.1×10^{14}
Ethylidene dibutyrate	33.0	1.8×10^{10}
Acetic anhydride	34.5	1.0×10^{12}
Ethyl nitrite	37.7	1.4×10^{14}
tert-Butyl chloride	41.4	2.5×10^{12}
Methyl iodide	43.0	3.9×10^{12}
Paracetaldehyde	44.2	1.3×10^{15}
Ethylidene dichloride	49.5	1.2×10^{12}
Nitromethane	50.6	4.1×10^{13}
Azomethane	52.5	3.5×10^{16}
Propylene oxide	58.0	1.2×10^{14}
Dimethylethylacetic acid	60.0	3.3×10^{13}
1-Butene	63.0	5.0×10^{12}
Trimethylacetic acid	65.5	4.8×10^{14}
p-Xylene	76.2	5.0×10^{13}
Toluene	77.5	2.0×10^{13}
Second-order gaseous reactions between stable molecules:		ml/mole-sec
$NO + O_3 \rightarrow NO_2 + O_2$	2.5	8×10^{11}
Cyclopentadiene	14.9	8.5×10^{7}
Cyclopentadiene + crotonaldehyde	15.2	1×10^{9}
Isoprene + acrolein	18.7	1.0×10^{9}
Butadiene + acrolein	19.7	1.5×10^{9}
Butadiene + crotonaldehyde	22.0	9.0×10^{8}
Isobutylene + HBr	22.5	1.6×10^{10}
$2NOCl \rightarrow 2NO + Cl_2$	24.0	9×10^{12}
1,3-Butadiene	25.3	4.7×10^{10}
1,3-Pentadiene	26.0	3.5×10^{10}
Isobutylene + HCl	28.8	1.0×10^{11}
Ethylene	37.7	7.1×10^{10}
Propylene	38.0	1.6×10^{10}
$H_2 + I_2 \rightarrow 2HI$	40.0	1×10^{14}
Isobutylene	43.0	2.0×10^{12}
Ethylene + H_2	43.2	4.0×10^{13}
$2HI \rightarrow H_2 + I_2$	44.0	6×10^{13}
Second-order reactions involving atoms or radicals:		
$H + HBr \rightarrow H_2 + Br$	1.2	
$H + Br_2 \rightarrow HBr + Br$	1.2	
$CH_3 + i\text{-}C_4H_{10}$	7.6	
$CH_3 + n\text{-}C_4H_{10}$	8.3	
$CH_3 + C_2H_6$	10.4	
Third-order gaseous reactions:		$ml^2/mole^2$-sec
$2NO + O_2 \rightarrow 2NO_2$	0 or negative	8×10^{9}
$2NO + Br_2 \rightarrow 2NOBr$	~4	$\sim 10^{11}$
$2NO + Cl_2 \rightarrow 2NOCl$	~4	$\sim 10^{9}$
$I + I + He \rightarrow I_2 + He$	0	0.34×10^{16}
$I + I + Ar \rightarrow I_2 + Ar$	0	0.72×10^{16}
$I + I + H_2 \rightarrow I_2 + H_2$	0	0.95×10^{16}
$I + I + CO_2 \rightarrow I_2 + CO_2$	0	2.7×10^{16}

TABLE 6. REACTION FREQUENCY FACTORS

Reaction	A, liter/mole-sec	Steric Factor
2-atoms	$10^{10} - 10^{12}$	1
Atom + linear molecule, linear complex	$10^{8} - 10^{10}$	10^{-2}
Atom + linear molecule, nonlinear complex	$10^{9} - 10^{11}$	10^{-1}
Atom + nonlinear molecule, linear complex	$10^{8} - 10^{10}$	10^{-2}
2 linear molecules, linear complex	$10^{6} - 10^{8}$	10^{-4}
1 linear + 1 nonlinear molecule, nonlinear complex	$10^{7} - 10^{9}$	10^{-3}
2 nonlinear molecules, nonlinear complex	$10^{5} - 10^{7}$	10^{-4}
3 atoms, linear complex	10^{8}	10^{-5}

where k_B is the Boltzmann constant (1.38×10^{-16} erg/°K), μ the reduced mass in grams and σ the hard-sphere collision diameter in cm. For a reaction involving the collision of species A with species B, the reaction collision diameter is

$$\sigma_{AB} = \tfrac{1}{2}(\sigma_A + \sigma_B)$$

and

$$\frac{1}{\mu} = \frac{1}{M_A} + \frac{1}{M_B}$$

where σ_A and σ_B represent the diameter of A and B, and M_A and M_B, their respective masses.* Typical values of collision diameters for various molecules are given in Table 7. The steric factor can be expressed as

$$p = \frac{\pi\sigma_R^2}{\pi\sigma_{AB}^2}$$

where σ_R is the reactive collision diameter and $\pi\sigma_R^2$ is often defined as the reactive collision cross section. Ranges of values for p for different types of reactions are presented in Table 6. Using the above relationships the reaction frequency factor can be written as

$$A = e^{1/2}\left(\frac{8\pi k_B T}{\mu}\right)^{1/2}\sigma_R^2 \text{ cm}^3\text{/molecule-sec}$$

where $e^{1/2}$ results from the conversion of the exponential from $e^{-E_0/RT}$ to $e^{-E_A/RT}$. The relationship between E_A and E_0 is

$$E_A = \frac{R}{k_B}(E_0 + \tfrac{1}{2}k_B T)$$

where k_B is defined above and R is the gas constant (1.9872 cal/mole-°K). Since p is less than unity for the bimolecular reactions, the above equations can be used to compute the upper limit of bimolecular reaction rates by taking p=1. Further details on reaction rate constants will be presented in a subsequent section of this report which covers more comprehensive information for estimating rate constants. For an exothermic reaction the smallest value of E_0 is zero; for an endothermic reaction the smallest value is the heat of reaction $E_0 = \Delta H_T^0$.

---

*Molecular weights may be converted from atomic mass units (AMU) to grams by multiplying by 1.662×10^{-24} gm/AMU.

TABLE 7. EFFECTIVE COLLISION DIAMETERS

Molecule	Effective Diameter, Å*	Reference
H_2	2.730	(13)
O_2	3.620	(13)
CO	3.766	(13)
NO	3.690	(13)
N_2	3.756	(13)
CO_2	4.630	(13)
H_2O	4.320	(13)
SO_2	2.747	(13)
CH_4	4.19	(14)
C_2H_6	5.37	(14)
C_3H_8	6.32	(14)
n-C_4H_{10}	7.06	(14)
n-C_5H_{12}	7.82	(14)
n-C_6H_{14}	8.42	(14)
cyclo-C_6H_{12}	7.620	(13)
C_6H_6	7.160	(13)
C_5H_5N	7.160	(13)
CH_3Cl	5.662	(13)
C_2H_4	4.956	(13)
$(C_2H_5)_2O$	7.060	(13)
$C_6H_5CH_3$	7.800	(13)

*1 Å = 10^{-8} cm.

Integrated rate equations for first- and second-order reactions are presented in Table 8. The integrated reactions are expressed in terms of residence time (τ) and the fraction of vapor consumed in a simple isothermal afterburner system under steady-state conditions assuming plug flow. The residence time can be calculated from

$$\tau = \frac{V}{Q} = \frac{a\,L}{Q}$$

where V is the volume of the afterburner, a and L its cross-sectional area and length, respectively, and Q the volumetric flow rate. Nonisothermal conditions, kinetics involving reactions other than those of first and second orders, and other complicating conditions lead to a need for more detailed modeling and mathematical procedures. A compilation of integrated rate expressions for both simple and complex homogeneous reaction kinetics can be found in the *Chemical Engineer's Handbook*.(9)

Heterogeneous (Surface) Reaction Rates. The overall rate of heterogeneous reactions is complicated because of the interaction between physical and chemical processes. Rates for heterogeneous reactions have upper limits which depend on the rate at which reactant molecules reach the interface where reaction occurs. The rate for a gas reaction catalyzed at a solid surface of area S can be written in terms of molecules of F reacting per second as

$$r = k_S\, S\, C_F$$

TABLE 8. DIFFERENTIAL AND INTEGRATED FORMS FOR SIMPLE-ORDER REACTIONS

Reaction Order	Differential Rate Expression	Integrated Expression for Fraction of Vapor Removed (Assumes Constant Volume Reactions)
1	$\frac{dC_F}{dt} = - k\, C_F$	$f = \left(1 - \frac{C_F}{C_F^0}\right) = (1 - e^{-k\tau})$
2	$\frac{dC_F}{dt} = - k\, C_F\, C_{O_2}$	$f = \left(1 - \frac{C_F}{C_F^0}\right) = \frac{\left(1 - e^{-k(C_{O_2}^0 - C_F^0)\tau}\right)}{\left(1 - \frac{C_F^0}{C_{O_2}^0}\, e^{-k(C_{O_2}^0 - C_F^0)\tau}\right)}$ for $C_{O_2}^0 \neq C_F^0$
		$f = \left(1 - \frac{C_F}{C_F^0}\right) = \frac{k\, C_F^0 \tau}{k\, C_F^0 \tau + 1}$ for $C_{O_2}^0 = C_F^0$
1/2	$\frac{dC_F}{dt} = - k\, C_F^{1/2}$	$f = \left(1 - \frac{C_F}{C_F^0}\right) = \frac{k\tau}{\sqrt{C_F^0}} \left(1 - \frac{k\tau}{4\sqrt{C_F^0}}\right)$
1/j	$\frac{dC_F}{dt} = - k\, C_F^{1/j}$	$f = \left(1 - \frac{C_F}{C_F^0}\right) = \left\{1 - \left[1 - \frac{(j-1)}{j(C_F^0)^{(j-1)/j}}\, k\tau\right]^{j/(j-1)}\right\}$

$C_{O_2}^0$ = initial concentration of O_2.

C_F^0 = initial concentration of fuel.

The maximum value of the rate constant can be written as

$$k_S = \left(\frac{k_B T}{2\pi M_F}\right)^{1/2} \qquad \text{(maximum value)}$$

To account for the fact that all surface collisions do not result in a reaction, the above equation can be modified to be

$$k_S = \left(\frac{k_B T}{2\pi M_F}\right)^{1/2} p\, e^{-E/kT}$$

where p takes into account a collision efficiency and E the energy barrier for the reaction.

The reaction rate for oxidation in a catalytic bed can be written as

$$Q \cdot \frac{dc_F}{dz} = -k_s\, c_F \frac{S}{V}$$

where z is the position in the direction of flow through the catalytic bed, S/V is the surface-to-volume ratio of the catalytic bed, and Q is the volumetric flow rate as defined before. The integrated form of this equation expressed in terms of the fraction of the hydrocarbon removed is

$$f = \left(1 - \frac{c}{c_0}\right) = 1 - e^{-\frac{k_s}{Q}\frac{S}{V}L}$$

where L is the length of the catalytic bed.

In the case where mass transport effects are important in the catalyst bed it is necessary to replace the catalytic rate constant with the effective or overall rate k_e given by

$$\frac{1}{k_e} = \frac{1}{k_m} + \frac{1}{k_s}$$

where k_m is the rate constant for mass transfer. The overall rate constant k_e approaches k_m in the high-temperature limit and approaches k_s, the chemical rate, at low temperatures. k_m is controlled by the geometry of the catalyst bed and the aerodynamics of the flow through the bed.

Relationships involving the Sherwood, Schmidt, and Reynolds numbers are effective for correlating data on k_m. The Sherwood number (N_{Sh}) is generally found to be a function of the Reynolds (N_{Re}) and Schmidt (N_{Sc}) numbers

$$N_{Sh} = \frac{k_m \ell}{D_i} = f(N_{Re}, N_{Sc})$$

with

$$N_{Re} = \frac{\ell G}{\mu \epsilon} \qquad N_{Sc} = \frac{\mu}{\rho_g D_i}$$

The above variables are defined below:

D_i = diffusion coefficient for component i

G = superficial mass velocity, mass/area-sec

μ = gas viscosity

ϵ = void fraction for catalyst matrix

ρ_g = gas density

ℓ = matrix length dimension usually taken as hole diameter for matrices, or effective diameter of catalytic wire or pellet.

Appropriate correlations of N_{Sh}, N_{Sc}, and N_{Re} for typical afterburner catalysts are presented in Table 9. Further details on afterburner catalysts are summarized in the article by Hawthorn.(10) The variable X used in Table 9 is basically the length between boundary layer interruptions in honeycomb matrices or the thickness of individual layers of catalyst in the bed.

TABLE 9. PROPERTIES OF AFTERBURNER CATALYSTS AND CORRELATIONS FOR MASS TRANSPORT COEFFICIENTS(10)

Catalyst Type	S/V, ft^{-1}	ϵ	ℓ, ft	X, ft	Sherwood Number Correlation
Torvex 2B (⅛-in. hexcell honeycomb)	268	0.61	0.0091	0.0833	$N_{Sh} = 3.66(1 + 0.095\, N_{Re} N_{Sc}\, \ell/X)^{0.45}$
Thermo Comb (8-c/in. honeycomb)	695	0.6	0.00345	0.167–0.333	$N_{Sh} = 2.35(1 + 0.095\, N_{Re} N_{Sc}\, \ell/X)^{0.45}$
Oxycats	36.5	0.515	0.0133	–	$N_{Sh} = 0.51\, N_{Re}^{0.56}\, N_{Sc}^{0.333}$
Metal Ribbon (D series)	336	0.93	0.004	–	$N_{Sh} = 0.55\, N_{Re}^{0.5}\, N_{Sc}^{0.333}$
Spherical Catalyst Pellets*	$\frac{6\epsilon}{d_p}$	0.35 – 0.4	d_p	–	$N_{Sh} = 2.42\, N_{Re}^{1/3}\, N_{Sc}^{1/3} + 0.129\, N_{Re}^{0.8} N_{Sc}^{0.4} + 1.4\, N_{Re}^{0.2}$

*For this case the Reynolds number is defined as $N_{Re} = d_p G/\mu$ where d_p is the diameter of spherical catalyst pellet.

Rate Data Compilations

A survey of the literature prior to and through May 1978 was made for chemical-rate data relevant to afterburner systems. Most of the available kinetic data were found to involve individual steps in complex reaction mechanisms; detail kinetic calculations can be made using the more complex kinetic mechanisms, however, these calculations generally require complicated computer modeling and are usually not necessary for afterburner applications. The data reported in this compilation emphasize mainly the global or overall reaction rates which are amenable to engineering calculations. In general, the amount of global rate data in the literature is very limited, however, there is increasing interest in expressing combustion kinetics in terms of global rate constants; hence, more data of this kind should become available in the future. When global data are not available, it is often useful to extrapolate rate constants from other data, or to use estimation procedures as described in another section of this report.

Most all the detailed data on single-step reaction rates for complex mechanisms can be found through the sources listed in Table 10. Common sources of new data as they become available can be found in the references listed in Table 11. New or updated compilations are also frequently being published by the National Bureau of Standards.(15,16)

TABLE 10. SOURCES OF REACTION RATE DATA FOR AFTERBURNERS

Author	Type of Information	Reference
NBS	General homogeneous reaction rate data	(17–21)
Trotman-Dickenson and Milne	Bimolecular reactions	(22)
Kondratiev	Covers bimolecular and termolecular rate constants reported in literature through 1969	(23)
Baulch et al.	H_2-O_2 system	(24)
Baulch et al.	H_2-N_2-O_2 system	(25)
Baulch et al.	O_2-O_3 and CO-O_2H_2 systems and sulfur containing species	(26)
Engleman	Methane-air combustion rate data	(27)
Westley	Bibliography through June 1971 on kinetics of C-O-S and H-N-O-S systems	(28)
Westley	Bibliography on N-O-NO_x systems	(29)
Hampson and Garvin	Rate data for atmospheric species	(30)
Franklin	Kinetic data on hydrocarbon oxidation	(31)
Westley	Bibliography on rates and mechanisms of hydrocarbon oxidation	(32)
Walker	Review of rate constants for hydrocarbon oxidation	(33)
Wall	Mechanisms for pyrolysis, oxidation, and burning of organics	(34)
Shtern	Mechanisms for hydrocarbon oxidation	(35)
McKay	Mechanisms and rate constants for low-temperature oxidation of hydrocarbons	(36)
Knox, Fish	Oxidation of organic compounds	(37)
Schofield	Reaction rates for H_2, O_2, N_2, H_2O, H, O, N, OH, HO_2, O_3, oxides of nitrogen, and hydrocarbons	(38)
Hampson et al.	Atmospheric species	(39)
Herron and Huie	Oxygen atom reactions with organics	(40)
Schofield	Reaction rates for small molecules and atoms involving H, O, N, C, and S	(41)
Wilson	Reaction kinetics of hydroxyl radicals	(42)
NBS	Pyrolysis, oxidation, and burning of organics	(43)
Aerospace Corporation	Compilation of experimental and estimated rate data which includes many combustion reactions	(44)
Benson and O'Neal	Rate data on unimolecular reactions	(45)
Jensen and Jones	Compilation of rate coefficients for flame reactions to 1977	(156)

TABLE 11. LITERATURE SOURCES OF CHEMICAL KINETIC RATE DATA

- Journal of Chemical Physics
- Journal of Physical Chemistry
- Journal of Physical and Chemical Reference Data
- Combustion and Flame
- International Journal of Chemical Kinetics
- Combustion Science and Technology
- Chemical Abstracts
- Journal of the American Chemical Society
- Journal of Catalysis
- Chemical Engineering Science

For completeness, information on pyrolysis and pollutant-formation reactions is also summarized in Appendices A and B.

HOMOGENEOUS OXIDATION REACTIONS

Homogeneous Oxidation Rate Data

The reactions discussed in this section are summarized in terms of global reaction rates.

CH_4. A number of investigators have reported global rate constants for CH_4.(46–50) Expressions developed by the different investigators are presented in Table 12. The equation of Dryer and Glassman is considered to be the best rate expression and is the one recommended here for afterburner applications.

C_2H_6. For ethane oxidation in the presence of excess oxygen the rate expression,

$$\frac{d[C_2H_6]}{dt} = -10^{7.18}\, e^{-32,900/RT}\, ([C_2H_6]_0 - [C_2H_6])^{0.8}$$

was obtained by Glassman, Dryer, and Cohen.(51) The temperature range over which this relationship applies is about 900 to 1050°K. A detailed 32-step mechanism for the partial oxidation of ethane is described by Geisbrecht and Daubert.(52)

Higher C_nH_{2n+2} Hydrocarbons. Flame speed and kinetic measurements indicate that oxidation rates for paraffinic hydrocarbons in the series from propane (C_3H_8) beyond decane ($C_{10}H_{22}$) are well within an order of magnitude of those of propane.(53,54)

The burning rate of propane has been measured in terms of CO_2 formation to be

$$\frac{d[C_3H_8]}{dt} = -2.9 \times 10^{10}\, e^{-15,000/RT}\, f_{O_2}^{0.35}\, f_{CO}\, f_{H_2O}^{0.4} \left(\frac{P}{RT}\right)^{1.75} \text{ moles/cm}^3\text{-sec}$$

TABLE 12. GLOBAL RATE CONSTANTS FOR CH_4 OXIDATION TO CO

Investigators	Rate Expression	Temperature Range	Reference
Nemeth and Sawyer	$\frac{d[CH_4]}{dt} = -6 \times 10^{10} [CH_4]^{-0.4} [O_2]^{1.4} e^{-57,000/RT}$ mole/cm^3-sec	>1200°K	(47)
Kozlov	$\frac{d[CH_4]}{dt} = -7 \times 10^{8} [CH_4]^{-0.5} [O_2]^{1.5} T^{-1} e^{-60,000/RT}$ mole/cm^3-sec	1200–1400°K	(48)
Williams et al.	$\frac{d[CH_4]}{dt} = -5.3 \times 10^{15} e^{-57,000/RT} f_{CH_4} f_{O_2}^{0.5} f_{H_2O}^{0.5} \left(\frac{P}{RT}\right)^2$ mole/liter-sec f = mole fraction, and P/RT is in moles/liter	1450–1750°K	(49)
Dryer and Glassman	$\frac{d[CH_4]}{dt} = -10^{13.2} e^{-48,400/RT} [CH_4]^{0.7} [O_2]^{0.8}$ mole/cm^3-sec	1100–1400°K	(50)

where f represents the mole fraction.(55) The temperature range over which the data were obtained was from about 1400 to 1800°K. Karim and Khan(56) have determined a global rate for propane from heat release data. They analyzed their data using the expression

$$m_f''' = k \, m_f^a \, m_o^b \, \rho^{(a+b)} \, e^{-E/RT} \ \mathrm{lb_m/ft^3\text{-}sec}$$

where m_f''', the rate of reaction per unit volume per unit time, is given in terms of the m_f, the fuel concentration, m_o, the oxygen concentration, and ρ, the density, all in units of lb_m/ft^3. For propane a and b were taken as unity and k and E were found to be 9×10^{13} and 60 kcal/mole, respectively, below 900°K, and 3.5×10^1 and 8 kcal/mole, respectively, above 900°K. Using the detailed chemical kinetic mechanism of Chinitz and Bauer(58) which involved 31 chemical species participating in 69 elementary reaction steps, Edelman and Fortune(54) give the overall rate expression for propane oxidation as

$$\frac{d[C_3H_8]}{dt} = -k[C_3H_8]^{0.5} [O_2]$$

where

$$k = 1.8 \times 10^9 \left[\frac{T(°K)}{1111} - 0.5\right] T^{0.5} P^{0.2} e^{-13,700/RT}$$

with P in atmospheres. The applicable temperature range is estimated to be from 800 to 3000°K. The above equation is based on the stoichiometric equation

$$C_3H_8 + \frac{3}{2}O_2 \rightarrow 4H_2 + 3CO \quad .$$

Complete combustion to CO_2 and H_2O must take into account the kinetics of the H_2 and CO reactions. A more representative expression for k,

$$k = 5.52 \times 10^8\ P^{-0.815}\ T\ e^{-12{,}200/T}$$

has been suggested by Edelman.(51,59) The above reaction rate expression has also been suggested as being applicable to the overall oxidation of hydrocarbons represented by the generalized chemical equation

$$C_aH_b + \frac{a}{2}O_2 \rightarrow \frac{b}{2}H_2 + aCO$$

with the rate given as

$$\frac{d[C_aH_b]}{dt} = -\ 5.52 \times 10^8\ P^{-0.815}\ T\ e^{-12{,}200/T}\ [C_aH_b]^{0.5}\ [O_2]\ \text{moles/cm}^3\text{-sec}$$

A general overall mechanism based on the above rate expression is given in Table 13.

Avery and Hart(53,57) developed the equation

$$\frac{d[C_4H_{10}]}{dt} = -\ [C_4H_{10}]^{3/2}\ [O_2]\ 5.4 \times 10^{13}\ e^{-21{,}000/RT}\ \text{moles/cm}^3\text{-sec}$$

for butane at a temperature in the range of 800°K.

TABLE 13. GENERAL OVERALL MECHANISM FOR COMPLETE OXIDATION OF HYDROCARBONS(60)

$$k = AT^b \exp(-E/RT)^*$$

Reaction	Forward A	Forward b	Forward E/R
$C_aH_b + \frac{a}{2}O_2 \rightarrow \frac{b}{2}H_2 + nCO$	$\frac{5.52 \times 10^8}{P^{0.825}} \cdot C_{C_aH_b}^{1/2}\ C_{O_2}$	1	12.2×10^3
$CO + OH = H + CO_2$	5.6×10^{11}	0	0.543×10^3
$OH + H_2 = H_2O + H$	2.19×10^{13}	0	2.59×10^3
$OH + OH = O + H_2O$	5.75×10^{12}	0	0.393×10^3
$O + H_2 = H + OH$	1.74×10^{13}	0	4.75×10^3
$H + O_2 = O + OH$	2.24×10^{14}	0	8.45×10^3
$M + O + H = OH + M$	1×10^{16}	0	0
$M + O + O = O_2 + M$	9.38×10^{14}	0	0
$M + H + H = H_2 + M$	5×10^{15}	0	0
$M + H + OH = H_2O + M$	1×10^{17}	0	0

*Units: cm^3/mole-sec for bimolecular reactions; cm^6/mole-sec for termolecular reactions.

Roberts et al.(61) have devised a quasi-global mechanism for the vapor-phase combustion of JP-5 fuel which they treat as C_8H_{16}. Their mechanism and rate constants, which take into account the formation of a hypothetical intermediate aldehyde (C_4H_8O), are given in Table 14. Kinetic calculations at combustion temperatures showed the aldehyde to have a negligible effect on the overall kinetics.

Nettleton(62) developed a global rate expression for hexadecane. His relationship is based on the expression

$$\frac{d[C_{16}H_{34}]}{dt} = -k\,[C_{16}H_{34}]\,[O_2]$$

where

$$k \cong 10^{14}\,e^{-13,200/T}\ \mathrm{cm^3/mole\text{-}sec.}$$

The above equation is probably applicable over the temperature range from 1000 to 2000°K.

Global rate constants for a number of organic oxidation reactions complied by Seshadri and Williams(63) are listed in Table 15. In general there is a strong similarity in the rate constants for the different species.

Hemsath and Susey(64) have made oxidation rate-constant measurements in actual thermal-type afterburner systems. Their rate constants which are presented in Table 16 are based on the equation

$$\frac{dn_{HC}}{dt} = -k\,e^{-E_A/RT}n_{HC} \quad .$$

A number of values for activation energies have been reported for various hydrocarbon oxidation reactions. Typical activation energies for the combustion of various species in air are given in Table 17. Falconer and Van Tiggelen(67) have observed a correlation between activation energies for hydrocarbon oxidation and the weakest C-H bond in the hydrocarbon. These results are summarized in Table 18 and Figure 5. For unsaturated compounds, a reaction at the multiple bond would normally control the activation energy for subsequent branching. In the case of an unsaturated hydrocarbon containing an easily abstracted hydrogen atom, as, for example, propylene, the reaction path with the lower activation energy would be expected to predominate in the chain branching. By extrapolating Figure 5, an activation energy of about 20 kcal/mole might be expected for propylene, based on a carbon-hydrogen bond strength of 77 kcal/mole in the paraffinic portion of the molecule.

Longwell and Weiss(68) in combustion experiments in a spherical reactor observed the oxidation of iso-octane to follow a temperature dependency of $\sqrt{T}\,e^{-E/RT}$ with $E = 42$ kcal/mole. Overall reaction order was about 1.8 and about 0.8 order in the iso-octane. Temperatures over which the data was obtained range from about 800 to 2500°K.

Global activation energies for reaction rates can also be obtained directly from ignition delay data. Henein(69) has determined the global activation energies of diesel No. 2, CITE (Compression-Ignition Turbine Engine), and gasoline fuels in the vapor phase to be 2920, 5790, and 8210 cal/mole, respectively. The cetane numbers for the above fuels are 57.5, 37.5, and 18, respectively, with the global activation energy increasing with a decrease in the cetane number of the fuel.

TABLE 14. HYDROCARBON OXIDATION KINETICS FOR JP-5 FUEL (C_8H_{16})(62)

C_8H_{16}	$+ O_2$	$= 2C_4H_8O$	$k_1 = 5 \times 10^7\ T^{1.5}\ e^{-7900/T}$
$2C_4H_8O$	$+ 3O_2$	$= 8CO + 8H_2$	$k_2 = 1 \times 10^{11}\ T^{4.5}$
O	$+ H_2O$	$= 2OH$	$k_3 = 5.75 \times 10^{13}\ e^{-9000/T}$
2H	+ M	$= H_2 + M$	$k_4 = 2 \times 10^{18}\ T^{-1}$
2O	+ M	$= O_2 + M$	$k_5 = 1 \times 10^{17}\ T^{-1}$
OH	+ H + M	$= H_2O + M$	$k_6 = 7 \times 10^{19}\ T^{-1}$
H	$+ O_2$	= OH + O	$k_7 = 2.24 \times 10^{14}\ e^{-8400/T}$
O	$+ H_2$	= OH + H	$k_8 = 1.74 \times 10^{13}\ e^{-4730/T}$
CO	+ OH	$= CO_2 + H$	$k_9 = 5.6 \times 10^{11}\ e^{-540/T}$
H	$+ H_2O$	$= OH + H_2$	$k_{10} = 8.41 \times 10^{13}\ e^{-10050/T}$

Units: cm^3/mole-sec.

TABLE 15. RATE CONSTANTS FOR OXIDATION OF MISCELLANEOUS ORGANIC COMPOUNDS(64)

Hydrocarbon Vapor	Chemical Formula	Activation Energy, kcal/mole	Preexponential Factor, cm^3/mole-sec
Isopropyl ether	$[(CH_3)_2CH]_2O$	50	1.2×10^{17}
Butyl-vinyl ether	$CH_3(CH_2)_3OCH{:}CH_2$	31	5.0×10^{14}
Methyl methacrylate	$C_5H_8O_2$	37	2.4×10^{15}
Polymethyl methacrylate	$(C_5H_8O_2)_n$	42	7.6×10^{15}
Methanol	CH_3OH	40	4.6×10^{15}
Heptane	C_7H_{16}	38	2.2×10^{15}
Decane	$C_{10}H_{22}$	37	1.6×10^{15}
Hexadecane	$C_{16}H_{34}$	35	8.2×10^{14}
Iso-octane	C_8H_{18}	35	4.5×10^{14}
Kerosene	$C_{10}H_{20}$ (approx.)	35	5.4×10^{14}

TABLE 16. RATE CONSTANTS MEASURED IN THERMAL AFTERBURNER SYSTEM(64)

Compound	Preexponential Constant, k, sec^{-1}	Activation Energy, E_A, kcal/mole
Hexane	4.5×10^{12}	52.5
Cyclohexane	5.13×10^{12}	47.6
Natural gas	1.65×10^{12}	49.3

TABLE 17. ACTIVATION ENERGIES (KCAL/MOLE) FOR COMBUSTION IN AIR(65,66)

Vapor	$E_{activation}$	Vapor	$E_{activation}$	Vapor	$E_{activation}$
Acetal	42.0	*trans*-Decalin	47.4	Methyl acetate	34.8
Acetaldehyde	45.4	*n*-Decyl alcohol	51.7	Methyl alcohol	41.3
Acetone	55.0	Diacetone alcohol	35.6	Methylcyclopentane	43.3
Acetonitrile	45.8	Diacetyl	42.0	Methylene chloride	41.9
Acetonyl acetone	48.9	Dichloroethylene	25.9	Methylethyl ketone	49.3
Acetylene (0.9 atm)	31	2,2-Dichloroethyl ether	42.5	Methyl formate	30.7
Acrolein	35.5	Diethanolamine	40.4	Methylpropyl ketone	48.2
Allyl alcohol	39.6	Diethylamine	37.0	Monoethanolamine	32.3
Allyl ether	32.8	Diethylaniline	41.1	Monoisopropylxylenes	36.6
Amyl acetate	37.2	Diethyl ether	52.5		
n-Amyl alcohol	48.0	Di-*iso*butylenes	36.8	Nitrobenzene	40.7
*iso*Amyl alcohol	48.5	Di-*iso*propyl ether	43.0	Nitroethane	42.6
tert-Amyl alcohol	48.5	Dimethylaniline	45.0	Nitromethane	39.2
Amyl nitrate	19.7	Dioxan	50.5	o-Nitrotoluene	39.3
Amyl nitrite	17.1	*iso*Dodecane	51.0	*m*-Nitrotoluene	36.4
*iso*Amyl nitrite	23.6				
Aniline	48.0	Ethane	49	*iso*Octane	32.4
o-Anisidine	35.5	Ethyl acetate	35.8		
Anisole	30.8	Ethyl alcohol (methylated spirits)	42.2	Paraldehyde	45.0
		Ethylbenzene	45.7	40–60° Petroleum ether	45.2
Benzaldehyde	40.0	Ethyl bromide	42.0	80–100° Petroleum ether	44.8
Benzene	47.2	Ethyl carbonate	38.4	(aromatic free)	
Benzyl acetate	36.2	Ethyleneglycolmonobutylether	48.8	100–120° Petroleum ether	42.3
Benzyl alcohol	44.0	Ethyleneglycolmonoethylether	49.7	(aromatic free)	
Bromobenzene	49.5	Ethyleneglycolmonoethylether-	44.6	*p*-Phenetidine	49.1
Buta gas	50	monoacetate		α-Picoline	39.3
n-Butyl acetate	36.5	Ethyleneglycolmonomethylether	52.6	Pinene	38.0
n-Butyl alcohol	48.4	Ethyl formate	44.0	*n*-Propyl acetate	32.3
*iso*Butyl alcohol	40.0	Ethyl nitrate	25.5	*n*-Propyl alcohol	45.3
sec-Butyl alcohol	56.4	Ethyl nitrite	23.8	*iso*Propyl alcohol	37.8
tert-Butylbenzene	39.4	Ethyl oxalate	41.0	Propylene dichloride	31.8
n-Butyl nitrite	16.5			Propylene oxide	46.4
Butyl phthalate	43.4	Formamide	40.7	Pyridine	31.7
		Furan	43.4		
Calor gas	52	Furfuraldehyde	37.0	Salicylic aldehyde	36.0
Carbon disulphide	27.2	Furfuryl alcohol	47.9	Styrene	31.8
Carbon monoxide	78				
Cetene	30.8	*n*Heptane	60.5	Tetrahydrofurfuryl alcohol	45.4
o-Chloroaniline	35.9	*n*-Hexane	50.7	Tetrahydrosylvan	38.9
m-Chloroaniline	33.9	*n*-Hexyl alcohol	50.8	Tetralin	42.5
m-Cresol	30.9	*iso*Hexyl alcohol	50.5	Tetramethylbenzene	37.7
Crotonaldehyde	33.6	Hydrogen (0.9 atm)	57	Toluene	41.0
Cumene	46.7			o-Toluidine	30.4
pseudo-Cumene	26.9	Kerosine	46	*m*-Toluidine	33.9
*cyclo*Hexane	46.4			Trichloroethylene	35.2
*cyclo*Hexanol	41.7	Ligroin	36.2	Tri-*iso*butylenes	34.8
*cyclo*Hexanone	40.0			Turpentine	40.6
*cyclo*Hexene	43.2	Mesityl oxide	42.7		
p-Cymene	38.1	Methane	29	Xylene	34.3

TABLE 18. ACTIVATION ENERGIES FOR HYDROCARBON–OXYGEN FLAMES(67)

Hydrocarbon	Weakest C–H Bond, kcal/mole^{-1}	Activation Energy, kcal/mole^{-1}
Methane	103.9	38, 40, 41
Ethane	98.3	39
Neopentane	99.3	38.3
n-Butane	94.6	33
Isobutane	91.4	30.5
Diethyl ether	95–100	38.5
Benzene	101.8	40
Ethylene	102.5, 105	36
Acetylene	121	32
Hydrogen sulfide	90	26

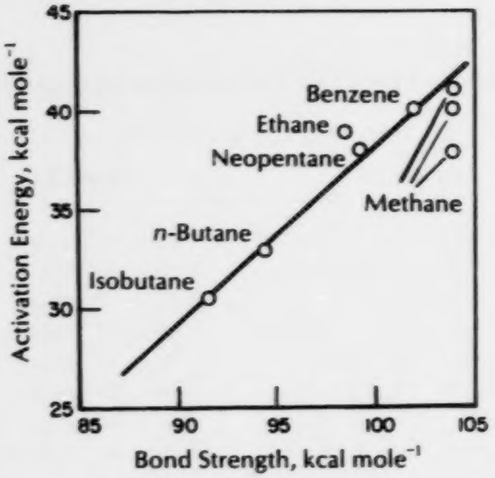

FIGURE 5. DEPENDENCE OF ACTIVATION ENERGY UPON BOND STRENGTH OF WEAKEST C–H BOND(67)

Unsaturated Hydrocarbons. Very few global rate data exist for the oxidation of unsaturated hydrocarbons. Details on the mechanisms of olefin oxidation mechanisms can be found in articles by Bolland(70), Bateman(71), and McKeon et al.(72). Detailed mechanisms along with the associated rate constants have been presented by Jackimowski(73) for the oxidation of C_2H_4 and C_2H_2. These mechanisms are summarized in Tables 19 and 20. An activation energy of E_A= 18,030 cal/mole was observed for C_2H_2 while a value of 34,250 cal/mole was observed for C_2H_4. A more abbreviated mechanism than given for C_2H_2 in Table 20 has been suggested by Shaub and Bauer.(157) Peeters and Mahnen(74) have observed an oxidation rate of 10^{-4} mole/cm^3-sec for C_2H_4 in a lean flame at a temperature of 1520°K. Levy and Weinberg(75,76) have determined the activation energy for C_2H_4 oxidation to be about 36 kcal/mole at 1250°K increasing to about 40 kcal/mole at higher temperatures. Induction time measurements by White(77) showed activation energies of about 39.8 kcal/mole for C_2H_4, C_2H_2, and H_2. Suzuki et at.(78) have observed that in the temperature range from about 1000 to 1315°K the activation energy is a function of the $[O_2]/[C_2H_4]$ ratio. Their results are summarized in Figure 6. Recent information on the modeling of the combustion of C_2H_2 and C_2H_4 has been reported by White and Gardiner.(163)

The only data found for the higher alkenes and alkynes were for low-temperature oxidation and are not applicable to the higher temperature afterburner conditions.

Aromatics. Global rate data for the oxidation of toluene based on the first-order equation

$$\frac{dn_{HC}}{dt} = -k\, e^{-E_A/RT}\, n_{HC}$$

are presented in Table 21. The values for benzene given in the table are based on second-order kinetics.

TABLE 19. ETHYLENE OXIDATION MECHANISM(73)

	Reaction	Rate Coefficient*
1.	$C_2H_4 + M \rightarrow C_2H_3 + H + M$	1.00×10^{14} exp (−109000/RT)
2.	$C_2H_4 + C_2H_4 \rightarrow C_2H_5 + C_2H_3$	5.00×10^{14} exp (−64700/RT)
3.	$C_2H_5 \rightarrow C_2H_4 + H$	3.16×10^{13} exp (−40700/RT)
4.	$C_2H_3 + M \rightarrow C_2H_2 + H + M$	7.94×10^{14} exp (−31500/RT)
5.	$H + C_2H_4 \rightarrow C_2H_3 + H_2$	1.10×10^{14} exp (−85000/RT)
6.	$OH + C_2H_4 \rightarrow C_2H_3 + H_2O$	1.00×10^{14} exp (−3500/RT)
7.	$O + C_2H_4 \rightarrow CH_2O + CH_2$	2.50×10^{13} exp (−5000/RT)
8.	$O + C_2H_4 \rightarrow CH_3 + HCO$	2.26×10^{13} exp (−2700/RT)
9.	$CH_2O + OH \rightarrow HCO + H_2O$	2.30×10^{13}
10.	$CH_2O + H \rightarrow HCO + H_2$	2.00×10^{13}
11.	$CH_2O + O \rightarrow HCO + OH$	2.00×10^{13}

*Units: cm, °K, cal, mole, sec.

TABLE 20. ACETYLENE OXIDATION MECHANISM(73)

	Reaction	Rate Coefficient*
1.	$C_2H_2 + M \rightarrow C_2H + H + M$	$1.00 \times 10^{14} \exp(-114000/RT)$
2.	$C_2H_2 + O_2 \rightarrow HCO + HCO$	$1.00 \times 10^{14} \exp(-38000/RT)$
3.	$H + C_2H_2 \rightarrow C_2H + H_2$	$2.00 \times 10^{14} \exp(-19000/RT)$
4.	$OH + C_2H_2 \rightarrow C_2H + H_2O$	$6.00 \times 10^{12} \exp(-7000/RT)$
5.	$O + C_2H_2 \rightarrow C_2H + OH$	$3.20 \times 10^{15}\, T^{-0.6} \exp(-17000/RT)$
6.	$O + C_2H_2 \rightarrow CH_2 + CO$	$5.20 \times 10^{13} \exp(-3700/RT)$
7.	$C_2H + O_2 \rightarrow HCO + CO$	$1.00 \times 10^{13} \exp(-7000/RT)$
8.	$C_2H + O \rightarrow CO + OH$	5.00×10^{13}
9.	$CH_2 + O_2 \rightarrow HCO + OH$	$1.00 \times 10^{14} \exp(-3700/RT)$
10.	$CH_2 + O \rightarrow CH + OH$	$1.90 \times 10^{11}\, T^{0.68} \exp(-25000/RT)$
11.	$CH_2 + H \rightarrow CH + H_2$	$2.70 \times 10^{11}\, T^{0.67} \exp(-25700/RT)$
12.	$CH_2 + OH \rightarrow CH + H_2O$	Obtained from $k_{12} = k_{11}$
13.	$CH + O_2 \rightarrow CO + OH$	Obtained from $k_{13} = 0.5\, k_{11}$
14.	$CH + O_2 \rightarrow HCO + O$	1.00×10^{13}
15.	$HCO + OH \rightarrow CO + H_2O$	1.00×10^{14}
16.	$HCO + H \rightarrow CO + H_2$	1.00×10^{14}
17.	$HCO + O \rightarrow CO + OH$	1.26×10^{14}
18.	$HCO + M \rightarrow H + CO + M$	$7.00 \times 10^{13} \exp(-15000/RT)$
19.	$CO + OH \rightarrow CO_2 + H$	$4.00 \times 10^{12} \exp(-8000/RT)$
20.	$CO + O + M \rightarrow CO_2 + M$	6.00×10^{13}
21.	$OH + H_2 \rightarrow H_2O + H$	$5.20 \times 10^{13} \exp(-6500/RT)$
22.	$H + O_2 \rightarrow OH + O$	$1.22 \times 10^{17}\, T^{-0.907} \exp(-16630/RT)$
23.	$O + H_2 \rightarrow OH + H$	$2.07 \times 10^{14} \exp(-13750/RT)$
24.	$OH + OH \rightarrow H_2O + O$	$5.5 \times 10^{13} \exp(-7000/RT)$
25.	$O_2 + M \rightarrow 2O + M$	$2.55 \times 10^{18}\, T^{-1.0} \exp(-18700/RT)$
26.	$H + H + M \rightarrow H_2 + M$	1.00×10^{15}
27.	$H + OH + M \rightarrow H_2O + M$	$8.40 \times 10^{21}\, T^{-2.0}$

*Units: cm, °K, cal, mole, sec.

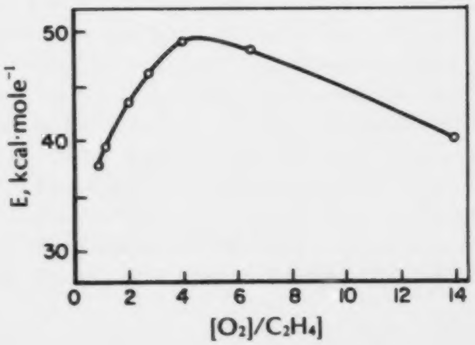

FIGURE 6. ACTIVATION ENERGY FOR C_2H_4 OXIDATION FROM 1000 TO 1315°K(78)

TABLE 21. GLOBAL RATE DATA FOR THE OXIDATION OF AROMATICS

Compound	Preexponential Term, A	Activation Energy, E_A, kcal/mole	Reference
Benzene	6.0×10^{14} cm^3/mole-sec	36	(63)
Toluene	6.56×10^{13} sec^{-1}	58.5	(64)

CO. A number of investigators have determined global rate constants for CO oxidation. The important CO oxidation reaction is

$$CO + OH \rightarrow CO_2 + H$$

with the direct oxidation reaction

$$CO + O_2 \rightarrow CO_2 + O$$

being very slow: hence, CO is quite difficult to oxidize in the absence of water.

Rolke et al.(1) and Williams et al.(79) have reviewed the early global rate data for CO oxidation. Selected results and more recent data are summarized in Table 22. A marked variation is observed in the different rate constants. The only actual afterburner rate data for CO are those by Hemsath and Susey.(64) These latter results are recommended for afterburner design applications.

H_2. A global rate for H_2 oxidation in air has been given as(66)

$$\frac{d[H_2]}{dt} = -1.6 = 10^{12} e^{-15{,}000/RT} [H_2] [O_2]^{1.17} \text{ mole/cm}^3\text{-sec}$$

A more detailed mechanism has been suggested by Bowman.(81) This mechanism is summarized in Table 23.

Another detailed mechanism has been suggested by Jenkins, Yumlu, and Spalding(82) for the temperature range from 1330 to 1560°K. The reaction mechanism is given in Table 24 and the reaction rate data are given in Table 25. Several conclusions were drawn regarding this reaction scheme by comparing theoretical modeling calculations with the performance characteristics of a steady-flow adiabatic stirred reaction. In the reaction scheme presented in Table 24, reactions 1, 4, and 7 are probably unimportant under all conditions. Reactions 2 and 5 are important only for near-stoichiometric mixtures. Reaction 9 is important for nearly all conditions and reaction 3 is important for all but the very low equivalence ratio values.* Reaction 6 is important only for large values of the equivalence ratio. Reaction 8 is unimportant for near-stoichiometric mixtures but even less important for very rich or very lean mixtures.

---

*Equivalence ratio is defined as $\phi = \frac{(\text{fuel/air})_{\text{actual}}}{(\text{fuel/air})_{\text{stoichiometric}}}$. $\phi > 1$ is fuel rich, $\phi = 1$ is stoichiometric and $\phi < 1$ is fuel lean. Fuel and air concentrations in moles.

TABLE 22. GLOBAL RATE CONSTANTS FOR CO OXIDATION

Investigators	Rate Expression, mole/cm^3-sec	Temperature Range	References
Williams, Hottel, and Morgan	$\frac{d\,[CO]}{dt} = -1.8 \times 10^7\ e^{-25{,}000/RT}\ f_{CO}\ f_{O_2}^{0.5}\ f_{H_2O}^{0.5}\ (P/RT)^2$	1450–1750°K	(49)
Howard, Williams, and Fine	$\frac{d\,[CO]}{dt} = -1.3 \times 10^{14}\ [CO]\ [O_2]^{1/2}\ [H_2O]^{1/2}\ e^{-30{,}000/RT}$	840–2360°K	(80)
Dryer and Glassman	$\frac{d\,[CO]}{dt} = -3.9 \times 10^{14}\ e^{-40{,}000/RT}\ [CO]^{1.0}\ [H_2O]^{0.5}\ [O_2]^{0.25}$	1030–1230°K	(50)
Hottel, Williams, Nerheim and Schneider	$\frac{d\,[CO]}{dt} = -1.2 \times 10^{11}\ e^{-16{,}000/RT}\ f_{O_2}^{0.3}\ f_{CO}\ f_{H_2O}^{0.5}\ (P/RT)^{1.8}$	1250–1550°K	(55)
Hemsath and Susey	$\frac{d\,f_{CO}}{dt} = -10^{23}\ e^{-100{,}000/RT}\ f_{CO}\ f_{O_2}^{0.5}\ sec^{-1}$	<1400°F (1033°K)	(64)
	$\frac{d\,f_{CO}}{dt} = -2.5 \times 10^{11}\ e^{-40{,}000/RT}\ f_{CO}\ f_{O_2}^{0.5}\ sec^{-1}$	>1400°F (1033°K)	(64)

All concentrations [ ] in mole/cm^3. f is the mole fraction.

TABLE 23. HYDROGEN-OXYGEN REACTION MECHANISM(81)

Reaction	Rate constant, k_f*
$H_2 + O_2 \leftrightarrow 2OH$	$2.5 \times 10^{12} \exp(-19650/T)$
$H + O_2 \leftrightarrow OH + O$	$2.2 \times 10^{11} \exp(-8450/T)$
$O + H_2 \leftrightarrow OH + H$	$1.7 \times 10^{13} \exp(-4760/T)$
$H + H_2O \leftrightarrow H_2 + OH$	$8.4 \times 10^{13} \exp(-10100/T)$
$O + H_2O \leftrightarrow 2OH$	$5.8 \times 10^{13} \exp(-9070/T)$
$H + H + \begin{bmatrix} Ar \\ N_2 \end{bmatrix} \leftrightarrow H_2 + \begin{bmatrix} Ar \\ N_2 \end{bmatrix}$	$\begin{bmatrix} 1.0 \\ 1.5 \end{bmatrix} \times 10^{18} T^{-1.0}$
$O + O + \begin{bmatrix} Ar \\ N_2 \end{bmatrix} \leftrightarrow O_2 + \begin{bmatrix} Ar \\ N_2 \end{bmatrix}$	$\begin{bmatrix} 3.0 \\ 4.0 \end{bmatrix} \times 10^{17} T^{-1.0}$
$H + OH + \begin{bmatrix} Ar \\ N_2 \\ H_2O \end{bmatrix} \leftrightarrow H_2O + \begin{bmatrix} Ar \\ N_2 \\ H_2O \end{bmatrix}$	$\begin{bmatrix} 0.2 \\ 0.4 \\ 4.0 \end{bmatrix} \times 10^{20} T^{-1.0}$
$H + O_2 + \begin{bmatrix} Ar \\ N_2 \end{bmatrix} \leftrightarrow HO_2 + \begin{bmatrix} Ar \\ N_2 \end{bmatrix}$	$\begin{bmatrix} 1.6 \\ 3.0 \end{bmatrix} \times 10^{15} \exp(504/T)$

*Units: cm, mole, sec, °K, cal.

TABLE 24. REACTION SCHEME FOR COMBUSTION OF HYDROGEN AND OXYGEN(82)

Reaction Number	Reaction
1	$H_2 + O_2 = 2OH$
2	$H_2 + OH = H_2O + H$
3	$O_2 + H = O + OH$
4	$H_2 + O = H + OH$
5	$H_2O + O = 2OH$
6	$H + H + M = H_2 + M$
7	$O + O + M = O_2 + M$
8	$H + O + M = OH + M$
9	$H + OH + M = H_2O + M$

TABLE 25. REACTION RATE CONSTANTS FOR COMBUSTION OF HYDROGEN AND OXYGEN(82)

$(k_i = A_j e^{-E_j/RT})$

Reaction j	A_j	E_j, kcal/mole	A_{-j}	E_{-j}, kcal/mole
1	8.0×10^{14}	45.0	2.0×10^{13}	25.0
2	2.2×10^{14}	10.3	1.1×10^{15}	25.49
3	1.9×10^{14}	17.9	1.34×10^{13}	1.838
4	2.25×10^{12}	7.75	9.8×10^{11}	5.88
5	8.3×10^{13}	18.1	7.6×10^{12}	1.0
6	$5.0 \times 10^{18} T^{-1.15}$	0	3.7×10^{14}	97.36
7	$4.7 \times 10^{15} T^{-0.23}$	0	5.1×10^{15}	115.0
8	5.3×10^{15}	−2.78	3.6×10^{16}	96.37
9	1.2×10^{17}	0.5	9.2×10^{17}	117.73

Units of A_j are cm^3, mole, sec.

Oxygenated Organics. Except for some simple aldehydes no global rate data are available for oxygenated compounds such as alcohols, aldehydes, and ketones. Information on detailed reaction mechanisms for these classes of compounds and associated rate constants have been summarized by Dixon, Skirrow, and Barnard.(4)

Aldehydes are often observed as intermediates in combustion processes. All aldehydes except formaldehyde are generally found to promote combustion, however, it is doubtful that the aldehydes are kinetically important intermediates in terms of contributing to chain branching in hydrocarbon combustion.(83) The combustion characteristics of the saturated aldehydes differ from those of the hydrocarbons in that their ease of oxidation does not generally increase with increasing molecular size. For example, of the first five straight-chain homologues, formaldehyde is the least reactive while acetaldehyde is the most reactive, and n-butyraldehyde is less reactive than propionaldehyde while n-valderaldehyde is more reactive. In general, most aldehydes are far more reactive than the corresponding hydrocarbon. The fact that formaldehyde is exceptionally resistant to oxidation despite a weak C−H bond is attributed to the stability of the formyl (HCO) radical. The bond dissociation energy for the HCO radical is much higher than that in the CH_3CO radical. The large amounts of CO formed during the early stages of acetaldehyde oxidation are attributed to the low bond dissociation energy of the acetyl radical. The fact that smaller amounts of CO are produced from propionaldehyde and higher aldehydes indicate that the higher carbonyl radicals are thermally more stable than the acetyl radicals. Unsaturated aldehydes usually cause a marked inhibition in the early stages of reaction and an equally marked promotion in later stages. The promoting effect increases with temperature and eventually is much greater than that of the saturated analogs.

Most formaldehyde rate studies have been conducted under conditions where wall effects are important. A reaction scheme suggested for the high-temperature (~850°K) oxidation in vessels coated with boric acid, $K_2B_4O_7$, KCl, and KBr is presented in Table 26.

TABLE 26. HIGH-TEMPERATURE MECHANISM FOR FORMALDEHYDE OXIDATION[84]

Reaction	Rate Constant, cm^3/molecule-sec
$CH_2O + O_2 = HCO + HO_2$	7.5×10^{-11} exp (−41,000/RT)
$HCO + O_2 = HO_2 + CO$	10^{-13}
$HO_2 + CH_2O = H_2O_2 + HCO$	1.9×10^{-11} exp (−11,000/RT)
$H_2O_2 + M = 2OH + M$	2.83×10^{-7} exp (−46,300/RT)
$OH + CH_2O = H_2O + HCO$	1.6×10^{-10}
$OH + H_2O_2 = HO_2 + H_2O$	1.6×10^{-11}
$HO_2 + HO_2 = H_2O_2 + O_2$	3×10^{-12}
$H_2O_2 \xrightarrow{\text{wall}}$ chain termination	10.5 sec^{-1}
$HO_2 \xrightarrow{\text{wall}}$ chain termination	10.5 sec^{-1}

Baldwin, Matchon and Walker[85] have derived a simple rate equation for the oxidation of acetaldehyde:

$$\frac{d[CH_3CHO]}{dt} = k_9 \left(\frac{k_1}{k_{10}}\right)^{1/2} [CH_3CHO]^{3/2} [O_2]^{1/2} .$$

The above rate constants are associated with the following reactions:

$$CH_3CHO + O_2 = CH_3CO + HO_2 \tag{1}$$

$$CH_3 + CH_3CHO = CH_4 + CH_3CO \tag{9}$$

$$CH_3 + CH_3 + M = C_2H_6 + M \tag{10}$$

Rate constant values are given in Table 27. The above reaction orders are in fairly good agreement with the average experimental values of 1.5 and 0.7 for CH_3CHO and O_2, respectively, however, the mechanism is not detailed enough to account for the distribution of oxidation

TABLE 27. RATE CONSTANTS FOR SIMPLE MECHANISM FOR ACETALDEHYDE OXIDATION[85]

	Rate Constant, liter/mole-sec	
Reaction	440°C	540°C
(1)	0.076	4.0
(9)	6.0×10^6	9.7×10^6
(10)	1.09×10^{10}	8.4×10^9

products. Around 540°C, CH_4 is a major product and significant yields of C_2H_6, H_2, and CH_3OH occur while at 440°C only minor yields of CH_4 and C_2H_6 are produced. A detailed mechanism for CH_3CHO combustion has been suggested by Beeley, Griffiths, Hunt, and Williams.(86) The reaction mechanism and kinetic data for the temperature, which range from about 1500 to 1850°K, are presented in Table 28. A global expression for the overall disappearance of acetaldehyde has been given by Colket, Naegeli, and Glassman(87) as

TABLE 28. REACTION MECHANISM AND KINETIC DATA(86)

	Reaction		Rate Constant, $cm^3\ mole^{-1}\ s^{-1}$, unless stated Activation Energies, $kJ\ mole^{-1}$
1	CH_3CHO	$\rightarrow CH_3 + CHO$	$4 \times 10^{14} \exp(-333.5/RT)\ s^{-1}$
2	CH_3CHO	$\rightarrow CH_3CO + H$	$5 \times 10^{14} \exp(-367.8/RT)\ s^{-1}$
3	$CH_3CHO + O_2$	$\rightarrow CH_3CO + H_2$	$10^{12} \exp(-175.56/RT)$
4	$CH_3CHO + CH_3$	$\rightarrow CH_3CO + CH_4$	$1.7 \times 10^{12} \exp(-35.28/RT)$
5	$CH_3CHO + O$	$\rightarrow CH_3CO + OH$	$10^{13} \exp(-16.72/RT)$
6	$CH_3CHO + OH$	$\rightarrow CH_3CO + H_2O$	$5.25 \times 10^{13} \exp(-9.99/RT)$
7	$CH_3CHO + H$	$\rightarrow CH_3CO + H_2$	$8.7 \times 10^{13} \exp(-28.97/RT)$
8	CH_3CO	$\rightarrow CH_3 + CO$	$2 \times 10^{10} \exp(-62.7/RT)\ s^{-1}$
9	$CH_3 + O_2$	$\rightarrow CH_2O + OH$	$1.2 \times 10^{11} \exp(-41.38/RT)$
10	$CH_3 + O$	$\rightarrow CH_2O + H$	2×10^{13}
11	$CH_3 + H$	$\rightarrow CH_4$	$1.17 \times 10^{12} \exp(-0.2/RT)$
12	$CH_4 + O$	$\rightarrow CH_3 + OH$	$2.0 \times 10^{13} \exp(-9.0/RT)$
13	$CH_4 + OH$	$\rightarrow CH_3 + H_2O$	$3.2 \times 10^{13} \exp(-5.0/RT)$
14	$CH_3 + CH_3 + M$	$\rightarrow C_2H_6 + M$	$1.54 \times 10^{12}\ T^{1/2} \times$ RRKM factor $cm^6\ mole^{-2}\ s^{-1}$
15	$C_2H_6 + M$	$\rightarrow 2CH_3 + M$	$3.2 \times 10^{16} \exp(-367.8/RT) \times$ RRKM factor
16	$C_2H_6 + OH$	$\rightarrow C_2H_4 + H + H_2O$	$6.5 \times 10^{13} \exp(-5.6/RT)$
17	$C_2H_4 + O$	$\rightarrow CH_3 + CHO$	$2.3 \times 10^{13} \exp(-2.7/RT)$
18	CH_2O	$\rightarrow CHO + H$	$10^{12} \exp(-171.6/RT)\ s^{-1}$
19	$CH_2O + O$	$\rightarrow CHO + OH$	$5 \times 10^{13} \exp(-12.54/RT)$
20	$CH_2O + OH$	$\rightarrow CHO + H_2O$	$3.1 \times 10^{14} \exp(-17.72/RT)$
21	$CH_2O + H$	$\rightarrow CHO + H_2$	$6 \times 10^{13} \exp(-19.35/RT)$
22	$CH_2O + CH_3$	$\rightarrow CHO + CH_4$	$2.2 \times 10^{13} \exp(-21.53/RT)$
23	$CHO + O_2$	$\rightarrow CO + HO_2$	$4.2 \times 10^{13} \exp(-30.09/RT)$
24	CHO	$\rightarrow CO + H$	$7 \times 10^{13} \exp(-79.5/RT)\ s^{-1}$
25	$CHO + O$	$\rightarrow CO + OH$	1×10^{13}
26	$CHO + OH$	$\rightarrow CO + H_2O$	3×10^{13}
27	$H + O_2$	$\rightarrow OH + O$	$2.2 \times 10^{14} \exp(-70.22/RT)$
28	$O + H_2$	$\rightarrow OH + H$	$1.8 \times 10^{10}\ T \exp(-35.97/RT)$
29	$OH + H_2$	$\rightarrow H + H_2O$	$2.2 \times 10^{13} \exp(-21.53/RT)$
30	$H + O_2 + M$	$\rightarrow HO_2 + M$	$1.5 \times 10^{15} \exp(+4.16/RT)$
31	$OH + OH$	$\rightarrow O + H_2O$	$2 \times 10^{14} \exp(-9.20/RT)$
32	$H + H + M$	$\rightarrow H_2 + M$	$6.4 \times 10^{17}\ T^{-1}\ cm^6\ mole^{-2}\ s^{-1}$
33	$H + HO_2$	$\rightarrow OH + OH$	$2 \times 10^{14} \exp(-9.20/RT)$
34	$OH + CO$	$\rightarrow H + CO_2$	$5.6 \times 10^{11} \exp(-4.51/RT)$
35	$HO_2 + CO$	$\rightarrow OH + CO_2$	$2 \times 10^{14} \exp(-96.14/RT)$

$$\frac{d[CH_3CHO]}{dt} = -2\gamma\,[CH_3CHO] + k_4 \left(\frac{\gamma}{k_6}\right)^{1/2} [CH_3CHO]^{3/2}$$

where $\gamma = k_1 + 2k_{23}\,[O_2]$. When $[O_2]$ is zero, the above expression reduces to the rate expression for pyrolysis. The rate constants for the above reactions along with those for a more comprehensive mechanism are tabulated in Table 29.

Methanol is more resistant to oxidation than formaldehyde. Outside of the global rate data listed for methanol in Table 15, no information was located for other alcohols. A detailed mechanism for methanol oxidation proposed by Bowman(88) is tabulated in Table 30.

TABLE 29. REACTION MECHANISM AND RATE CONSTANTS(a) FOR THE OXIDATION OF ACETALDEHYDE(87)

No.	Elementary Reaction	Log_{10} A	n	E, kcal/mole
1	$CH_3CHO \rightarrow CH_3 + CHO$	15.85	0	81.755
2	$HCO + M \rightarrow H + CO + M$	12.3	0.5	28.8
2a	$HCO + O_2 \rightarrow HO_2 + CO$	13.7	0	1.6
3	$H + CH_3CHO \rightarrow H_2 + CH_3CO$	−4.23	5.6	−1.36
4	$CH_3 + CH_3CHO \rightarrow CH_4 + CH_3CO$	−7.22	6.1	1.72
4a	$CH_3 + CH_3CHO \rightarrow CH_4 + CH_2CHO$	−0.26	4.0	8.28
5	$CH_3CO \rightarrow CH_3 + CO$	13.5	0	17.24
6	$CH_3 + CH_3 \rightarrow C_2H_6$	13.34	0	0
7	$CH_3 + C_2H_6 \rightarrow CH_4 + C_2H_5$	−0.26	4.0	8.28
8	$H + C_2H_6 \rightarrow H_2 + C_2H_5$	2.73	3.5	5.2
9	$C_2H_5 \rightarrow H + C_2H_4$	13.58	0	38.0
10	$CH_2CHO \rightarrow H + CH_2CO$	13.2	0	35.0
23	$O_2 + CH_3CHO \rightarrow HO_2 + CH_3CO$	13.3	0.5	42.2
28	$CH_3O \rightarrow H + H_2CO$	13.95	0	30.0
29	$H + O_2 \rightarrow OH + O$	14.35	0	16.8
30	$H + O_2 + M \rightarrow HO_2 + M$	15.5	0	−1.0
32	$H_2O_2 + M \rightarrow 2OH + M$	17.07	0	45.5
33	$HO_2 + CH_3CHO \rightarrow H_2O_2 + CH_3CO$	12.23	0	10.7
34	$OH + CH_3CHO \rightarrow H_2O + CH_3CO$	14.51	0	4.24
36	$CO + OH \rightarrow CO_2 + H$	3.37	2.45	−2.18
38	$HO_2 + HO_2 \rightarrow H_2O_2 + O_2$	13.0	0	1.0
39	$HO_2 + CH_3 \rightarrow CH_3O + OH$	13.3	0	0.0
39a	$HO_2 + CH_3 \rightarrow CH_4 + O_2$	12.3	0	0.0
40	$CH_3 + H_2CO \rightarrow CH_4 + HCO$	−7.22	6.1	1.72
41	$O + CH_3HCO \rightarrow OH + CH_3CO$	13.03	0	2.3
42	$CO + HO_2 \rightarrow CO_2 + OH$	14	0	23

(a) Expressed as $k = AT^n e^{-E/RT}$ where A is in units of cm^3, moles, sec; E in cal/mole and T in degrees K.

TABLE 30. METHANOL OXIDATION MECHANISM[88]

Reaction	Rate Coefficient, k
$CH_3OH + (M) \rightarrow CH_3 + OH + (M)$	$4 \times 10^{15} \exp(-34{,}200/T)$
$CH_3 + CH_3OH \rightarrow CH_2OH + CH_4$	$1.8 \times 10^{11} \exp(-4940/T)$
$O + CH_3OH \rightarrow CH_2OH + OH$	$1.7 \times 10^{12} \exp(-1150/T)$
$H + CH_3OH \rightarrow CH_3 + H_2O$	$1.3 \times 10^{13} \exp(-2670/T)$
$OH + CH_3OH \rightarrow CH_2OH + H_2O$	$3.0 \times 10^{13} \exp(-3000/T)$
$CH_2OH + O_2 \rightarrow CH_2O + HO_2$	5×10^{10}
$CH_2OH \rightarrow CH_2O + H$	$3 \times 10^{9} \exp(-14600/T)$
$CH_4 + OH \rightarrow CH_3 + H_2O$	$6 \times 10^{14} \exp(-6290/T)$
$CH_4 + H \rightarrow CH_3 + H_2$	$2.24 \times 10^{4}\, T^{3} \exp(-4400/T)$
$CH_4 + O \rightarrow CH_3 + OH$	$2.1 \times 10^{13} \exp(-4560/T)$
$CH_3 + O \rightarrow CH_2O + H$	1×10^{14}
$CH_3 + O_2 \rightarrow CH_2O + OH$	$1.2 \times 10^{11} \exp(-5000/T)$
$CH_2O + OH \rightarrow CHO + H_2O$	$5.4 \times 10^{14} \exp(-3170/T)$
$CH_2O + H \rightarrow CHO + H_2$	$1.35 \times 10^{13} \exp(-1890/T)$
$CH_2O + O \rightarrow CHO + OH$	$5 \times 10^{13} \exp(-2300/T)$
$CH_2O + M \rightarrow CHO + H + M$	$1 \times 10^{14} \exp(-18500/T)$
$CHO + OH \rightarrow CO + H_2O$	1×10^{14}
$CHO + H \rightarrow CO + H_2$	2×10^{14}
$CHO + O \rightarrow CO + OH$	1×10^{14}
$CHO + M \rightarrow CO + H + M$	$5 \times 10^{14} \exp(-9570/T)$
$H_2 + OH \rightarrow H_2O + H$	$2.9 \times 10^{14} \exp(-5530/T)$
$O + H_2 \rightarrow OH + H$	$3.2 \times 10^{14} \exp(-7540/T)$
$H + O_2 \rightarrow OH + O$	$4.4 \times 10^{14} \exp(-8450/T)$
$OH + OH \rightarrow H_2O + O$	$5.5 \times 10^{13} \exp(-3520/T)$
$CO + OH \rightarrow CO_2 + H$	$4.0 \times 10^{12} \exp(-4030/T)$
$H + HO_2 \rightarrow OH + OH$	$2.5 \times 10^{14} \exp(-950/T)$
$H + OH + Ar \rightarrow H_2O + Ar$	$8.4 \times 10^{21}\, T^{-2}$
$H + O_2 + M \rightarrow HO_2 + M$	$1.5 \times 10^{15} \exp(500/T)$

Units: cm^3, mole, sec, °K.

Afterburner Calculations

Presented below are some examples showing how chemical rate data may be used to design afterburner systems. The following examples are based on a removal efficiency of 90 percent for 1000 ppm of organic in air, and assume that complete mixing exists. Incomplete mixing would increase the estimated residence time based on the chemistry alone.

Example 1. Methanol destruction in thermal afterburner

The appropriate rate data can be found in Table 15 to determine the rate constant for methanol oxidation

$$k = A\,e^{-E_A/RT} = 4.6 \times 10^{15}\,e^{-40,000/1.987\,T}\ \text{cm}^3/\text{mole-sec} \;.$$

At 1300°F (977°K), k is equal to 5.18×10^6 cm^3/mole-sec. Treating the reaction as pseudo first order, the rate expression can be obtained from Table 8

$$f = 1 - e^{k_1 \tau}$$

where f is the fraction of organic destroyed, k_1 is the first-order rate constant, and τ the residence time in the afterburner. The above expression can be rearranged to give τ as

$$\tau = \frac{1}{k_1} \ln\left(\frac{1}{1-f}\right) \;.$$

The pseudo first-order rate constant is obtained by multiplying k by the oxygen concentration (2.61×10^{-6} moles/cm^3) to give $k_1 = 1.35 \times 10^1$ sec^{-1}. For 90 percent destruction of the methanol ($f = 0.9$), the residence time is

$$\tau = \frac{1}{k_1} \ln\left(\frac{1}{1-f}\right) = \frac{1}{1.35 \times 10^1} \ln\left(\frac{1}{1-0.9}\right) = 0.17\ \text{sec} \;.$$

Assuming a linear velocity of 30 ft/sec, the required length of the heat section in the afterburner would be

$$L = \tau v = 0.17 \times 30 = 5.1\ \text{ft}.$$

If f were increased to 0.95, the required residence time would be 0.22 sec corresponding to L = 6.6 ft.

Example 2. Cyclohexane destruction in thermal afterburner

Rate parameters from Table 16 give the rate constant expression for cyclohexane oxidation as

$$k = A\,e^{-E_A/RT} = 5.13 \times 10^{12}\,e^{-47,600/1.987T}\ \text{sec}^{-1}$$

At 1300°F (977°K), $k = 1.15 \times 10^2$ sec^{-1}, and for 90 percent destruction the residence time is

$$\tau = \frac{1}{k_1} \ln\left(\frac{1}{1-f}\right) = \frac{1}{1.15 \times 10^2} \ln\left(\frac{1}{1-0.9}\right) = 0.02\ \text{sec}$$

which corresponds to a heat length of 0.6 ft for a gas velocity of 30 ft/sec.

Example 3. Toluene destruction in thermal afterburner

Based on rate data from Table 21, the rate expression for toluene is

$$k_1 = A\,e^{-E_A/RT} = 6.56 \times 10^3\,e^{-58,500/1.987T}\ \text{sec}^{-1}$$

The rate constant at 1300°F would be 5.4 sec^{-1} which gives a residence time for 90 percent destruction of the toluene as

$$\tau = \frac{1}{k_1} \ln\left(\frac{1}{1-f}\right) = \frac{1}{5.4} \ln\left(\frac{1}{1-0.9}\right) = 0.43\ \text{sec}$$

which is equivalent to a length of 12.9 ft for a linear velocity of 30 ft/sec.

Example 4. Methane destruction in thermal afterburner

The available global rate data for methane oxidation to CO_2 and H_2O are expressed in two steps

$$CH_4 + \frac{3}{2}O_2 = CO + 2H_2O$$

$$CO + \frac{1}{2}O_2 = CO_2 \quad .$$

The first step can be represented by the equation of Dryer and Glassman in Table 12

$$\frac{d[CH_4]}{dt} = -10^{13.2}\, e^{-48,400/RT}\, [CH_4]^{0.7}\, [O_2]^{0.8} \text{ mole/cm}^3\text{-sec}$$

Step 2 can be obtained from the equation of Hemsath and Susey in Table 22

$$\frac{d[CO]}{dt} = -10^{23}\, e^{-100,000/RT} [CO]\, [O_2]^{1/2} \left[\frac{RT}{P}\right]^{1/2} \text{mole/cm}^3\text{-sec} \quad .$$

At 1400°F (1033°K), assuming the O_2 concentration is a constant (2.469×10^{-6}) the methane oxidation step is

$$\frac{d[CH_4]}{dt} = -2.974 \times 10^{-2}\, [CH_4]^{0.7} \text{ mole/cm}^3\text{-sec}$$

which can be integrated to give

$$[CH_4] = (4.185 \times 10^{-3} - 8.921 \times 10^{-3}\, t)^{1/0.3}$$

for an initial methane concentration of 1000 ppm (1.181×10^{-8} moles/cm^3). This can be combined with the expression for CO oxidation to give

$$\frac{d[CO]}{dt} + 31.76\, [CO] = 8.393 \times 10^{-8}\, (1 - 2.132\, t)^{0.7/0.3}$$

for $0 \leqslant t \leqslant 0.469$ sec.

Replacing the right side of the above expression with a quadratic approximation gives

$$\frac{d[CO]}{dt} + 31.76\, [CO] = 8.393 \times 10^{-8}\, (1 - 4.683t + 5.438t^2)$$

which can be integrated to give

$$[CO] = 3.001 \times 10^{-9}\, (1 - e^{-31.76t}) - 1.328 \times 10^{-8}t + 1.437 \times 10^{-8}t^2$$

The formation of CO_2 can be determined by integrating the expression

$$\frac{d[CO_2]}{dt} = 31.76\, [CO]$$

to give

$$[CO_2] = 9.722 \times 10^{-8}\, [t - 1/31.76\ (1 - e^{-31.76t})] - 2.109 \times 10^{-7}t^2 + 1.521 \times 10^{-7}t^3 \quad .$$

Defining f as $[CO_2]/[CH_4]_0$ and t as τ the residence time, then

$$f = \frac{[CO_2]}{[CH_4]_0} = 8.232 \left[\tau - \frac{1}{31.76}\,(1 - e^{-31.76\tau})\right]$$
$$- 1.786 \times 10^1 \tau^2 + 1.288 \times 10^1 \tau^3 \quad .$$

For a removal of 90 percent of the organic (f = 0.9), a trial-and-error solution of the above equation gives a residence time $\tau = 0.26$ sec, which is equivalent to a length of 7.8 ft for a flow velocity of 30 ft/sec. Assuming that Step 1 leads directly to CO_2 and H_2O gives a residence time of 0.234 sec which indicates that initial oxidation of the methane is the rate controlling step.

CATALYTIC OXIDATION REACTIONS

Heterogeneous catalytic oxidation of hydrocarbon vapors can be considered as falling into two categories. These are: (1) selective or partial oxidation, and (2) complete oxidation. Selective catalytic oxidation is commonly used in the commercial production of oxygenated organic compounds, while the intention of complete oxidation is to convert an organic completely to CO_2 and H_2O. A typical selective oxidation process would be the conversion of benzene to maleic anhydride. Most of the information reported here is concerned with complete oxidation or combustion in oxygen or air.

The kinetics and mechanisms of gas-surface oxidations are usually explained in terms of the redox mechanism or the Langmuir-Hinshelwood mechanism or a combination of the two mechanisms.(89) In the redox mechanism, the substance to be oxidized is assumed to reduce the catalyst which in turn is reoxidized by oxygen from the gas phase. The Langmuir-Hinshelwood mechanism assumes that the molecule to be oxidized and the oxygen are first absorbed on the surface of the catalyst where the oxidation reaction then occurs.

The mathematical relations generally used to express heterogeneous catalytic reaction rates fall into two classifications.(90) In one case, a power function equation of the form

$$r = k\,P_A^a\,P_B^b$$

is used. The reaction rate is represented by r, k is the rate constant, and the P's represent pressure. This form utilizes the concept of reaction order. The second classification often possesses the general functional form

$$r = \frac{kK_AP_A}{1 + K_AP_A + K_BP_B}$$

where the K's can be interpreted either as absorption equilibrium for active sites on the catalyst surface, or as empirical constants. Specific forms of this type of expression have been developed by Hougen and Watson(91) for different rate controlling steps. Details on the redox approach have been developed by Mars and van Krevelen.(92)

Empirical rate equations representing the catalytic oxidation of hydrocarbons are frequently used to correlate experimental rate data.(93) Assuming ideal plug flow, an isothermal reactor can be represented by the expression

$$\int_0^f \frac{df}{r} = \frac{V}{C_F^0 Q}$$

where

$$r = k\,C_F^a\,C_{O_2}^b$$

and V is the volume of the catalyst bed, Q the volumetric flow rate, and f is the fraction of the hydrocarbon or organic oxidized defined as

$$C_F = C_F^0\,(1 - f) \quad .$$

The zero superscript denotes the initial concentration.

When O_2 is in excess, the above equation can be written as

$$\int_0^f \frac{df}{k'C_F^a} = \frac{V}{C_F^0 Q}$$

where $k' = kC_{O_2}^b$. This equation can now be rewritten in terms of f to give

$$\frac{1}{k'(C_F^0)^a} \int_0^f \frac{df}{(1-f)^a} = \frac{V}{C_F^0 Q} \quad .$$

For a first-order reaction, a = 1, and the above equation integrates to give

$$f = \left(1 - \frac{C_F}{C_F^0}\right) = 1 - e^{-k'V/Q} \quad .$$

The volumetric flow rate, Q, must be at the temperature of the reactor. The ratio V/Q is essentially the residence time in the reactor or afterburner.

For reactions other than first order, $a \neq 1$

$$f = 1 - \left[1 - \frac{Vk'(C_F^0)^{(a-1)}}{Q}(1-a)\right]^{1/(1-a)}$$

Catalysis by surfaces generally involves specific chemical interactions between a surface and reacting gas molecules which must first become absorbed on the surface before a reaction occurs.(94) Of the two main types of adsorption that occur on surfaces: van der Waals and chemisorption; only the chemisorption is sufficiently strong to influence the reactivity of adsorbed molecules. Generally the heat of reaction for chemisorption is in the range from 10 to 100 kcal/mole, the same range as that observed for chemical reactions, while van der Waal adsorption values are less than 5 kcal/mole. Activation energies of about 20 kcal/mole are associated with chemisorption processes, and consequently adsorption is slow at low temperatures. Surfaces are usually not uniform and some surface sites tend to be more reactive than others for promoting reactions. Also interactions of a repulsive nature occur between atoms or molecules adsorbed on a surface causing the heat of chemisorption to decrease with increasing surface coverage.

Adsorption on surfaces is often represented by the Langmuir adsorption isotherm. If θ is the fraction of the surface covered and $(1 - \theta)$ the fraction that is bare, then the rate of adsorption can be expressed as $K_aP(1 - \theta)$ where P is the gas pressure and k_a a rate constant. The desorption rate can be expressed as $k_d\theta$ where k_d is the desorption rate constant. At equilibrium, the adsorption and desorption rates are equal giving

$$\frac{\theta}{1-\theta} = \frac{k_a}{k_d} P = KP$$

where K is an equilibrium constant equal to k_a/k_d. The above equation can be written as

$$\theta = \frac{KP}{1+KP} \quad .$$

In a situation where the process of adsorption is accompanied by dissociation, the simple Langmuir equation requires modification. In this case, the adsorption process can be considered to be a reaction between a gas molecule and two surface sites with the rate of adsorption being written as $k_aP(1 - \theta)^2$; the rate of desorption, which is assumed to involve the reaction between two adsorbed atoms, is written as $k_d\theta^2$. At equilibrium where the rates are equal

$$\frac{\theta}{1-\theta} = \left(\frac{k_a}{k_d} P\right)^{1/2} = K^{1/2}P^{1/2}$$

or

$$\theta = \frac{K^{1/2}P^{1/2}}{1 + K^{1/2}P^{1/2}} \quad .$$

When two gases react on a surface, such as in the case of a catalytic afterburner, the above equation must be modified to take into account the adsorption of two gases. If the fraction of the surface covered by molecules A is θ, and the fraction covered by molecules B is θ', then the fraction of uncovered surface is $1 - \theta - \theta'$. Molecules A and B are assumed to be adsorbed without dissociation. Appropriate modifications can be made for dissociation. The rate of adsorption of A can be written as $k_aP(1 - \theta - \theta')$ with the rate of desorption equal to $k_d\theta$. At equilibrium the two rates can be set equal to give

$$\frac{\theta}{1-\theta-\theta'} = \frac{k_a}{k_d} P = KP \quad .$$

The equilibrium absorption of B can also be represented by

$$\frac{\theta'}{1-\theta-\theta'} = K'P' \quad .$$

The two above equations can be solved simultaneously to give

$$\theta = \frac{KP}{1 + KP + K'P'}$$

and

$$\theta' = \frac{K'P'}{1 + KP + K'P'} \quad .$$

These equations represent what is sometimes called competitive chemisorption, which is where both gases compete for the same surface sites. In some cases, the adsorption of the two gases takes place on two different types of sites, in which case competition does not occur.

Surface reactions can be considered to occur in five consecutive steps:

1. Diffusion to surface
2. Surface adsorption
3. Reaction on the surface
4. Desorption of products
5. Diffusion of products away from surface.

In the case of a porous catalyst, the diffusion in the first step involves both mass transport from the bulk gas to the external surface of the catalyst and mass transport within the internal pore structure of the catalyst. Details on the effects of pore structure, pore diffusion, effectiveness factors and catalyst poisoning can be found in a comprehensive article by Wheeler.(158)

The adsorption or desorption steps are most likely to be the slow or rate controlling steps, which is consistent with the high activation energies usually observed with heterogeneous reactions. Because it is usually difficult to separate out the desorption step, Steps 3 and 4 are usually treated as one step. This is the basis of the Langmuir-Hinshelwood mechanism. This approach is based on obtaining an expression for the concentrations of reactant molecules on the surface, and then expressing the rate of formation of gaseous products in terms of the surface concentrations. The rate is then expressed in terms of the concentrations of the gaseous reactants.

A less common mechanism, called the Langmuir-Rideal mechanism, assumes that the reaction occurs between a gas molecule and an adsorbed molecule. In this case only one reactant is adsorbed.

A simple unimolecular reaction can be treated in terms of the Langmuir adsorption isotherm with the reaction rate, r, expressed as

$$r = k_2\theta = \frac{k_2KP}{1 + KP}$$

where k_2 is a rate constant. This formulation assumes that adsorption equilibrium is not affected by the reaction which is usually the case.

Frequently a substance other than the reactant is adsorbed on a surface reducing the effective surface area and the reaction rate. This is called inhibition, and the nonreacting substance is called an inhibitor or poison. If the fraction of surface covered by the reactant is θ and the fraction covered by the inhibitor θ_i, then

$$\theta = \frac{KP}{1 + KP + K_iP_i}$$

and the rate of reaction is

$$r = \frac{k_2KP}{1 + KP + K_iP_i}$$

where P_i is the partial pressure of the inhibitor and K_i its equilibrium absorption constant.

The rate constant k_2 follows the Arrhenius expression

$$\frac{d \ln k_2}{dT} = \frac{E}{RT^2}$$

and the temperature dependence of the equilibrium constant follows the van't Hoff equation

$$\frac{d \ln K}{dT} = -\frac{\lambda}{RT^2}$$

where λ is the heat evolved per mole of reactant gas in the adsorption process. If the pressure is low, then

$$r = k_2KP$$

and

$$\frac{d \ln r}{dT} = \frac{d \ln k_2K}{dT} = \frac{d \ln k_2}{dT} + \frac{d \ln K}{dT} = \frac{E - \lambda}{RT^2} \quad .$$

The apparent activation E_{app} is then given by $E - \lambda$, which is the true activation energy minus the heat of adsorption of the reactant. If the pressure is high,

$$r = k_2$$

and the apparent activation energy is equal to the true activation energy.

When a reaction is inhibited, the activation energy is changed by the heat of adsorption of the inhibitor, which can be expressed as

$$\frac{d \ln r}{dT} = \frac{d \ln k_2}{dT} + \frac{d \ln K}{dT} - \frac{d \ln K_i}{dT} = \frac{E - \lambda + \lambda_i}{RT^2}$$

where the apparent activation energy is

$$E_{app} = E - \lambda + \lambda_i \quad .$$

The activation energy is increased by λ_i because it is necessary for an inhibitor molecule to be desorbed for a reactant molecule to be adsorbed and undergo reaction.

In the case of bimolecular surface reactions where the reaction occurs between two adsorbed molecules following the Langmuir-Hinshelwood mechanism, the reaction rate between molecules A and B is given by

$$r = k_2\theta\theta' = \frac{k_2KK'PP'}{(1 + KP + K'P')^2} \quad .$$

If the Langmuir-Rideal mechanism applies and the reaction involves a molecule from the gas phase reacting with a surface molecule, then the rate expression can be written as

$$r = k_2\theta P = \frac{k_2KPP'}{1 + KP + K'P'} \quad .$$

This mechanism does take into account absorption of the species at P', however this species when adsorbed does not react; only the gaseous molecule undergoing a surface collision reacts.

When adsorption of two gases takes place without mutual displacement and the reaction is between molecules adsorbed on two different types of surface sites, another mechanism can be developed. The isotherm for molecules A on sites of type 1 can be represented by

$$\frac{\theta}{1-\theta} = KP$$

and for the adsorption of molecules B on sites of type 2

$$\frac{\theta'}{1-\theta'} = K'P' \quad .$$

The reaction rate is proportional to $\theta\theta'$, so that

$$r = \frac{k_2KK'PP'}{(1 + KP)(1 + K'P')} \quad .$$

When a bimolecular surface reaction is inhibited by a substance at partial pressure, P_i, the fraction covered by A and B are

$$\theta = \frac{KP}{1 + KP + K'P' + K_iP_i}$$

$$\theta' = \frac{K'P'}{1 + KP + K'P' + K_iP_i}$$

which can be combined to give the reaction rate

$$r = k_2\theta\theta' = \frac{k_2KK'PP'}{(1 + KP + K'P' + K_iP_i)^2} \quad .$$

If the inhibitor is a diatomic molecule which is adsorbed as dissociated atoms, then the corresponding equation is

$$r = \frac{k_2KK'PP'}{(1 + KP + K'P' + K_i^{1/2}P_i^{1/2})^2} \quad .$$

When appropriate the partial pressures in the above relationships can be converted to concentrations.

A summary of kinetic mechanisms for surface catalyzed oxidation reactions assembled by Young and Greene(95) are presented in Table 31. The integrated expressions listed in the table are based on the expression

$$\int_0^f \frac{df}{r} = \frac{V}{C_F^0 Q}$$

which was defined earlier in this section.

Catalytic Oxidation Rate Data

The data presented here should be considered as only typical of the types of catalysts used for afterburner applications. Information on catalysts actually used in afterburners is generally of a proprietary nature available only from the catalyst manufacturers.

For complete methane oxidation, it has been found that the activity of catalytic components(96) supported on alumina decreases in the following order: rhodium, palladium, iridium, ruthenium, platinum, and silver. Rate data based on the Arrhenius rate equation

$$k = A\,e^{-E/RT}$$

and the rate equation

$$r = -k\,C_F$$

which can be integrated to give

$$k = -\frac{Q}{V} \ln(1-f)$$

are presented in Figures 7 and 8, and Table 32. On alumina, the activity of the metals or metal oxides per gram of active metal decreases in the order of Pt, Pd, Cr, Mn, Cu, Ce, Co, Fe, Ni, and Ag. Although Co_3O_4 is the most active catalyst for oxidizing hydrocarbons, its activity is decreased by impregnation on alumina. In general methane is the most difficult hydrocarbon to oxidize. Table 33 compares the temperatures needed for complete oxidation of methane, 2-pentene, and benzene on four of the most active catalysts. 2-pentene is an easily oxidized higher hydrocarbon while benzene is one of the most difficult to oxidize.

Mezaki and Watson(97) have investigated the catalytic oxidation of methane on a catalyst consisting of palladium on alumina over the temperature range from 320 to380°C at a pressure of 1 atm. The data were analyzed using a Langmuir-Hinshelwood mechanism based on the rate expression

$$r = \frac{LS\,(S-1)\,k_{SR}\,K_{O_2}\,a_{CH_4}\,a_{O_2}^2}{(1 + a_{O_2}\sqrt{K_{O_2}} + a_{CO_2}K_{CO_2} + a_{H_2O}K_{H_2O} + a_{N_2}K_{N_2})^2}$$

where

$a_{CH_4} = a(1-f)P$
$a_{O_2} = (b-2af)P$
$a_{CO_2} = (c+af)P$
$a_{H_2O} = (d+2af)P$
$a_{N_2} = \zeta P$
a = volume fraction of methane in feed
b = volume fraction of oxygen in feed
c = volume fraction of carbon dioxide in feed
d = volume fraction of water vapor in feed

TABLE 31. INTEGRATED RATE EXPRESSIONS FOR SURFACE CATALYZED OXIDATION[(95)]

Rate Expression	Integrated Equation	Comments
$r_A = kC_{O_2}{}^b$	$\frac{V}{Q} = C_F{}^0 f/kC_{O_2}{}^b$	Empirical model Zero order wrt hydrocarbon
$r_A = kC_F$	$\frac{V}{Q} = -\frac{1}{k} \ln(1 - f)$	Empirical order wrt oxygen Empirical model First order wrt hydrocarbon
$r_A = kC_F{}^a$	$\frac{V}{Q} = \frac{C_F{}^{0(1-a)}}{k(1-a)} \left\{(1-f)^{(1-a)} - 1\right\}$	Zero order wrt oxygen Empirical model Empirical order wrt hydrocarbon
$r_A = kC_F{}^a C_{O_2}{}^b$	$\frac{V}{Q} = \frac{C_F{}^{0(1-a)}}{k(1-a)C_{O_2}{}^b} \left\{(1-f)^{(1-a)} - 1\right\}$	Zero order wrt oxygen Empirical model Empirical order wrt hydrocarbon
$r_A = kC_F C_{O_2}{}^b$	$\frac{V}{Q} = \frac{1}{kC_{O_2}{}^b} \ln(1 - f)$	Empirical order wrt oxygen Empirical model First order wrt hydrocarbon
$r_A = \frac{k_1 C_F k_2 C_{O_2}}{Nk_1 C_F + k_2 C_{O_2}}$	$\frac{V}{Q} = \frac{C_F{}^0 f}{(k_2/N)C_{O_2}} - \frac{1}{k_1} \ln(1 - f)$	Empirical order wrt oxygen Redox model Oxygen adsorbs irreversibly onto catalyst surface Gas phase hydrocarbon reacts with adsorbed oxygen Oxygen adsorption is the rate-controlling step
$r_A = \frac{k_1 C_F k_2 C_{O_2}}{[k_2 C_{O_2} + (k_1 k_2/k_3) C_F C_{O_2} + k_1 C_F]}$	$\frac{V}{Q} = C_F{}^0 f \left(\frac{1}{k_3} + \frac{1}{k_2 C_{O_2}}\right) - \frac{1}{k_1} \ln(1 - f)$	[S–] + oxygen → [S–O][a] [S–O] + hydrocarbon → [hyd.–S–O] [hyd.–S–O] → [S–] + products

TABLE 31. (Continued)

Rate Expression	Integrated Equation	Comments
$r_A = \dfrac{kC_F}{1 + kC_F}$	$\dfrac{V}{Q} = C_F{}^0 f - \dfrac{1}{k_1} \ln (1 - f)$	Langmuir adsorption model Assuming hydrocarbon reversibly adsorbs on catalyst surface Rate is proportional to surface fraction covered Independent of oxygen concentration
$r_A = \dfrac{k_1 C_F k_2 C_{O_2}{}^b}{(1 + k_1 C_F)}$	$\dfrac{V}{Q} = \dfrac{1}{k_2 C_{O_2}{}^b} \left\{ C_F{}^0 f - \dfrac{1}{k_1} \ln (1 - f) \right\}$	Langmuir adsorption model as above but assuming empirical gas phase oxygen dependence
$r_A = \dfrac{k_1 k_2 C_F C_{O_2}}{(k_3 + k_1 C_F + k_2 C_{O_2})}$	$\dfrac{V}{Q} = \dfrac{C_F{}^0 f}{k_2 C_{O_2}} - \left(\dfrac{k_3 + k_2 C_{O_2}}{k_1 k_2 C_{O_2}} \right) \ln (1 - f)$	Redox model assuming reversible oxygen adsorption
$r_A = \dfrac{k_1 C_F k_2 C_{O_2}{}^{1/2}}{N k_1 C_F + k_2 C_{O_2}{}^{1/2}}$	$\dfrac{V}{Q} = \dfrac{C_F{}^0 f}{(k_2/N) C_{O_2}{}^{1/2}} - \dfrac{1}{k_1} \ln (1 - f)$	Redox model assuming rate of oxygen adsorption is ½ order wrt oxygen
$r_A = \dfrac{k_1 k_2 k_3 C_F C_{O_2}}{(1 + k_2 C_F + k_3 C_{O_2})^2}$	$\dfrac{V}{Q} = \dfrac{2C_F{}^0}{k_1 k_3 C_{O_2}} \times \left\{ \left(1 + k_3 C_{O_2} + \dfrac{1}{2} k_2 C_F{}^0\right) f - \dfrac{1}{4} k_2 C_F{}^0 f^2 - \dfrac{(1 + k_3 C_{O_2})^2}{2 k_2 C_F{}^0} \ln (1 - f) \right\}$	Langmuir-Hinshelwood dual-site model assuming both reactants adsorbed on catalyst surface with reaction occurring between adsorbed species
$r_A = \dfrac{k_1 k_2 C_F C_{O_2}}{1 + k_2 C_{O_2}}$	$\dfrac{V}{Q} = \dfrac{1}{k_1} \left(1 + \dfrac{1}{k_2 C_{O_2}} \right) \ln (1 - f)$	Langmuir-Rideal model assuming equilibrium oxygen adsorption and reaction with gas phase hydrocarbon molecule

[a] S, site; O, oxygen; hyd., hydrocarbon.

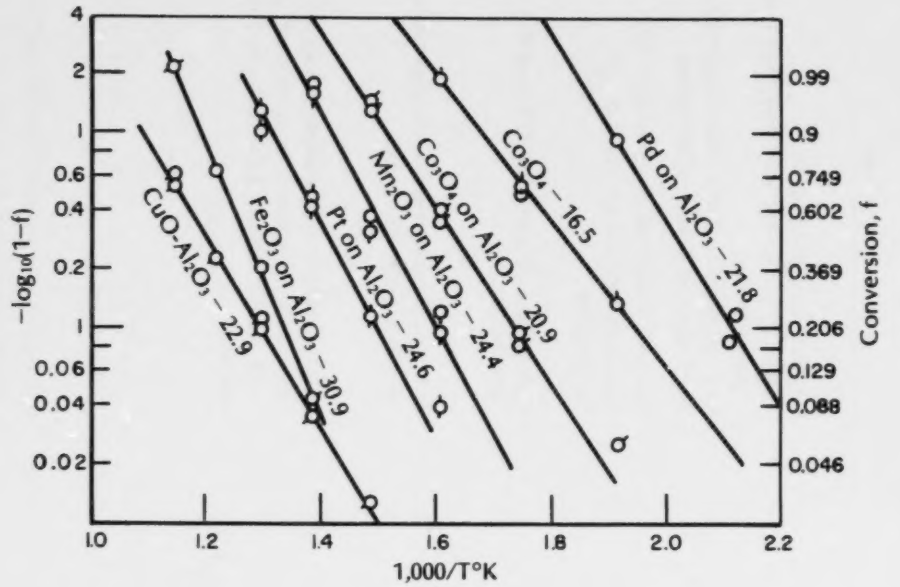

FIGURE 7. ARRHENIUS PLOTS SHOWING TEMPERATURE DEPENDENCE IN CATALYTIC OXIDATION OF METHANE

(Activation energies are in kilocalories per mole)(96)

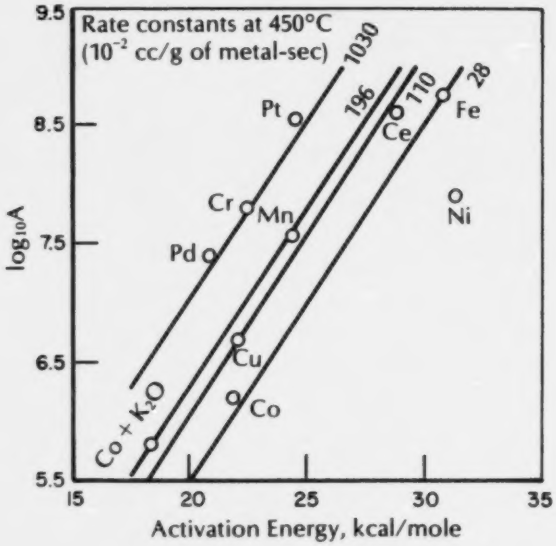

FIGURE 8. PLOTS OF THE LOGARITHM OF FREQUENCY FACTOR, A, AS A FUNCTION OF ACTIVATION ENERGY FOR METAL OXIDES AND METALS SUPPORTED ON ALUMINA(96)

(Oblique lines represent constant values of the rate constant at 450°C. Rate constants and frequency factors are expressed per gram of active metal.)

TABLE 32. RATE CONSTANTS FOR CATALYSTS FOR THE OXIDATION OF METHANE[96]

Catalyst No.	Catalyst Components and Wt % Active Metal	Bulk Density, grams/cc	Activation Energy, kcal/mole	Rate Constants x 10^{-2}				Log_{10} A, cc/cc-sec
				cc/cc-sec		cc/gram-sec		
				300°C	450°C	300°C	450°C	
	Precipitated and Sintered							
6	Co_3O_4	0.80	16.5	7.2	144	9.0	180	5.12
18	$ZnCrO_4$ (48 Zn, 27.5 Cr)	0.310	15.4	–	5.3	–	17.1	3.35
9	Co-ThO_2-MgO-kieselguhr (24.7 Co)	0.213	19.2	–	3.3	–	15.5	4.29
25	$CuCrO_4$ (33.4 Cu, 17.9 Cr)	0.541	23.1	–	0.84	–	1.55	4.87
33	$PbCrO_4$	1.745	25.0	–	0.056	–	0.032	4.26
	Decomposition–All Mixed Oxides							
24	9.4 Co-61 Fe	1.30	21.1	–	0.64	–	0.50	4.15
19	50 Co-26 Cu	1.41	18.4	–	0.51	–	0.36	3.24
31	34 Cu-30 Al	0.712	22.9	–	0.48	–	0.67	4.57
20	30 Cu-45 Fe	1.30	13.0	–	0.37	–	0.28	1.48
29	38 Fe-39 Cd	1.073	30.7	–	0.16	–	0.15	6.44
	Impregnated Catalysts							
14	Pd on alumina (0.5 Pd)	0.765	21.8	76	3960	99.3	5180	8.14
8	Pt on alumina (0.5)	0.861	23.5	2.8	199	3.3	235	7.35
1	Co_3O_4 on Kaosorb clay (6.5 Co)	0.636	22.2	1.6	90	2.5	140	6.62
5	Co_3O_4 on alumina-622 (7.2 Co)	1.186	20.9	1.1	49	0.93	41	5.97
22	PdO on alumina-151 (3.5 Pd)	0.851	20.9	0.88	39	1.03	46	5.88
10	Cr_2O_3 on alumina-151 (3.1 Cr)	0.817	22.6	0.43	26	0.53	32	6.20
7	Mn_2O_3 on alumina-151 (13.6 Mn)	0.912	24.4	0.25	21	0.25	23	6.66
15	CuO on alumina-151 (7.0 Cu)	0.836	22.1	–	6.4	–	7.7	5.45
28	Pt on alumina-151 (0.51 Pt)	0.775	24.6	–	5.5	–	7.1	6.13
17	Co_3O_4 + K_2CO_3 on alumina-151 (2.4 Co)	0.845	18.4	–	4.0	–	4.7	4.13
23	CeO_2 on alumina-151 (1.2 Ce)	0.827	28.9	–	0.79	–	0.96	6.59
13	Co_3O_4 on alumina-151 (2.0 Co)	0.899	21.9	–	0.75	–	0.83	4.46
32	Fe_2O_3 on alumina-151 (2.9 Fe)	0.753	30.9	–	0.61	–	0.81	7.07
11	V_2O_5 on alumina (8.8 V)	0.877	23.9	–	0.43	–	0.49	4.82
21	NiO on alumina-151 (3.8 Ni)	0.852	31.3	–	0.13	–	0.15	6.41
16	Ag on alumina-151 (4.7 Ag)	0.784	50.6	–	0.073	–	0.093	12.07
27	MoO_3 on alumina-151 (3.2 Mo)	0.770	35.9	–	0.069	–	0.090	7.63
26	TiO_2 on alumina-151 (7.9 Ti)	0.792	32.4	–	0.069	–	0.087	6.58

TABLE 33. TEMPERATURES FOR COMPLETE OXIDATION OF HYDROCARBONS[96]

Catalyst Number*	Catalyst	Temperature for Complete Oxidation of Hydrocarbon, °C		
		2-Pentene	Benzene	Methane
6	Co_3O_4 (unsupported)	200	200	400
10	Cr_2O_3 on alumina	–	350	500
8	Pt on alumina	200	200	400
14	Pd on alumina	250	300	300

*Catalyst numbers correspond to those listed in Table 32.

ζ = volume fraction of nitrogen in feed
k_{SR} = surface reaction rate constant
K_{CH_4} = adsorption equilibrium constant of methane on catalytically active sites
K_{CO_2} = adsorption equilibrium constant of carbon dioxide
K_{H_2O} = adsorption equilibrium constant of water vapor
K_{N_2} = adsorption equilibrium constant of nitrogen
K_{O_2} = adsorption equilibrium constant of oxygen
L = total concentration of active sites
S = number of equidistant active centers adjacent to each other
f = fraction of methane oxidizer
P = total pressure
$\theta = LS(S-1)k_{SR}$.

Assuming nitrogen is not adsorbed and the nitrogen term in the above equation can be neglected, the following Arrhenius parameters were determined:

$$\ln \theta = \frac{36.35}{R} - \frac{8228}{RT}$$

$$\ln K_{O_2} = \frac{6.71}{R} + \frac{8631}{RT}$$

$$\ln K_{CO_2} = -\frac{0.55}{R} + \frac{5079}{RT}$$

$$\ln K_{H_2O} = -\frac{4.66}{R} + \frac{8006}{RT} \quad .$$

In the above correlations, T and R represent the absolute temperature and the gas constant, respectively. Typical values of the above rate parameters are listed in Table 34.

Accomazzo and Nobe[93] measured heterogeneous rate constants for the oxidation of methane, ethane, and propane over a cupric oxide-aluminum oxide (1:1) catalyst with a BET surface area of 120 sq m/g and a mean pore radius of 65 Å. The measurements were conducted for initial hydrocarbon concentrations in the range from 650 to 5,000 ppm over the temperature range from 313 to 591°C and gas space velocities from 6,000 to 16,000 hr^{-1}. The

TABLE 34. RATE PARAMETERS FOR CATALYTIC OXIDATION OF METHANE(97)

Temperature, °C	θ	K_{O_2}	K_{CO_2}	K_{H_2O}
320	79,700	45,300	54.2	86.7
350	120,000	30,000	50.0	60.4
380	151,000	23,200	36.3	46.5

results showed that for gas space velocities up to 10,000 hr^{-1}, 90 percent combustion was attained at temperatures above 580, 500, and 480°C for methane, ethane, and propane, respectively. The results indicate that the degree of oxidation increases with increased chain length. The rate data were correlated using the following relations

$$r_{CH_4} = 9.0 \times 10^{10}\, e^{-23,600/RT}\, C_{CH_4}$$

$$r_{C_2H_6} = 1.1 \times 10^{9}\, e^{-21,200/RT}\, C_{C_2H_6}^{0.75}$$

$$r_{C_3H_8} = 1.8 \times 10^{8}\, e^{-21,400/RT}\, C_{C_3H_8}^{0.6} \quad .$$

Concentrations are in moles/cm^3 and the activation energies in cal/g-mole.

In more recent work by Accomazzo and Nobe(98) with CuO:Al_2O_3, complete catalytic oxidation measurements were made on a number of hydrocarbons at initial concentrations between 182 and 1450 ppm at temperatures from 140 to 510°C and at gas flow rates of 160, 275, and 525 liters per hr (NTP). Empirical rate expressions of the form

$$r = A\, e^{-E/RT}\, P_F^n$$

were used to correlate the data. P_F represents the pressure of the fuel or hydrocarbon in atmospheres. The appropriate reaction rate parameters are listed in Table 35. A relative comparison of oxidation rates are also shown in Figure 9.

Juusola et al.(99) have measured the catalytic oxidation of o-xylene over a vanadium oxide/potassium sulfate-promoted/silica catalyst at temperatures from 290 to 310°C and concentrations of (0.5 to 3.0) $\times 10^{-4}$ g-mole/liter o-xylene and (5 to 100) $\times 10^{-4}$ g-mole/liter oxygen. The data were correlated using the models presented in Table 36. Of the 5 models, Model 1 was found to offer the best correlation for the data. The rate constants for o-xylene based on Model 1 are

$$\ln k_a = 11.8 - \frac{26,000}{RT}$$

$$\ln k_r = 16.8 - \frac{28,000}{RT}$$

which apply to the temperature range from 290 to 310°C. Rate data for the o-xylene along with naphthalene, toluene, and benzene, based on Model 1, are plotted in Figures 10 and 11, and listed in Table 37.

TABLE 35. EMPIRICAL REACTION RATE PARAMETERS(98)

Hydrocarbon	A, mole/g-sec-atm^n	E, cal	n
Methane	5.53×10^2	23,000	0.9
Ethane	9.20×10^3	26,000	0.7
Ethylene	5.82×10^1	18,000	0.5
Acetylene	6.67×10^2	19,000	0.2
Propane	1.26×10^1	17,300	0.6
Propylene	6.58×10^1	17,500	0.5
Propadiene	4.44×10^0	15,000	0.3
Propyne	4.15×10^0	17,000	0.0
Cyclopropane	2.12×10^1	16,000	0.8

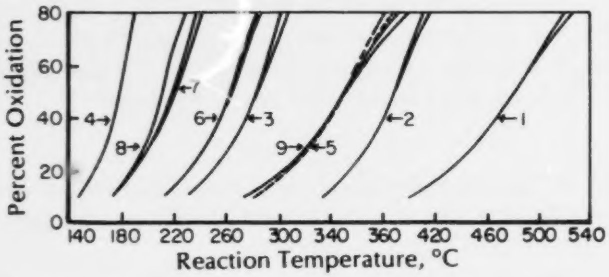

Flow rate = 525 liters/hr   Initial concentration = 500 ppm

1. Methane
2. Ethane
3. Ethylene
4. Acetylene
5. Propane
6. Propylene
7. Propadiene
8. Propyne
9. Cyclopropane

FIGURE 9. COMPARISON OF CATALYTIC COMBUSTION OF C_1 TO C_3 HYDROCARBONS(98)

TABLE 36. SUMMARY OF REACTION RATE MODELS TESTED[99]

Model	Assumptions	Rate Equation for Initial Rate Conditions
1	A steady-state adsorption model (SSAM)—a steady state is assumed between the rate of adsorption of oxygen on the surface and the rate of removal of oxygen by reaction with R from the gas phase	$r_R = \dfrac{k_a k_r C_o C_R}{k_a C_o + n\, k_r C_R}$
2	SSAM—additional assumption to Model 1 is made that oxygen dissociates	$r_R = \dfrac{k_a k_r C_R (C_o)^{1/2}}{k_a (C_o)^{1/2} + n\, k_r C_R}$
3	SSAM—additional assumption to Model 1 is made that the oxygen desorption rate is not negligible	$r_R = \dfrac{k_a k_r C_o C_R}{k_d + k_a C_o + n\, k_r C_R}$
4	Rideal mechanism—equilibrium concentration of oxygen is assumed established on the surface, with reaction occurring between adsorbed oxygen and gas phase hydrocarbon	$r_R = \dfrac{k_r K_A C_o C_R}{1 + K_A C_o}$
5	Langmuir-Hinshelwood model—equilibrium concentrations of oxygen and hydrocarbon are assumed established on the surface, with reaction occurring between adsorbed reactants	$r_R = \dfrac{k_r K_A K_R C_o C_R}{(1 + K_A C_o + K_R C_R)^2}$

Nomenclature:

C_o = concentration of oxygen, moles/liter
C_R = concentration of hydrocarbon, moles/liter
k_a = specific rate of oxygen adsorption, liter/g catalyst see (in Model 1)
K_a = oxygen equilibrium adsorption constant
k_d = specific rate of oxygen desorption, liter/g catalyst sec
k_r = reaction rate constant, liter/g catalyst sec
K_R = hydrocarbon equilibrium adsorption constant
n = stoichiometric number, moles oxygen required/mole hydrocarbon reacted
r_R = rate of hydrocarbon reaction, moles/g catalyst sec.

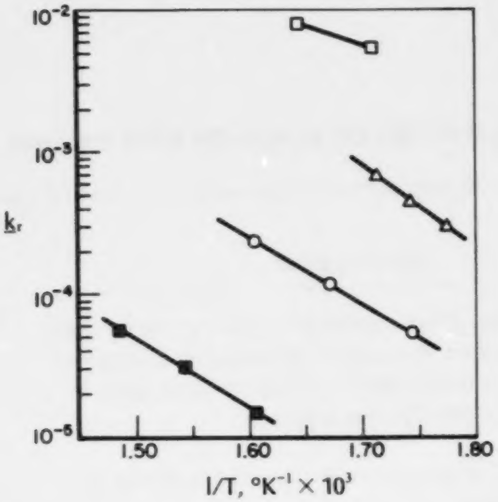

FIGURE 10. ARRHENIUS PLOTS OF k_r FROM NAPHTHALENE, TOLUENE, BENZENE, AND o-XYLENE

(□, naphthalene; o, toluene; ■, benzene, △, o-xylene)(99)

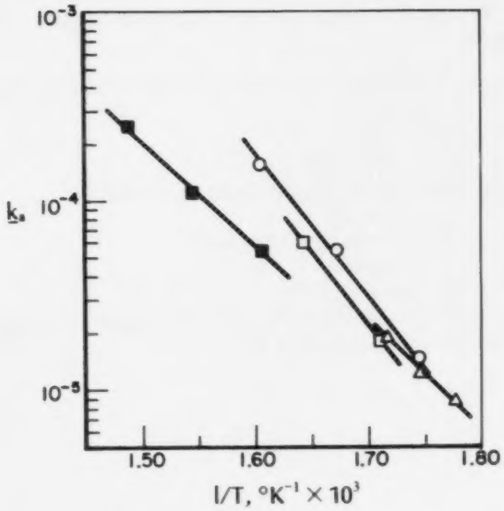

FIGURE 11. ARRHENIUS PLOTS OF k_a FROM NAPTHALENE, TOLUENE, BENZENE, AND o-XYLENE

(□, naphthalene; o, toluene; ■, benzene; △, o-xylene)(99)

TABLE 37. RATE CONSTANTS FOR MODEL 1[99]

Hydrocarbon	Temperature, °C	k_a, liter/ g-catalyst sec	k_r, liter/ g-catalyst sec
Naphthalene	312	1.81×10^{-5}	5.40×10^{-3}
	335	6.17×10^{-5}	7.85×10^{-3}
Toluene	300	1.11×10^{-5}	5.24×10^{-5}
	325	5.59×10^{-5}	1.18×10^{-4}
	350	1.58×10^{-4}	2.38×10^{-4}
Benzene	350	5.48×10^{-5}	1.42×10^{-5}
	375	1.10×10^{-4}	3.07×10^{-5}
	400	2.49×10^{-4}	5.50×10^{-5}
Oxylene	290	8.66×10^{-6}	2.88×10^{-4}
	300	1.26×10^{-5}	4.39×10^{-4}
	310	1.91×10^{-5}	6.74×10^{-4}

Benzo(α)pyrene oxidation on a mixed vanadium pentoxide-molybdenum oxide catalyst was observed to follow a redox mechanism(95) for temperatures from 275 to 345°C; benzo(α)pyrene concentrations 0.002 to 0.05 g-mole/m^3; and oxygen concentrations 4 to 26 g-mole/m^3. The redox model assumes that the gas-phase hydrocarbon reacts rapidly with an oxidized catalyst site to form the reaction products and the gas-phase oxygen slowly adsorbs onto reduced sites (S):

$$\text{Hydrocarbon} + [\text{S–O}] \xrightarrow[\text{fast}]{k_1} \text{Products} + [\text{S–}]$$

$$[\text{S–}] + \text{Oxygen} \xrightarrow[\text{slow}]{k_2} [\text{S–O}] \quad .$$

If it is assumed that N moles of oxygen are required for the oxidation of a mole of hydrocarbon, then the redox mechanism can be expressed as

$$-r_F = \frac{k_1 C_F k_2 C_{O_2}^{\alpha}}{N k_1 C_F + k_2 C_{O_2}^{\alpha}}$$

For a process where the catalyst reoxidation involves atomic oxygen, $\alpha = \frac{1}{2}$; for the molecular process, $\alpha = 1$. It appears that the experimental data favors the mechanistic model with $\alpha = 1$. An empirical correlation based on

$$-r_F = \phi\, e^{-E/RT} C_F^{a} C_{O_2}^{b}$$

has the reaction rate parameters listed in Table 38. In the above equation the units for r_F are g-mole/hr·kg catalyst for the values given in Table 38. The integrated form of the above equation can be written as

$$\frac{W}{Q} = \frac{C_F^{(1-a)}}{\phi\, e^{-E/RT} C_{O_2}^{b}} \left[(1-f)^{(1-a)} - 1\right]$$

where W represents the weight of catalyst, Q the flow rate, and f the fraction of hydrocarbon oxidized.

TABLE 38. REACTION RATE PARAMETERS FOR THE CATALYTIC OXIDATION OF BENZO(α)PYRENE[95]

Parameter	Value
ϕ	$(8.3 \pm 1.4) \times 10^9$
E	31.9 ± 4.3 kcal/mole
a	0.20 ± 0.03
b	0.60 ± 0.05

Voltz et al. have studied the oxidation of CO and propylene on a platinum-alumina catalyst between 200 and 370°C.[100] The oxidation rate was found to increase with increasing oxygen and was inhibited by CO, propylene, and nitric oxide. The rate data can be represented by

$$r_{CO} = -k_{r_1}\,(CO)(O_2)/R(\theta)$$

$$r_{C_3H_6} = -k_{r_2}\,(C_3H_6)(O_2)/R(\theta)$$

where

$$R(\theta) = [1 + k_{a_1}\,(CO) + k_{a_2}\,(C_3H_6)]^2 \times \{1 + k_{a_3}[(CO)(C_3H_6)]^2\} \times [1 + k_{a_4}\,(NO)^{0.7}] \quad .$$

The concentration units are expressed as: (CO) = mole percent CO, (O_2) = mole percent O_2; (C_3H_6) = ppm propylene, (NO) = ppm of NO; k_{a_1} = intrinsic rate constant based on catalyst volume, $sec^{-1}(O_2)^{-1}$; k_{r_2} = intrinsic rate constant based on catalyst volume, $sec^{-1}(O_2)^{-1}$; k_{a_1} = adsorption constant for CO, $(CO)^{-1}$; k_{a_2} = adsorption constant for C_3H_6, $(C_3H_6)^{-1}$; k_{a_3} = adsorption constant for combined effect of CO and C_3H_6, $[(CO)(C_3H_6)]^{-2}$; and k_{a_4} = adsorption constant for NO, $(NO)^{-1}$. The temperature dependency of the rate constants are given by

$$k_{r_j} = k_{r_j}^0 \exp\left[-\frac{E_{rj}}{R(T_s + 460)}\right] \qquad \begin{pmatrix} j = 1 \text{ for CO} \\ j = 2 \text{ for } C_3H_6 \end{pmatrix}$$

$$k_{a_i} = k_{a_i}^0 \exp\left[-\frac{E_{ai}}{R(T_s + 460)}\right] \qquad (i = 1, 2, 3, 4)$$

E_{rj} and E_{ai} are activation energies in Btu/lb-mole; R is the gas constant, 1.987 Btu/lb-mole °R, and T_s the catalyst temperature, °F. Values of the frequency factors and activation energies are given in Table 39.

The rate for complete catalytic oxidation to CO_2 of CO, C_2H_4, and C_2H_6 over Co_3O_4 and Co_3O_4 supported on alumina was found[101] to be described by an expression

$$r_s = k\, p_{O_2}^m\, p_{CO\ (or\ HC)}^n\, p_{H_2O}^{-1}\, e^{-E/RT} \quad .$$

r_s is the specific rate in ml (NTP) of CO_2 formed per minute per m^2 of catalyst surface, k is the rate constant, p_{O_2}, p_{CO}, p_{HC}, and p_{H_2O} are the partial pressures in mole percent for O_2, CO, hydrocarbon and water, respectively. Kinetic parameters for the unsupported Co_3O_4 catalyst

TABLE 39. REACTION RATE PARAMETERS FOR CATALYTIC OXIDATION OF CO AND PROPYLENE(100)

$k_{r1}^0 = 1.83 \times 10^{12}$	$E_{r1}/R = 22{,}600$
$k_{r2}^0 = 3.80 \times 10^{13}$	$E_{r2}/R = 26{,}200$
$k_{a1}^0 = 6.55 \times 10^{-1}$	$E_{a1}/R = -1{,}730$
$k_{a2}^0 = 2.08 \times 10^{-3}$	$E_{a2}/R = -650$
$k_{a3}^0 = 3.98 \times 10^{-16}$	$E_{a3}/R = -20{,}900$
$k_{a4}^0 = 3.02 \times 10^{1}$	$E_{a4}/R = 6{,}720$

are presented in Tables 40 and 41, while data on the alumina-supported catalyst are given in Tables 42 and 43. For the unsupported Co_3O_4 it was observed that CO oxidation at 200 to 250°C was severely retarded by the presence of C_2H_4 even though the oxidation of the latter was negligible at low temperatures. Competition between CO and C_2H_4 for the surface sites is more likely responsible for the retardation. Kinetic parameters for the oxidation of CO and several hydrocarbons are summarized in Table 44 and Figure 12.(102)

Afterburner Calculation

An example of a design calculation for a catalytic afterburner system is given below.

Example 5. Toluene destruction in catalytic afterburner

Toluene oxidation over a V_2O_5-type catalyst can be represented by the relationship

$$\frac{1}{W_c}\frac{dc_T}{dt} = \frac{k_a\, k_r\, c_{O_2}\, c_T}{k_a\, c_{O_2} + n\, k_r\, c_T}$$

from Table 36. W_c is the weight of catalyst per liter and n is defined by

$$C_6H_5CH_3 + nO_2 = 7CO_2 + 4H_2O$$

where n = 9. The above expression can be integrated to give

$$\tau = \frac{n\, c_T^0}{W_c\, k_a\, c_{O_2}}\, f - \frac{1}{W_c k_r} \ln (1 - f)$$

Extrapolating the rate data in Figures 9 and 10 to 1000°F (811°K) gives

$k_r = 1.330 \times 10^{-2}$ liter/g-catalyst sec
$k_a = 1.820 \times 10^{-1}$ liter/g-catalyst sec
$W_c = 880$ g-catalyst/liter.

At 1000°F and 1000 ppm of toluene

$c_{O_2} = 3.144 \times 10^{-3}$ mole/liter
$c_T^0 = 1.504 \times 10^{-5}$ mole/liter

for which a residence time of 0.20 sec can be determined from the above equation. In the case of the thermal afterburner (Example 3) a residence time of 0.43 sec was required at 1300°F.

TABLE 40. KINETIC PARAMETERS OVER Co_3O_4 [(101)(a)]

Reactant	Temperature Range, °C	l	m	n	f	E, kcal/mole
CO	150–200	0.3 ± 0.1	0.46 ± 0.12	0.45 ± 0.10	0	20 ± 2
CO	300–350	0.1 ± 0.1	0.10 ± 0.04	0.93 ± 0.10	0.3 ± 0.1	5 ± 2
C_2H_4	275–450	0.35 ± 0.1	0.29 ± 0.07	0.51 ± 0.10	0	23 ± 2
C_2H_6	300–450	0.3 ± 0.1	0.33 ± 0.07	0.62 ± 0.08	0	21 ± 2

(a) Rate = $k(p_{O_2})^m (p_{CO \text{ or } HC})^n (p_{H_2O})^l (\text{flow rate})^f e^{-E/RT}$.

TABLE 41. SPECIFIC RATES OVER Co_3O_4 [(101)(a)]

Catalyst	Surface Area, m^2/g	CO + O_2 T, °C	CO + O_2 R, ml CO_2/min-m^2	C_2H_4 + O_2 T, °C	C_2H_4 + O_2 R, ml CO_2/min-m^2	C_2H_6 + O_2 T, °C	C_2H_6 + O_2 R, ml CO_2/min-m^2
Co_3O_4I	0.44	150	2.2	300	0.3	400	0.6
		200	28	350	1.8		
		300	70	400	10.5		
Co_3O_4II—600°C (diluted with Linde A)	10	150	1.0	300	0.3	400	1.3
		200	17	350	1.3		
		300	120	400	4.3		
Co_3O_4II—850°C	0.93	150	1.1	300	0.4	400	0.8
		200	20	350	1.5		
		300	60	400	5.0		
Co_3O_4III—600°C	5.0	150	2.3	300	0.45		
		200	28	350	2.2		
		300	95	400	9.5		
Co_3O_4III—850°C	1.2	150	1.2	300	0.3		
		200	21	350	1.1		
		300	35	400	3.5		
$CoAl_2O_4$	11.3	300	0.003	400	0.0005		

(a) CO + O_2, 1% O_2, 1% CO, 0% H_2O; C_2H_4 + O_2, 1% O_2, 0.1% C_2H_4, 0.1% H_2O; C_2H_6 + O_2, 1% O_2, 0.1% C_2H_6, 0.1% H_2O.

TABLE 42. KINETIC PARAMETERS OF OXIDATIONS OVER SUPPORTED Co_3O_4 CATALYSTS[(101)(a)]

Reactant	Temperature Range, °C	l	m	n	f	E, kcal/mole
			600°C Pretreatment (25–60 m^2/g)			
CO	125–200	–	0.44 ± 0.11	0.47 ± 0.14	0	15 ± 1
CO	250–350	–	0.25 ± 0.1	0.90 ± 0.13	~0.5	3–7
C_2H_4	300–450	0.4 ± 0.1	0.26 ± 0.08	0.39 ± 0.04	0	20 ± 2
C_2H_6	300–450	0.35 ± 0.1	0.24 ± 0.04	0.53 ± 0.05	0	18.5 ± 1
			850°C Pretreatment			
CO	150	–	0.31 ± 0.07	0.38 ± 0.11	–	10 ± 2
CO	300	–	0.16 ± 0.1	0.80 ± 0.07	–	–
C_2H_4	350–450	0.3 ± 0.1	0.31 ± 0.07	0.47 ± 0.08	0	16 ± 2
C_2H_6	350–450	–	0.4	0.48	–	21

(a) Rate = $k(p_{O_2})^m(p_{CO\ or\ HC})^n(p_{H_2O})^l e^{-E/RT}$.

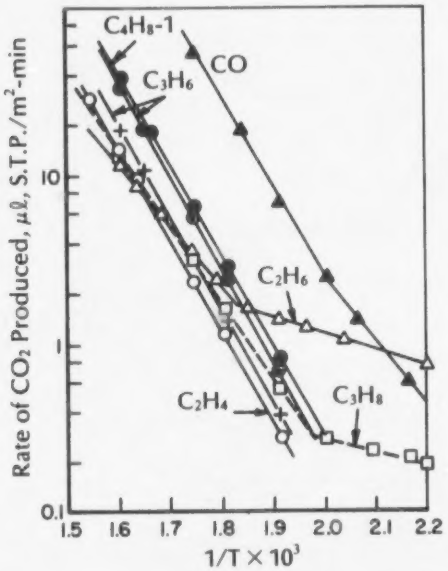

FIGURE 12. ARRHENIUS PLOTS FOR OXIDATION OVER NiO[(102)]: ○ C_2H_4, 2.5%; O_2, 6.2%; H_2O, 0.4%; (+) C_3H_6, 0.8%; O_2, 3.5%; H_2O, 0.4%; (⊕) C_3H_6, 3.2%; O_2, 7%; H_2O, 0.5%; (●) C_4H_8-1, 1.8%; O_2, 5.3%; H_2O, 0.5%; (□) C_3H_8, 0.4%; O_2, 3.6%; H_2O, 0.3%; (△), C_3H_6, 1.6%; O_2, 2.5%; H_2O, 0.25%; (▲) CO, 2.1%; O_2, 2.7%; H_2O, 0%

TABLE 43. SPECIFIC RATES OVER SUPPORT Co_3O_4 CATALYSTS(101)(a)

Catalyst	Wt % Co_3O_4	$CO + O_2$(b)		$C_2H_4 + O_2$(d)		$C_2H_6 + O_2$(e)
		$R_{150°C}$	$R_{200°C}$	$R_{350°C}$	$R_{400°C}$	$R_{400°C}$
			600°C Pretreatment			
Co_3O_4-DAL(1)	25.2	90	900	41	102	12
Co_3O_4-DAL(3)	45	46	530	28	65	–
Co_3O_4-DAL(4)	10	45	1000	42	102	14
Co_3O_4-DAL(6)	13.1	75	940	38	122	15.5
Co_3O_4-DAL(10)	9.8	105	700	29.5	90	
Co_3O_4-DAL(11)	8.4	120	600	19	48	
Co_3O_4-DAL(13)(c)—600 C	10.1	6.7	20.5	0.1	0.4	
Co_3O_4-DAL(13)(c)—850 C (1 day)	10.1	23.5	105	0.5	3.6	
Co_3O_4-DAL(13)(c)—850 C (3.5 days)	10.1	21	80	–	3.0	
Co_3O_4-Linde A	9.2	140	1000	20	–	
Co_3O_4-Linde B	15.4	–	61	6.9	18	
Co_3O_4-Mullite	9.1	–	~1	–	1.6	
Co_3O_4-Cab-O-Sil	13.3	–	4	–	–	
Co_3O_4-Al_2O_3(k)(ImN)	10.4	–	2	–	0.6	
Co_3O_4-Al_2O_3(ImNI)	17.2	–	0.3	–	0.3	
Co_3O_4-Al_2O_3(ImNN)	3.3	70	180	1.6	8.1	
Co_3O_4-Al_2O_3(ImA)	5.5	12	44	0.6	1.35	
Co_3O_4-Al_2O_3(F) (ImNN)	6.05	60	450	20.5	55	
			850°C Pretreatment			
Co_3O_4-DAL(1)	25.2	33	100	3.2	–	0.8
Co_3O_4-DAL(3)	45	–	20	1.6	–	–
Co_3O_4-DAL(6)	10	27	90	1.8	–	0.9
Co_3O_4-DAL(10)	9.8	17	74	1.3	3.4	
Co_3O_4-DAL(11)	8.4	27	91	1.7	4.2	
Co_3O_4-Linde A	9.2	–	20	–	–	
Co_3O_4-Linde B	15.4	–	~6	–	–	
Co_3O_4-Al_2O_3(ImNN)	17.2	13	40	–	–	
Co_3O_4-Al_2O_3(ImA)	5.5	11	43	0.4	0.05	

(a) Rate in ml CO_2/min-g Co_3O_4.
(b) 1% O_2, 1% CO, 0% H_2O.
(c) Co_3O_4 III—850 C used as starting material.
(d) 1% O_2, 0.1% C_2H_4, 0.1% H_2O.
(e) 1% O_2, 0.1% C_2H_6, 0.1% H_2O.

TABLE 44. KINETIC PARAMETERS FOR HYDROCARBON OXIDATION OVER NiO(I)(102)(a)

Reactant	l	m	n		E, kcal/mole, °C	
C_2H_4	0.33	0.47	0.33		25.4	(250–400)
C_3H_6	0.27	0.53	0.23		25.0	(250–400)
C_4H_8-1	0.35	0.55	0.14		24.7	(300–350)
trans-C_4H_8-2	0.33	0.48	0.20		~25	(300–350)
i-C_4H_8	0.35	0.58	0.10		~25	(300–350)
C_2H_6	0.27	0.44	0.50	(350°C)	17.0	(>270)
	–	0.07	0.95	(240°C)	6.8	(<270)
C_3H_8	0.26	0.29	0.53		21.0	(>230)
					~7	(<230)
CO	–	0.47	0.55		25.1	(>220)
					15	(<220)

(a) Temp, 250–400°C; rate of CO_2 produced = $k(p_{O_2})^m p_{HC}{}^n p_{H_2O}{}^l$.

ESTIMATION PROCEDURES FOR CHEMICAL KINETIC RATE DATA

The development of the theory of chemical-reaction rates has received considerable attention in the past and promises to be an area of intense activity in the future. Theoretical methods for accurately predicting chemical rate constants are extremely complex to apply and are only successful for a limited number of very simple reactions. No attempt is made here to delve into the detailed quantum-mechanical aspects of chemical kinetics. Major emphasis is on the presentation of simple estimation procedures that can be easily adapted to the design and analysis of afterburner systems. The estimation procedures presented here are for gas-phase homogeneous reactions. A recent collection of papers summarizes the current status of the theory of elementary gas reactions.(159)

There are several sources that cover procedures for estimating kinetic rate constants for combustion reactions.(121-127) These references can be consulted for details beyond those covered here. The approach outlined in this report for estimating oxidation rate constants for organics is based essentially on modified collision theory.

REACTION RATE THEORY

The simple collision treatment of chemical reactions is based on hard sphere collisions and suffers from the fact that the internal states of reactants are neglected. A more realistic theory which has improved the quality of calculated rate constants is commonly called the transition-state theory. In this approach an attempt is made to follow a reaction in terms of the changes in potential energy of the reactants and products as they approach each other and then separate. Unimolecular reactions which typify hydrocarbon pyrolysis can with some degree of success be treated as a special case of transition rate theory.

From transition rate theory[128], the parameters in the standard rate expression

$$k = A\, e^{-E_a/RT}$$

can be written as

$$A = \left(\frac{e\, k_B\, T_m}{h}\right) e^{-\Delta S^{\ddagger}/R}$$

and

$$E_a = \Delta H^{\ddagger} + RT_m$$

where T_m is a mean temperature, k_B is Boltzmann's constant, and h is Planck's constant. $\Delta H^{\ddagger}$ and $\Delta S^{\ddagger}$ are the enthalpy of activation and the entropy of activation, respectively, for the transition-state complex. In order to determine the thermodynamic parameters of the transition-state complex it is necessary to know its structure, which is the main limitation in trying to use transition-state theory to obtain practical rate constants. It is often possible to make good estimates of $\Delta S^{\ddagger}$; however, determination of $\Delta H^{\ddagger}$ requires a very detailed knowledge of the potential energy surface as a function of reaction coordinates. Detailed procedures for estimating $\Delta S^{\ddagger}$ and $\Delta H^{\ddagger}$ for combustion reactions can be found through correlations in References (125) or (126).

Unimolecular Reactions

In the case of unimolecular reactions the frequency factors, $A(\Delta S^{\ddagger})$, can be estimated with reasonable success. For the simple removal of an atom from a molecule, the entropy increase in going to the transition state is usually in the range of 0 to 9 cal/mole. This is equivalent to an A-value in the range from $10^{13.5}$ to $10^{15.5}$ sec^{-1}. A more accurate value may be determined by taking into account whether a light or heavy atom is being removed, or whether multiple bond formation occurs in the transition state. For detachment of a hydrogen atom from ethane, $3.6 \leqslant \Delta S^{\ddagger} \leqslant 7$ cal/mole-°K and $10^{14} \leqslant A \leqslant 6 \times 10^{14}$ sec^{-1}. If the atom being separated is relatively heavy such as in the case of the removal of I from CH_3I then $A \sim 10^{15}$ sec^{-1}. In cases where internal changes occur with bond breaking such as in the case of

$$C_2H_5 \rightarrow [H_2C - CH_2 \text{--} H]^{\ddagger} \rightarrow C_2H_4 + H$$

then $A \sim 2 \times 10^{13}$ sec^{-1}. Activation energies of these types of reactions can often be estimated from the reverse reactions which are about zero for atom-radical reactions and about 2 kcal/mole for atom-molecule reactions of this type. When fission produces two polyatomic fragments as in the case of

$$C_2H_6 \rightarrow CH_3 + CH_3$$

there is a large entropy increase in going from the reactants to the transition state. Most of these reactions have $\Delta S^{\ddagger}$ values of around 11.5 cal/mole°K, which corresponds to an A of about 10^{16} sec^{-1}. If the products are stiffened by double bond formation, then the value of A will be reduced. Activation energies for simple fission reactions can be estimated from

$$E_A\,(\text{unimolecular}) = \Delta E^0_T = \Delta E^0_{298} + \langle \Delta C_V \rangle\,(T - 298°K) \quad .$$

This is based on the fact that the activation energy of the back reaction, the recombination of two free radicals, is zero. Strength of the bonds being broken is given by

$$\Delta H^0_{298} = \Delta H^0_f\,(\text{products}) - \Delta H^0_f\,(\text{reactants})$$

and

$$\Delta E^0_{298} = \Delta H^0 - RT \quad .$$

$$<\Delta C_V^0> \cong \tfrac{1}{2}\,[\Delta C_V^0(T_0) + \Delta C_V^0(T_1)]$$

where C_V is the constant volume heat capacity and

$$\Delta C_V^0 = r\,C_V^0\,(R) + q\,C_V^0\,(Q) - a\,C_V^0\,(A) - b\,C_V^0\,(B)$$

based on the chemical reaction

$$a\,A + b\,B \rightarrow r\,R + q\,Q \quad .$$

Thermodynamic data can be obtained from the *JANAF Thermochemical Tables* or other compilations of thermodynamic data. General information on a number of organic substances is given in Table C-1 in Appendix C.

Fissions where two or more bonds are broken and two or more bonds are formed are generally divided into three classes: four-center, five-center, and six-center reactions. Four-center reactions which have 4 cyclic transition states such as in the case of the reaction $C_2H_5I \rightarrow C_2H_4 + HI$ have frequency factors of $10^{13\pm1}$ sec^{-1}, while five-center reactions, such as $C_2H_5NO_2 \rightarrow C_2H_4 + HONO$ have frequency factors of about 10^{12} sec^{-1}. Six-center reactions fall into 3 groups. In ethers, such as ethyl vinyl ether, where there is nearly free rotation about the vinyl C—O bond, A is equal to around 3×10^{11} sec^{-1}. With esters, where the acyl C—O bond has a large torsion barrier, the frequency factors run around 3×10^{12} sec^{-1}. On the other hand, for the pyrolysis of symmetrical trioxanes the A values are about 3×10^{14} sec^{-1}.

A large number of complex fissions occur through rather complex mechanisms involving biradicals. This type of reaction includes the pyrolysis of ring compounds. The simplest reactions involving a biradical transition state are cis-trans isomerizations. For this type of reaction frequency factors lie in the range from 10^{11} to 3×10^{13}. Further details on the use of transition-state theory may be found by consulting the paper by Golden(121) and the accompanying references. A detailed method for estimating Arrhenius A factors for four- and six-center unimolecular reactions is given by O'Neal and Benson.(164)

Bimolecular Reactions

Gas-phase bimolecular reactions can be classified as three main types: atom transfer, addition to double bonds, and association reactions. These types of reactions are often exothermic producing products in vibrationally excited states which must be deactivated through collisions or the products will react further or revert to the original reactants.

From transition-state theory, the frequency factor, A, for a bimolecular reaction is given by

$$A = \frac{e\,k\,T}{h}\,e^{\Delta S^\ddagger/R}$$

where $\Delta S^\ddagger$ is the entropy change for forming the transition state from the reactants. There is always a loss of entropy in going to the transition state $A + B \rightarrow AB^\ddagger$, so $\Delta S^\ddagger$ is always negative. An upper limit for A is about $10^{11.5}$ liter/mole-sec at 600°K, which corresponds to the gas kinetic collision frequency.

For a wide variety of metathesis reactions involving atoms the A's fall in the range from $10^{11.0}$ to $10^{11.5}$ M^{-1} sec^{-1} with minimum values all above 10^{10} M^{-1} sec^{-1}. Reactions between radicals and molecules have A's in the range of 10^{8} M^{-1} sec^{-1}. A-values for an abstraction or an addition to a double bond are in the range from $10^{10.5}$ to $10^{11.0}$ M^{-1} sec^{-1}. Reactions involving the association of two free radicals have A's falling from 10^9 to 10^{10} M^{-1} sec^{-1}. Frequency factors for association reactions also can be estimated from the A's for the reverse unimolecular process and the equilibrium constant for the reaction.

There is little difference between the activation energies for bimolecular reactions of atoms or polyatomic radicals. In the case of both abstraction and addition of atoms and polyatomic radicals to double bonds, the activation energy, to a good approximation is 8 ± 3 kcal/mole plus an endothermicity. Exceptions are the reactions involving very reactive halogen atoms, which have activation energies in the range from 0 to 5 kcal/mole, and radical-radical combination and disproportionation reactions which have values of the order of zero.

Several procedures have been reported recently for estimating activation energies.(127,129–131)

The intrinsic activation energy of a reaction, defined as the activation energy in the exothermic direction, is a measure of the amount by which the electron clouds around the reactants must be deformed so that the reaction can proceed. Intrinsic activation energies for the three different bimolecular reactions are given in Table 45. It has been found by Alfassi and Benson(129) that for the reaction

$$A + BC \leftrightarrow (A\cdots B\cdots C)^{\ddagger} \leftarrow AB + C + \text{energy}$$

the intrinsic activation energy can be correlated using the empirical relationship

$$E_A\ (\text{intrinsic}) = 13.0 - 3.30\mathrm{I}$$

where I is the sum of the electron affinities in eV of A and C with E_A (intrinsic) in kcal/mole. Negative values of E_A (intrinsic) are taken as zero. Taking into account the exothermicity of the reaction, ΔH_r, the expression can be improved in the form

$$E_A\ (\text{intrinsic}) = \frac{14.8 - 3.64\,\mathrm{I}}{1 + \Delta H_r/40} \quad .$$

A simpler and improved form is given by the bond additivity relation

$$E_A\ (\text{intrinsic}) = X_A + X_C$$

where X_A and X_C are additive group contributions. Best results are found with the expression

$$E_A\ (\text{intrinsic}) = (F_A)\ (F_B) \quad .$$

Values of electron affinities, X's and F's are presented in Tables C-2 and C-3 in Appendix C.

TABLE 45. INTRINSIC ACTIVATION ENERGIES FOR BIMOLECULAR REACTIONS(132)

Reaction Class	Electronic Structures	Range of Intrinsic Activation Energy, kcal/mole
Molecule + molecule	Two closed shells	20–50
Radical + molecule	One closed shell/one open shell	0–15
Radical + radical	Two [illegible]en shells	0

ESTIMATION PROCEDURES

There are also a number of procedures that can be used for estimating rate constants when experimental data are unavailable. If data are available at temperatures other than those in the range of interest, it is sometimes possible to apply extrapolation procedures. One common method for extrapolating data is to use a plot of the logarithm of the rate constant versus the reciprocal of the absolute temperature. When the rate data have been correlated in terms of an Arrhenius equation such as $k = A\ e^{-E/RT}$, the procedure is equivalent to using the equation over a greater temperature range than that covered experimentally.

If reaction rate data are available for the reverse direction of a reaction, it is possible to obtain rate data for the reaction proceeding in the forward direction through use of the equilibrium constant for the reaction.(133) As an example, consider the reaction

$$aA + bB \underset{k_r}{\overset{k_f}{\rightleftharpoons}} cC + dD \quad .$$

The equilibrium expression is

$$K = \frac{(C)^c\ (D)^d}{(A)^a\ (B)^b} \quad ,$$

where K is the equilibrium constant. The rate of the forward reaction can be expressed as $k_f\ (A)^a\ (B)^b$, while the reverse reaction is given as $k_r\ (C)^c\ (D)^d$. At equilibrium the forward and reverse reaction rates are equal

$$k_f\ (A)^a\ (B)^b = k_r\ (C)^c\ (D)^d \quad ,$$

which when rearranged give the ratio

$$\frac{k_f}{k_r} = \frac{(C)^c\ (D)^d}{(A)^a\ (B)^b} \quad ,$$

where

$$\frac{k_f}{k_r} = K \quad .$$

Thus, if either the reverse or forward reaction is known it is possible to determine the opposing reaction rate assuming the principle of microscopic reversibility to be valid.

Theoretical Procedures

Reaction rates may also be estimated on the basis of theoretical considerations. In considering the derivation of a reaction rate constant, it is often convenient to express it in the following form

$$k = A\ e^{-E_A/RT} \quad ,$$

where A is a constant and E_A is the Arrhenius activation energy.

For the purpose of afterburner design applications it is recommended that when rate constants cannot be inferred from experimental data, the rate constants be calculated using simple collision theory augmented by appropriate transition-state corrections. The more complicated theoretical procedures that are available require very expensive computer calculations and usually do not warrant the effort.

For the simple bimolecular reaction

$$A + B \rightarrow C + D \quad ,$$

the differential rate equation is

$$\frac{-dC_A}{dt} = \frac{-dC_B}{dt} = \frac{dC_C}{dt} = \frac{dC_D}{dt} = k\, C_A\, C_B \quad ,$$

where C represents the species concentration and t is the reaction time. The collision rate of molecules A and B in a gaseous mixture can be expressed using kinetic theory as

$$z = \sigma_{AB}^2 \,(8\pi k_B T)^{1/2} \left(\frac{M_A + M_B}{M_A\, M_B}\right)^{1/2} n_A n_B \quad \text{collisions/(sec)(cm}^3\text{)} \quad ,$$

$\sigma_{AB} = (\sigma_A + \sigma_B)/2$
σ = molecular diameter, cm
M = molecular weight, g per molecule
k_B = Boltzmann constant, 1.38×10^{-16} erg per °K.
The n's represent particle number density.

The equation for z can also be expressed in terms of the gas constant as

$$z = \sigma_{AB}^2 \,(8\pi RT)^{1/2} \left(\frac{M_A + M_B}{M_A\, M_B}\right)^{1/2} n_A n_B \quad \text{collisions/(sec)(cm}^3\text{)} \quad ,$$

where

R = gas constant, 8.314×10^7 erg/(°K)(g mole)
M = molecular weight, AMU

Collision diameters for a number of the species of interest in this study are listed in Table 7. When data are not available, the collision diameter may be approximated using the equation

$$\sigma = 1.18\, V_B^{1/3} \quad ,$$

where V_B is the LeBas volume or the molal volume at the normal boiling point.(134) For organic compounds, V_B can be calculated by adding together the appropriate values for each of the constituent elements given in Table 46.(135) As an example, the atomic volume of C_2H_6 can be calculated to be $2 \times 14.8 + 6 \times 3.7 = 51.8$ cm^3 per g-mole.

Correlation techniques for determining molecular volumes of hydrocarbons have also been developed by Kurtz and Sankin.(137)

Hard-sphere collision diameters can also be determined from the Lennard-Jones parameters. A procedure for these calculations taken from Gardiner's book(8) is outlined in Table C-4 in Appendix C. Lennard-Jones parameters for a wide variety of compounds are given in Table C-5.

Not every collision results in the transformation of reactants into products, since only the more energetic collisions with certain orientations between reacting species lead to a reaction. From Maxwell's distribution law the fraction of all bimolecular collisions that involve energies above a certain minimum energy is given approximately by

$$e^{-E_0/RT} \quad ,$$

TABLE 46. ADDITIVE VOLUME INCREMENTS FOR ESTIMATING MOLAR VOLUMES AT THE NORMAL BOILING POINT[135,136]

Element[a]	Atomic Volume, cm^3 per g mole
Bromine	27.0
Carbon	14.8
Chlorine	
Terminal, as in R-Cl	21.6
Medial, as in R-CHCl-R	24.6
Fluorine	8.7
Hydrogen	
In compounds	3.7
In hydrogen molecule	7.15
Nitrogen	
Double-bonded	15.6
In primary amines	10.5
In secondary amines	12.0
In nitrogen molecule	15.6
Oxygen	
Double-bonded	7.4
In aldehydes and ketones	7.4
In methyl esters	9.1
In ethyl esters	9.9
In higher esters and ethers	11.0
In acids	12.0
In union with sulfur, phosphorus, nitrogen	8.3
Iodine	37.0
Sulfur	25.6

(a) For benzene ring deduct 15; for naphthalene ring deduct 30.

where R is the gas constant, T the absolute temperature, and E_0 is an energy term. The orientation factor, or steric factor, will be discussed in more detail below. If E_0 is expressed in calories, then R is equal to 1.987 cal/(g mole)(°K). For the bimolecular reaction, the disappearance of A may be expressed as

$$
\begin{aligned}
-\frac{dn_A}{dt} &= (\text{collision rate}) \times \left(\begin{matrix}\text{fraction of collisions involving} \\ \text{energies in excess of } E_0\end{matrix}\right) \times \quad (\text{steric factor}) \\
&= \sigma^2_{AB} (8\pi RT)^{1/2} \left[(M_A + M_B)/M_A M_B\right]^{1/2} n_A n_B \, p \, e^{-E_0/RT} \\
&= k \, n_A n_B \quad .
\end{aligned}
$$

Therefore,

$$k = \sigma_{AB}^2 \, (8\pi RT)^{1/2} \, p(M_A + M_B/M_A M_B)^{1/2} \, e^{-E_0/RT}$$

$$= Z'pT^{1/2} \, e^{-E_0/RT} \, \text{cm}^3/(\text{molecule})(\text{sec}) \quad ,$$

where

$$Z' = \sigma_{AB}^2 \, (8\pi R)^{1/2} \left(\frac{M_A + M_B}{M_A M_B}\right)^{1/2} \quad \text{cm}^3/(\text{molecule})(\text{sec})(\text{K}^{1/2}) \quad .$$

If the rate equation is expressed as

$$-\frac{dC_A}{dt} = k \, C_A \, C_B \quad ,$$

where C_A and C_B are in units of g moles per liter, then

$$Z' = \sigma_{AB}^2 \, (8\pi R)^{1/2} \frac{N}{10^3} \left(\frac{M_A + M_B}{M_A M_B}\right)^{1/2} \quad \text{liter}/(\text{mole})(\text{sec})(\text{K}^{1/2}) \quad ,$$

where

N = Avogadro's number, 6.023×10^{23} molecules/g mole and
σ_{AB} is still expressed in cm. Making the appropriate substitutions:

$$Z' = 2.76 \times 10^{25} \, \sigma_{AB}^2 \left(\frac{M_A + M_B}{M_A M_B}\right)^{1/2} \quad \text{liter}/(\text{mole})(\text{sec})(\text{K}^{1/2}) \quad .$$

Approximate values for the steric factors based on transition-state theory for various types of reactions are summarized in Table 6.

Several techniques have been proposed for estimating activation energies for bimolecular reactions. These techniques have been reviewed by Laidler and Polanyi(142) and Szabo(143). The most popular method of estimating activation energies is that suggested by Evans and Polanyi.(144) They found that for a series of closely related compounds the activation energy is proportional to the heat of reaction. Semenov(145) has shown that for a number of exothermic abstraction reactions the activation energy, E_A, is approximately related to the heat of reaction, ΔH, by

$$E_A = 0.25 \, \Delta H + 11.5 \quad .$$

A less reliable method has been proposed by Hirschfelder.(146) For an exothermic reaction of the type

$$A + BC = AB + C \quad ,$$

the activation energy follows roughly the relationship

$$E_A = 0.055 \, D_B \quad ,$$

where D_B is the dissociation energy of bond BC. If the reaction is endothermic, it is best to calculate E for the reverse reaction from which E_A can be calculated for the forward reaction. Szabo(143,147) has developed an empirical formulation for a homogeneous gas reaction based on the energies of the bonds broken and the bonds formed where

$$E_A = \sum_i D_i \, (\text{broken}) - \alpha \sum_j D_j \, (\text{formed}) \quad ,$$

and α is a constant for a given type of reaction. Values of α have been determined for several homologous series of reactions.(147) Values of α for several classes of reactions are tabulated in Table C-7 in Appendix C.

Bond energies or strengths for a number of simple bonds in small molecules are tabulated in Table C-8. A technique developed by Szabo(7) can be used to calculate strengths for bonds in large molecules. This approach is based on the bond strengths and decrements given in Table 47 and takes into account the fact that bond strength between two atoms is influenced by the adjacent atoms and groups. For example, the strength of the n-C_3H_7–$CH_2C_6H_5$ bond is calculated from the values in the table as

$$161 - 4 \times 13 - 16 - 34 = 59 \text{ kcal} \quad .$$

The general theory of three-body reactions is not well established and very difficult to apply.(148-150) It is sometimes of interest in estimating three-body reaction rates to know the number of three-body collisions occurring in a reacting system. The number of triple collisions per unit time and volume has been derived by Tolman(151) as

$$z = n_A n_B n_C \, (4\pi\sigma_{AB}^2) \, (4\pi\sigma_{BC}^2) \, \delta \sqrt{\frac{RT}{2\pi}} \left[\sqrt{\frac{M_A + M_B}{M_A M_B}} + \sqrt{\frac{M_B + M_C}{M_B M_C}} \right] \text{collisions/(cm}^3\text{)(sec)} \quad ,$$

where the n's are concentrations in terms of molecules per cm^3. This equation assumes that the colliding species are rigid elastic spheres and that a collision exists when these spheres are within a small distance, δ, of each other. It is also assumed that δ is much smaller than the diameter of a molecule and is in the neighborhood of about 1 Å. Upper limits have been calculated for δ for several different reactions which are listed in Table 48.(152) For the third-order reactions

$$A + B + C \rightarrow \text{products} \quad ,$$

the differential rate equation is

$$\frac{dn_A}{dt} = -\,k\, n_A n_B n_C \quad .$$

Assuming a collision efficiency factor of $pe^{-E_0/RT}$, the rate constant may be determined from the collision frequency as

$$k = (4\pi\sigma_{AB}^2) \, (4\pi\sigma_{BC}^2) \, \delta \sqrt{\frac{RT}{2\pi}} \left[\sqrt{\frac{M_A + M_B}{M_A M_B}} + \sqrt{\frac{M_B + M_C}{M_B M_C}} \right] pe^{-E_0/RT} \quad .$$

The ternary collision rate per unit volume has also been expressed by Moelwyn-Hughes(13) as the collisions of the molecular pair AB with all the C molecules. On this basis the collision equation is

$$Z = n_A n_B n_C \, 4\pi \, (r_A + r_B + r_C)^2 \, (r_A + r_B)^3 \sqrt{\frac{RT}{\pi}} \sqrt{\left(\frac{1}{M_C} + \frac{1}{M_A + M_B}\right)} \quad ,$$

where r represents the corresponding molecular radius.

In considering atomic recombination, two mechanisms have been postulated to account for experimental observations. At low temperatures, it appears that the principal mechanism involves first the combination of an atom with a molecule, forming a loose complex. Then a second atom collides with the complex, forming a diatomic molecule and the original molecule. At high temperatures, though, the principal mechanism appears to involve the direct single three-body collision as described by the Tolman or Moelwyn-Hughes collision equations covered in the preceding paragraphs.

The techniques just described are not intended to always produce accurate information. Often they do prove to be of value, though, when a kinetic analysis is attempted for situations where only a portion of the data is available. It is also sometimes valuable to be able to assess

TABLE 47. CONVENTIONAL BASIC VALUES AND DECREMENTS FOR THE CALCULATION OF BOND STRENGTHS(7)

Conventional Basic Values in kcal			
$\equiv C-C\equiv$	161	$\equiv C-S-$	127
$\equiv C-H$	142	$\equiv C-N=$	145
$\equiv C-F$	147	$-S-S-$	103
$\equiv C-Cl$	120	$-S-H$	104
$\equiv C-Br$	106	$-O-O-$	66
$\equiv C-I$	93	$-O-H$	123
$\equiv C-O-$	147	$=N-N=$	112
$=C=O$	200		
Decrements in kcal			
$-H$	13	$-CH=CH_2$	36
$-F$	14	$-COCH_3$	18
$-Cl$	19	$-CH_2C(CH_3)=CH_2$	37
$-Br$	18	$-OC(CH_3)_3$	15
$-O$	22	$-C_6H_5$[a]	32
$=O$	33	$-C_6H_5$	34
$\equiv N$	18	o-$C_6H_4CH_3$	41
$-CH_3$	15	m-$C_6H_4CH_3$	39
$=CH_2$	25	p-$C_6H_4CH_3$	40
$\equiv CH$	11	(o,m,p)$-CH_2C_6H_4F$	38
$-CH_2Cl$	22	$-\alpha$-naphthyl[a]	35
$-CHCl_2$	32	$-\beta$-naphthyl[a]	36
$-CCl_3$	42	9-phenanthryl[a]	38
$-C_2H_5$	16	9-anthracyl[a]	40

(a) A carbon atom in the aromatic ring forms part of the affected bond.

TABLE 48. UPPER LIMITS FOR δ IN TOLMAN'S THREE-BODY-COLLISION EQUATION(152)

Reaction	δ, cm
$H + H + H \rightarrow H_2 + H$	5×10^{-9}
$H + H + H_2 \rightarrow H_2 + H_2$	5×10^{-10}
$O + O + O_2 \rightarrow O_2 + O_2$	5×10^{-11}
$N + N + N_2 \rightarrow N_2 + N_2$	5×10^{-11}
$O + O_2 + O_2 \rightarrow O_3 + O_2$	5×10^{-11}
$H + O_2 + H_2 \rightarrow HO_2 + H_2$	6×10^{-14}

the importance of a particular reaction in an overall reaction scheme by either estimating the value of the rate constant or establishing an upper limit for it. This information may be used to determine the conditions for which a particular reaction is unimportant to the overall reaction scheme, or it may aid in choosing which particular reactions must be studied in the laboratory to develop a kinetic model of the overall reaction scheme for a complex chemical system.

PROCEDURES FOR RAPID ESTIMATION OF KINETIC DATA

Rate constants may be estimated on the basis of the modified Arrhenius expression

$$k = A\,T^{n}\,e^{-E_B/RT}$$

using the relations given below for various types of reactions.(153) Units for the rate constants are in terms of cc, g-mole, seconds, °K, and kcal.

- Exothermic termolecular reaction

$$B + C + M \rightarrow BC + M$$

$$k = 3 \times 10^{16}\,T^{-0.5}$$

- Exothermic bimolecular reactions with triatomic transition states

$$B + CD \rightarrow BC + D$$

$$k = 5 \times 10^{11}\,T^{0.5}\,e^{-E_B/RT}$$

where E_B = 5.5 percent of the CD bond energy.

- Exothermic bimolecular reactions with transition states of more than 3 atoms

$$BC + DE \rightarrow BCD + E$$

$$k = 1 \times 10^{11}\,T^{0.5}\,e^{-E_B/RT}$$

where E_B = 5.5 percent of the DE bond energy.

- Exothermic bimolecular binary exchange reactions

$$BC + DE \rightarrow BD + CE$$

$$k = 1 \times 10^{10}\,T^{0.5}\,e^{-E_B/RT}$$

where E_B = 28 percent of the sum of the BC and DE bond energies.

Appropriate bond energies for these calculations can be found in the appendix or estimated using the procedures outlined in the previous section on Estimation Procedures.

More refined approximations for rate constants may be obtained using the procedures already described.

SUMMARY AND CONCLUSIONS

Details of mechanisms have been reviewed for oxidation and pyrolysis reactions involving organic vapors. Rate data have been compiled for both global and complex mechanisms of interest for the design and analysis of fume afterburner systems. The available rate data are quite limited; so attention has been given to procedures for estimating reaction rates.

For estimating the rates of homogeneous gas phase reactions modified collision theory is recommended. This estimation procedure requires the determination of three factors: (1) the collision frequency, (2) the steric factor or collision efficiency, and (3) the activation energy. Recipes for the calculation of each of these factors and the required data are presented in the previous section and Appendix C. It is intended that these techniques will provide acceptable rate data for any afterburner application. Rapid, but probably less reliable, estimates can also be made by either comparing the unknown reaction with similar reactions for which known rate data are tabulated or by using the rapid estimation procedures that are outlined.

When kinetic rate data are not defined explicitly for either complete combustion to CO_2 and H_2O or for a specific yield of CO_2 and CO, it is probably reasonable to assume that the hydrocarbon oxidation results in only CO production which is then converted to CO_2 according to the kinetics of CO oxidation. The initial attack of an organic by oxygen is generally rapid and it is often the CO kinetics that largely control the overall kinetics of complete combustion.

Rates for catalytic surface reactions cannot be predicted with any degree of certainty. Reliable catalytic rate data can only be obtained through well-defined empirical measurements involving the catalyst of interest. However, in some cases, rate data can be estimated using the information compiled in this report for typical afterburner-type catalysts.

Various integrated rate expressions which can be used to estimate residence times for afterburner systems are presented in this report. These expressions are based on simple plug-flow models and do not take mixing and recirculation effects into account. Most afterburners can be divided conceptually into two sections: a mixing section and a combustion section. Generally good mixing can be achieved through proper design considerations; however, recirculation and backmixing in the combustion section and their effect on residence time can be more difficult to take into account. In many cases, however, the plug-flow model can provide adequate approximations for design applications.

For reliable modeling of afterburner systems detailed computer analyses are generally required to couple both the chemical and physical processes. A simplified analysis developed by Levenspiel and Bischoff(154), though, can often be used with good results to correct residence times calculated on the basis of plug flow for recirculation and backmixing effects.

REFERENCES

(1) R. W. Rolke, R. D. Hawthorne, C. R. Garbett, E. R. Slater, T. T. Phillips, and G. D. Towell, "Afterburner Systems Study", Final Report under U.S. EPA Contract EHS-D-71-3. U.S. Government Printing Office, PB 212560 (1972).

(2) J. L. Franklin, "Mechanisms and Kinetics of Hydrocarbon Combustion", *Annual Review of Physical Chemistry*, **18**, 261 (1967).

(3) J. N. Bradley, *Flame and Combustion Phenomena*, Mathuen & Co. Ltd., London (1969).

(4) C. H. Bamford and C.F.H. Tipper (Editors), *Comprehensive Chemical Kinetics*, Vol. 17, Gas-Phase Combustion, Elsevier Scientific Publishing Company (1977).

(5) I. Glassman, *Combustion*, Academic Press (1977).

(6) A. A. Boni and R. C. Penner, "Sensitivity Analysis of a Mechanism for Methane Oxidation Kinetics", *Combustion Science and Technology*, **15**, 99 (1977).

(7) Z. G. Szabó, *Advances in the Kinetics of Homogeneous Gas Reactions*, Methuen (1964).

(8) W. C. Gardiner, Jr., *Rates and Mechanisms of Chemical Reactions*, W. A. Benjamin, Inc. (1969).

(9) R. H. Perry and C. H. Chilton, *Chemical Engineers' Handbook*, 5th Edition, McGraw-Hill (1973).

(10) R. D. Hawthorn, "Afterburner Catalysts—Effects of Heat and Mass Transfer Between Gas and Catalyst Surface", AIChE Symposium Series No. 137, Vol. 70, 428 (1974).

(11) J. M. Smith, *Chemical Engineering Kinetics*, McGraw-Hill (1956).

(12) A. Kreglewski, "A Semiempirical Treatment of Properties of Fluid Mixtures", *J. Phys. Chem.*, **71**, 2860 (1967).

(13) E. A. Moelwyn-Hughes, *Physical Chemistry*, 2nd Edition, Pergamon Press (1961).

(14) S. Dushman, *Scientific Foundations of Vacuum Technique*, 2nd Edition, Wiley (1965).

(15) J. G. Koch, "Chemical Kinetics Tables, Data Evaluations, and Bibliographies. A Guide to the Literature", revised September, 1976, NBS List of Publications No. 73.

(16) R. F. Hampson, Jr. and D. Garvin, "Evaluation and Compilation of Reaction Rate Data", *J. Phys. Chem.*, **81**, 2317 (1977).

(17) "Tables of Chemical Kinetics. Homogeneous Reactions", NBS Circular 510 (PB 192339) (1951).

(18) "Tables of Chemical Kinetics. Homogeneous Reactions", Supplement 1 to NBS Circular 510 (PB 192340) (1956).

(19) "Alphabetical Index to Tables of Chemical Kinetics. Homogeneous Reactions", Supplement 2 to NBS Circular 510 (PB 192341) (1960).

(20) "Tables of Chemical Kinetics. Homogeneous Reactions", Supplementary Tables to Accompany Circular 510 and Supplements 1 and 2, NBS Monograph 34, U.S. Government Printing Office, Washington, D.C. 20402 (1961).

(21) "Tables of Chemical Kinetics. Homogeneous Reactions", Supplementary Tables, NBS Monograph 34, Vol. 2, U.S. Government Printing Office, Washington, D.C. 20402 (1964).

(22) A. F. Trotman-Dickenson and G. S. Milne, *Tables of Bimolecular Gas Reactions*, NSRDS-NBS 9 (1967).

(23) V. N. Kondratiev, *Rate Constants of Gas Phase Reactions*, NBS Publication COM-72-10014 (1972).

(24) D. L. Baulch, D. D. Drysdale, D. B. Horne, and A. C. Lloyd, "Evaluated Kinetic Data for High-Temperature Reactions, Vol. 1, Homogeneous Gas Phase Reactions of the H_2-O_2 Systems", Butterworths, London (1972).

(25) D. L. Baulch, D. D. Drysdale, and D. G. Horne, "Evaluated Kinetic Data for High-Temperature Reactions, Vol. 2, Homogeneous Gas Phase Reactions of the H_2-N_2-O_2 Systems", Butterworths, London (1973).

(26) D. L. Baulch, D. D. Drysdale, J. Duxbury, and S. Grant, "Evaluated Kinetic Data for High-Temperature Reactions, Vol. 3, Homogeneous Gas Phase Reactions of the O_2-O_3 System, the CO-O_2-H_2 System, and of Sulfur-Containing Species", Butterworths, London (1976).

(27) V. S. Engleman, "Survey and Evaluation of Kinetic Data on Reactions in Methane/Air Combustion", Report No. EPA-600/2-76-003 (1976).

(28) F. Westley, "Chemical Kinetics in the C-O-S and H-N-O-S Systems: A Bibliography 1899 through June 1971", NBS Special Publication 362 (1972).

(29) F. Westley, "A Supplementary Bibliography of Kinetic Data on Gas Phase Reactions of Nitrogen, Oxygen, and Nitrogen Oxides", NBS Special Publication 371 (1973).

(30) R. F. Hampson, Jr., and D. Garvin, "Chemical Kinetic and Photochemical Data for Modelling Atmospheric Chemistry", NBS Technical Note 866 (1975).

(31) J. L. Franklin, "Mechanisms and Kinetics of Hydrocarbon Combustion", *Annual Review of Physical Chemistry*, **18**, 261 (1967).

(32) F. Westley, "Chemical Kinetics of the Gas Phase Combustion of Fuels (A Bibliography on Rates and Mechanisms of Oxidation of Aliphatic C_1 to C_{10} Hydrocarbons and of Their Oxygenated Derivatives)", NBS Special Publication 449 (1976).

(33) R. W. Walker, "A Critical Survey of Rate Constants for Reactions in Gas-Phase Hydrocarbon Oxidation", *Reaction Kinetics*, Vol. 1, p. 161, A Specialist Periodical Report (The Chemical Society, Burlington House, London) (1975).

(34) L. A. Wall, "The Mechanisms of Pyrolysis, Oxidation, and Burning of Organic Materials", NBS Special Publication 357 (1972).

(35) V. Ya. Shtern, *The Gas-Phase Oxidation of Hydrocarbons*, Macmillan (1964).

(36) G. McKay, "The Gas-Phase Oxidations of Hydrocarbons", *Prog. Energy Combust. Sci.*, **3**, 105 (1977).

(37) F. R. Mayo, *Oxidation of Organic Compounds*, Vol. II. Gas-Phase Oxidations, Homogeneous and heterogeneous Catalysis, Applied Oxidations and Synthetic Processes, *Advan. Chem. Ser.*, **76** (1968).

(38) K. Schofield, "An Evaluation of Kinetic Rate Data for Reactions of Neutrals of Atmospheric Interest", *Planetary and Space Science*, **15**, 643 (1967).

(39) R. F. Hampson, W. Braun, R. L. Brown, D. Garvin, J. T. Herron, R. E. Huie, M. J. Kurylo, A. H. Laufer, J. D. McKinley, H. Okabe, M. D. Scheer, and W. Tsang, "Survey of Photochemical and Rate Data for Twenty-Eight Reactions of Atmospheric Chemistry", *J. Phys. Chem. Ref. Data*, **2**, 267 (1973).

(40) J. T. Herron and R. E. Huie, "Rate Constants for the Reactions of Atomic Oxygen (O^3P) With Organic Compounds in the Gas Phase", *J. Phys. Chem. Ref. Data*, **2**, 467 (1973).

(41) K. Schofield, "Evaluated Chemical Kinetic Rate Constants for Various Gas Phase Reactions", *J. Phys. Chem. Ref. Data*, **2**, 25 (1973).

(42) W. E. Wilson, Jr., "A Critical Review of the Gas-Phase Reaction Kinetics of the Hydroxyl Radical", *J. Phys. Chem. Ref. Data*, **1**, 535 (1972).

(43) L. A. Wall, Editor, "The Mechanisms of Pyrolysis, Oxidation, and Burning of Organic Materials", National Bureau of Standards Special Publication 357 (June 1972).

(44) R. Tunder, S. Mayer, E. Cook, and L. Schieler, "Compilation of Reaction Rate Data for Nonequilibrium Performance and Reentry Calculation Programs", Aerospace Report No. TR-1001 (9210-02)-1, Aerospace Corporation (1967).

(45) S. W. Benson and H. E. O'Neal, *Kinetic Data on Gas Phase Unimolecular Reactions*, NBS Publication NSRDS-NBS-21 (1970).

(46) R. W. Bilger, "Reaction Rates in Diffusion Flames", *Combustion and Flame*, **30**, 277 (1977).

(47) A. Nemeth and R. F. Sawyer, "The Overall Kinetics of High-Temperature Methane Oxidation in a Flow Reactor", *J. Phys. Chem.*, **73**, 2421 (1969).

(48) G. I. Kozlov, "On High-Temperature Oxidation of Methane", Seventh Symposium (International) on Combustion, p. 142, The Combustion Institute, Pittsburgh, Pa. (1959).

(49) G. C. Williams, H. C. Hottel, and A. C. Morgan, "The Combustion of Methane in a Jet-Mixed Reactor", Twelfth Symposium (International) on Combustion, p. 913, The Combustion Institute, Pittsburgh, Pa. (1969).

(50) F. L. Dryer, and I. Glassman, "High-Temperature Oxidation of CO and CH_4", Fourteenth Symposium (International) on Combustion, p. 987, The Combustion Institute, Pittsburgh, Pa. (1973).

(51) I. Glassman, F. L. Dryer, and R. Cohen, "Combustion of Hydrocarbons in an Adiabatic Flow Reactor: Some Considerations and Overall Correlations of Reaction Rate", paper presented at Joint Meeting of the Central and Western States Sections of the Combustion Institute, San Antonio, Texas (April 21-22, 1975).

(52) R. A. Geisbrecht and T. E. Daubert, "Chemical and Physical Processes of Hydrocarbon Combustion: Chemical Processes", *Ind. Eng. Chem. Process Des. Dev.*, **14**, 159 (1975).

(53) W. H. Avery and R. W. Hart, "Combustion Performance with Instantaneous Mixing", *Ind. Eng. Chem.*, **45**, 1634 (1953).

(54) R. B. Edelman and O. F. Fortune, "A Quasi-Global Chemical Kinetic Model for the Finite Rate Combustion of Hydrocarbon Fuels with Application to Turbulent Burning and Mixing in Hypersonic Engines and Nozzles", AIAA Paper No. 69-86, New York (1969).

(55) H. C. Hottel, G. C. Williams, N. M. Nerheim, and G. R. Schneider, "Kinetic Studies in Stirred Reactors: Combustion of Carbon Monoxide and Propane", Tenth Symposium (International) on Combustion, p. 111, The Combustion Institute, Pittsburgh, Pa. (1965).

(56) G. A. Karim and M. O. Khan, "The Determination of Gross Chemical Kinetic Data for the Combustion of Common Fuels Using a Motored-Piston Engine", *J. Inst. Fuel*, 190 (1969).

(57) W. G. Appleby, W. H. Avery, W. K. Meerbott, and A. F. Sartor, "The Decomposition of n-Butane in the Presence of Oxygen", *J. Am. Chem. Soc.*, **75**, 1809 (1953).

(58) W. Chinitz and T. Baurer, "An Analysis of Nonequilibrium Hydrocarbon/Air Combustion", *Pyrodynamics*, **4**, 119 (1966).

(59) V. S. Engleman, W. Bartok, J. P. Longwell, and R. B. Edelman, "Experimental and Theoretical Studies of NO_x Formation in a Jet-Stirred Combustor", Fourteenth Symposium (International) on Combustion, p. 775, The Combustion Institute, Pittsburgh, Pa. (1973).

(60) R. B. Edelman, O. Fortune, and G. Weilerstein, "Some Observations on Flows Described by Coupled Mixing and Kinetics", in *Emissions from Continuous Combustion Systems*, Edited by W. Cornelius and W. G. Agnew, Plenum Press, New York (1972).

(61) R. Roberts, L. D. Aceto, R. Kollrack, J. M. Bonnell, and D. P. Teixeira, "An Analytical Model for Nitric Oxide Formation in a Gas Turbine Combustion Chamber", AIAA Paper NO. 71-715, Salt Lake City, Utah (1971).

(62) M. A. Nettleton, "Ignition and Combustion of a Fuel of Low Volatility (Hexadecane) in Shock-Heated Air", *Fuel*, **53**, 88 (1974).

(63) K. Seshadri and F. A. Williams, "Effect of CF_3Br on Counterflow Combustion of Liquid Fuel with Diluted Oxygen", in *Halogenated Fire Suppressants*, R. G. Gann (Ed.), ACS Symposium Series 16 (1975).

(64) K. H. Hemsath and P. E. Susey, "Fume Incineration Kinetics and Its Applications", AIChE Symposium Series No. 137, Vol. 70, 439 (1974).

(65) B. P. Mullins and S. S. Penner, *Explosions, Detonations, Flammability, and Ignition*, Pergamon Press (1959).

(66) A Murty Kanury, *Introduction to Combustion Phenomena*, Gordon and Breach (1975).

(67) W. E. Falconer and A. Van Tiggelen, "A Kinetic Study of Hydrocarbon-Oxygen-Nitrogen Flame Systems and Molecular Weights of Chain Carries", Ninth Symposium (International) on Combustion.

(68) J. P. Longwell and M. A. Weiss, "High Temperature Reaction Rates in Hydrocarbon Combustion", *Ind. Eng. Chem.*, **47**, 1634 (1955).

(69) N. A. Henein, "Diesel Engines Combustion and Emissions", in *Engine Emissions, Pollutant Formation and Measurement*, Edited by G. S. Springer and D. J. Patterson, Plenum Press (1973).

(70) J. L. Bolland, "Kinetics of Olefin Oxidation", *Chemical Society London Quarterly Reviews*, **3**, 1 (1949).

(71) L. Bateman, "Olefin Oxidation", *Chemical Society London Quarterly Reviews*, **8**, 147 (1954).

(72) E. McKean, D.J.M. Ray, A. Redfearn, R. Ruiz Diaz, and D. J. Waddington, "Gas Phase Oxidation of Alkenes: Propagation Reactions" in *Combustion Institute European Symposium 1973*, F. J. Weinberg (Ed.), Academic Press (1973).

(73) C. J. Jachimowski, "An Experimental and Analytical Study of Acetylene and Ethylene Oxidation Behind Shock Waves", *Combustion and Flame*, **29**, 55 (1977).

(74) J. Peeters and G. Mahnen, "Structure of Ethylene-Oxygen Flames. Reaction Mechanism and Rate Constants of Elementary Reactions" in *Combustion Institute European Symposium 1973*, F. J. Weinberg (Ed.), Academic Press (1973).

(75) S. A. Miller, *Ethylene and Its Industrial Derivatives*, Ernest Benn Limited, London (1969).

(76) A. Levy and F. J. Weinberg, "Optical Flame Structure Studies: Examination of Reaction Rate Laws in Lean Ethylene-Air Flames", *Combustion and Flame*, **3**, 229 (1959).

(77) D. R. White, "Density Induction Times in Very Lean Mixtures of D_2, H_2, C_2H_2, and C_2H_4, with O_2", Eleventh Symposium (International) on Combustion, p. 147, The Combustion Institute, Pittsburgh (1967).

(78) M. Suzuki, T. Moriwaki, S. Okazaki, T. Okuda, and T. Tanzawa, "Oxidation of Ethylene in Shock Tube", *Astronautica Acta*, **18**, 359 (1973).

(79) G. C. Williams, A. F. Sarofim, and N. Lambert, "Nitric Oxide Formation and Carbon Monoxide Burnout in a Compact Steam Generator", in *Emissions from Continuous Combustion Systems*, W. Cornelius and W. G. Agnew (Eds.), Plenum Press, New York (1972).

(80) J. B. Howard, G. C. Williams, and D. H. Fine, "Kinetics of Carbon Monoxide Oxidation in Postflame Gases", Fourteenth Symposium (International) on Combustion, p. 975, The Combustion Institute, Pittsburgh, Pa. (1973).

(81) C. T. Bowman, "Investigation of Nitric Oxide Formation Kinetics in Combustion Processes: The Hydrogen-Oxygen-Nitrogen Reaction", *Combustion Science and Technology*, **3**, 37 (1971).

(82) D. R. Jenkins, V. S. Yumlu, and D. B. Spalding, "Combustion of Hydrogen and Oxygen in a Steady-Flow Adiabatic Stirred Reactor", Eleventh Symposium (International) on Combustion, p. 779, The Combustion Institute, Pittsburgh, Pa. (1967).

(83) K. C. Salooja, "The Role of Aldehydes in Combustion: Studies of the Combustion Characteristics of Aldehydes and of Their Influence on Hydrocarbon Combustion Processes", *Combustion and Flame*, **9**, 373 (1965).

(84) I. A. Vardanyan, G. A. Sachyan, A. G. Philiposyan, and A. B. Nalbandyan, "Kinetics and Mechanism of Formaldehyde Oxidation—II", *Combustion and Flame*, **22**, 153 (1974).

(85) R. R. Baldwin, M. J. Matchan, and R. W. Walker, "The High-Temperature Oxidation of Acetaldehyde", *Combustion and Flame*, **15**, 109 (1970).

(86) P. Beeley, J. F. Griffiths, B. A. Hunt, and A. Williams, "The Combustion of Acetaldehyde Behind Incident Shock Waves", Sixteenth Symposium (International) on Combustion, p. 1013, The Combustion Institute, Pittsburgh, Pa. (1977).

(87) M. B. Colket, III, D. W. Naegeli, and I. Glassman, "High Temperature Oxidation of Acetaldehyde", Sixteenth Symposium (International) on Combustion, p. 1023, The Combustion Institute, Pittsburgh, Pa. (1977).

(88) C. T. Bowman, "A Shock-Tube Investigation of the High-Temperature Oxidation of Methanol", *Combustion and Flame*, **25**, 343 (1975).

(89) A. Cappelli, "Oxidation Reaction Engineering" in *Chemical Reaction Engineering Reviews*, H. M. Hulburt (Ed.), Advances in Chemistry Series 148, American Chemical Society, Washington, D.C. (1975).

(90) J. R. Kittrell and R. Mezak, "Reaction Rate Modeling in Heterogeneous Catalysis", *Ind. Eng. Chem.*, **59**, 28 (1967).

(91) O. A. Hougen and K. M. Watson, "Solid Catalysts and Reaction Rates", *Ind. Eng. Chem.*, **35**, 529 (1943).

(92) P. Mars and D. W. van Krevelen, *Chem. Eng. Sci. (Special Supplement)*, **3**, 41 (1954).

(93) M. A. Accomazzo and K. Nobe, "Catalytic Combustion of Methane, Ethane, and Propane with Copper Oxide", *Chemical Engineering Progress Symposium Series 45*, **59**, 71 (1963).

(94) K. J. Laidler, *Chemical Kinetics*, 2nd Edition, McGraw-Hill (1965).

(95) G. W. Young and H. L. Greene, "Kinetic Modeling for the Catalytic Oxidation of Benzo(α)pyrene", *J. of Catalysis*, **50**, 258 (1977).

(96) R. B. Anderson, K. C. Stein, J. J. Feenan, and L.J.E. Hofer, "Catalytic Oxidation of Methane", *Ind. Eng. Chem.*, **53**, 809 (1961).

(97) R. Mezaki and C. C. Watson, "Catalytic Oxidation of Methane", *Ind. Eng. Chem. Process Design and Development*, **5**, 62 (1966).

(98) M. A. Accomazzo and K. Nobe, "Catalytic Combustion of C_1 to C_3 Hydrocarbons", *Ind. Eng. Chem. Process Design and Development*, **4**, 425 (1965).

(99) J. A. Juusola, R. F. Mann, and J. Downie, "The Kinetics of the Vapor-Phase Oxidation of o-Xylene Over a Vanadium Oxide Catalyst", *J. Catalysis*, **17**, 106 (1970).

(100) S. E. Voltz, C. R. Morgan, D. Liederman, and S. M. Jacob, "Kinetic Study of Carbon Monoxide and Propylene Oxidation on Platinum Catalyst", *Ind. Eng. Chem. Prod. Res. Development.*, **12**, 294 (1973).

(101) Yung-Fang Yu Yao, "The Oxidation of Hydrocarbons and CO Over Metal Oxides III. Co_3O_4", *J. Catalysis*, **33**, 108 (1974).

(102) Yung-Fang Yu Yao and J. T. Kummer, "The Oxidation of Hydrocarbons and CO Over Metal Oxides I. NiO Crystals", *J. Catalysis*, **28**, 124 (1973).

(103) J. N. Bradley and D. A. Durden, "The Role of Pyrolysis Reactions in Hydrocarbon Oxidation", *Combustion and Flame*, **19**, 452 (1972).

(104) A. S. Gordon, "A Review of the Kinetics and Mechanism of the Pyrolysis of Hydrocarbons", *Combustion and Propulsion*, Fifth Agard Colloquium, High-Temperature Phenomena, R. P. Hagerty, O. Lutz, A. L. Jaumotte and S. S. Penner (Eds.), A Pergamon Press Book, The Macmillan Company (1963).

(105) J. H. Purnell and C. P. Quinn, "The Pyrolysis of Paraffins", in *Photochemistry and Reaction Kinetics*, P. G. Ashmore, F. S. Dainton, and T. M. Sugden (Eds.), Cambridge University Press (1967).

(106) C.-J. Chen, M. H. Back, and R. A. Back, "Mechanism of the Thermal Decomposition of Methane", in *Industrial and Laboratory Pyrolysis*, L. F. Albright and B. L. Crynes (Eds.), ACS Symposium Series 32, American Chemical Society, Washington, D.C. (1976).

(107) M. S. Khan and B. L. Crynes, "Survey of Recent Methane Pyrolysis Literature", *Ind. Eng. Chem.*, **62**(10), 54 (1970).

(108) J. Happel and L. Kramer, "Acetylene and Hydrogen from the Pyrolysis of Methane", *Ind. Eng. Chem.*, **59**(1), 39 (1967).

(109) H. B. Palmer, J. Lahaye, and K. C. Hou, "On the Kinetics and Mechanism of the Thermal Decomposition of Methane in a Flow System", *J. Phys. Chem.*, **72**, 348 (1968).

(110) A. Holmen, O. A. Rokstad, and A. Solbakken, "High-Temperature Pyrolysis of Hydrocarbons. I. Methane to Acetylene", *Ind. Eng. Chem. Process Des. Dev.*, **15**, 439 (1976).

(111) J. E. Taylor and D. M. Kulich, "Oxidative Pyrolyses of Selected Hydrocarbons Using the Wall-less Reactor", in *Industrial and Laboratory Pyrolysis*, L. F. Albright and B. L. Crynes (Eds.), ACS Symposium Series 32, American Chemical Society, Washington, D.C. (1976).

(112) B. L. Crynes and L. F. Albright, "Pyrolysis of Propane in Tubular Flow Reactors", *Ind. Eng. Chem. Process Design and Development*, **8**, 25 (1969).

(113) H. J. Hepp and F. E. Frey, "Pyrolysis of Propane and Butanes at Elevated Pressure", *Ind. Eng. Chem.*, **45**, 410 (1953).

(114) S. B. Zdonik, E. J. Green, and L. P. Hallee, "How Cracking Proceeds in the Ethylene-Pyrolysis Reaction", *The Oil and Gas Journal*, 96 (June 26, 1967).

(115) S. B. Zdonik, E. J. Green, and L. P. Hallee, "Here's More on How Cracking Occurs in Ethylene Pyrolysis", *The Oil and Gas Journal*, 192 (July 10, 1967).

(116) G. G. Smith and F. W. Kelly, "Structure Reactivity Relationships", *Progress in Physical Organic Chemistry*, **8**, 209 (1971).

(117) R. J. Harris, M. Nasralla, and A. Williams, "The Formation of Oxides of Nitrogen in High Temperature CH_4-O_2-N_2 Flames", *Combustion Science and Technology*, **14**, 85 (1976).

(118) P. A. Leonard, S. L. Plee, and A. M. Mellor, "Nitric Oxide Formation from Fuel und Atmospheric Nitrogen", *Combustion Science and Technology*, **14**, 183 (1976).

(119) N. M. Laurendeau, "Fast Nitrogen Dioxide Reactions: Significance During NO Decomposition and NO_2 Formation", *Combustion Science and Technology*, **11**, 89 (1975).

(120) E. G. Paulson, "How to Get Rid of Toxic Organics", *Chemical Engineering, Deskbook Issue*, **84** (22), 21 (October 17, 1977).

(121) D. M. Golden, "Estimation of Rate Constants of Elementary Processes—A Review of the State of the Art", Fourteenth Symposium (International) on Combustion, p. 121, The Combustion Institute, Pittsburgh, Pa. (1973).

(122) S. W. Mayer, L. Schieler, and H. S. Johnson, "Computation of High-Temperature Rate Constants for Bimolecular Reactions of Combustion Products", Eleventh Symposium (International) on Combustion, p. 837, The Combustion Institute, Pittsburgh, Pa. (1967).

(123) R. Shaw, "Estimation of Rate Constants as a Function of Temperature for the Reactions $W + XYZ = WX + YZ$ Where W, X, Y, and Z are H or O Atoms", *Int. J. Chem. Kinet.*, **9**, 929 (1977).

(124) S. W. Benson, "Current Status of Methods for the Estimation of Rate Parameters", *Int. J. Chem. Kinet.*, Symposium 1, 359 (1975).

(125) S. W. Benzon, D. M. Golden, R. W. Lawrence, R. Shaw, and R. W. Woolfolk, "Estimation of Rate Constants for Reactions $X + YZ \rightarrow XY + Z$, $X + Y + M \rightarrow XY + M$, and $X + YZ + M \rightarrow XYZ + M$, Where X, Y, and Z are Atoms, H, N, O", *Int. J. Chem. Kinet.*, Symposium 1, 399 (1975).

(126) S. W. Benson, D. M. Golden, R. W. Lawrence, R. Shaw, and R. W. Woolfolk, "Estimating the Kinetics of Combustion Including Reactions Involving Oxides of Nitrogen and Sulfur", U.S. EPA Report No. EPA-600/2-75-019 (1975) (PB-245054).

(127) S. W. Benson, *Thermochemical Kinetics*, Methods for the Estimation of Thermochemical Data and Rate Parameters, Second Edition, Wiley (1976).

(128) S. W. Benson, *The Foundation of Chemical Kinetics*, McGraw-Hill (1960).

(129) Ze'ev B. Alfassi and S. W. Benson, "A Simple Empirical Method for the Estimation of Activation Energies in Radical Molecule Metathesis Reactions", *Int. J. Chem. Kinet.*, **5**, 879 (1973).

(130) T. N. Bell and P. G. Perkins, "Calculation of the Energies of Activation for Some Gas-Phase Reactions", *J. Phys. Chem.*, **81**, 2012 (1977).

(131) R. D. Gilliam, "Activation Energies from Bond Energies. A Modification", *J. Am. Chem. Soc.*, **99**, 8399 (1977).

(132) R. H. Krech and D. L. McFadden, "An Empirical Correlation of Activation Energy With Molecular Polarizability for Atom Abstraction Reactions", *J. Am. Chem. Soc.*, **99**, 8402 (1977).

(133) W. J. Moore, *Physical Chemistry*, p. 528, Prentice-Hall, Inc., New York (1955).

(134) C. R. Wilke, and C. Y. Lee, "Estimation of Diffusion Coefficients for Gases and Vapors", *Ind. Eng. Chem.*, **47**, 1253 (1955).

(135) E. R. Gilliland, "Diffusion Coefficients in Gaseous Systems", *Ind. Eng. Chem.*, **26**, 681 (1934).

(136) T. K. Sherwood and R. L. Pigford, *Absorption and Extraction*, p. 11, McGraw-Hill (1952).

(137) S. S. Kurtz, Jr. and A. Sankin, "Calculation of Molecular Volumes of Hydrocarbons", *Ind. Eng. Chem.*, **46**, 2186 (1954).

(138) J. O. Hirschfelder, C. F. Curtiss, and R. B. Bird, *Molecular Theory of Gases and Liquids*, Wiley (1954).

(139) D. K. Edwards, V. E. Denny, and A. F. Mills, *Transfer Processes*, Holt, Rinehart and Winston (1973).

(140) R. B. Bird, J. O. Hirschfelder, and C. F. Curtiss, "Theoretical Calculation of the Equation of State and Transport Properties of Gases and Liquids", *Trans. Am. Soc. Mech. Eng.*, **76**, 1011 (1954).

(141) R. A. Svehla, "Estimated Viscosities and Thermal Conductivities of Gases at High Temperatures", National Aeronautics and Space Administration Technical Report No. NASA TR R-132 (1962).

(142) K. J. Laidler and J. C. Polanyi, "Theories of the Kinetics of Bimolecular Reactions", *Progress in Reaction Kinetics, 3,* G. Porter (Ed.), Pergamon Press Inc., New York (1965).

(143) Z. G. Szabo, *Advances in the Kinetics of Homogeneous Gas Reactions*, Methuen and Co., Ltd., London (1964).

(144) M. G. Evans and M. Polanyi, "Further Considerations on the Thermodynamics of Chemical Equilibria and Reaction Rates", *Trans. Faraday Soc.*, **32**, 1333 (1936).

(145) N. N. Semenov, *Some Problems of Chemical Kinetics and Reactivity*, Vol. I, Pergamon Press, Inc., New York (1958).

(146) J. O. Hirschfelder, "Semi-Empirical Calculations of Activation Energies", *J. Chem. Phys.*, **9**, 645 (1941).

(147) Z. G. Szabo, Chemical Society Special Publication 16 (1962), p 113.

(148) D. W. Jepson and J. O. Hirschfelder, "Idealized Theory of the Recombination of Atoms by Three-Body Collision", *J. Chem. Phys.*, **30**, 1032 (1959).

(149) J. C. Keck, "Variational Theory of Chemical Reaction Rates Applied to Three-Body Recombinations", *J. Chem. Phys.*, **32**, 1035 (1965).

(150) S. K. Kim, "The Rate of Termolecular Atomic Recombinations", Project Squid Technical Report BNR-18-P (March, 1966).

(151) R. C. Tolman, *Statistical Mechanics with Applications to Physics and Chemistry*, Chemical Catalog Co., New York (1927).

(152) G. von Elbe and B. Lewis, *Combustion Flames and Explosions of Gases*, Academic Press Inc., New York (1961).

(153) C. H. Waldman, R. P. Wilson, Jr., and K. L. Maloney, "Kinetic Mechanism of Methane/Air Combustion with Pollutant Formation", U.S. Environmental Protection Agency Report EPA-650/2-74-045 (1974).

(154) O. Levenspiel and K. B. Bischoff, "Backmixing in the Design of Chemical Reactors", *Ind. Eng. Chem.*, **51**, 1431 (1959).

(155) M. Szwarc, "The Transition State in Radical Reactions" in *The Transition State*, A Symposium at Sheffield on April 3 and 4, 1962, The Chemical Society, Special Publication No. 16.

(156) D. E. Jensen and G. A. Jones, "Reaction Rate Coefficients for Flame Calculations", *Combustion and Flame*, **32**, 1 (1978).

(157) W. M. Shaub and S. H. Bauer, "The Reduction of Nitric Oxide During the Combustion of Hydrocarbons: Methodology for a Rational Mechanism", *Combustion and Flame*, **32**, 35 (1978).

(158) A. Wheeler, "Reaction Rates and Selectivity in Catalyst Pores" in *Advances in Catalysis, Volume III*, pp. 249–327, Edited by W. G. Frankenburg, V. I. Komarewsky and E. K. Rideal, Academic Press (1951).

(159) Symposium on Current Status of Kinetics of Elementary Gas Reactions: Predictive Power of Theory and Accuracy of Measurement, *J. Phys. Chem.*, **83**, No. 1 (January 11, 1979).

(160) J. C. Dechaux and L. Delfosse, "The Negative Temperature Coefficient in the C_2 to C_{13} Hydrocarbon Oxidation. I. Morphological Results", *Combustion and Flame*, **34**, 161 (1979).

(161) J. C. Dechaux and L. Delfosse, "The Negative Temperature Coefficient in the C_2 to C_{12} Hydrocarbon Oxidation. II. Analytical Results", *Combustion and Flame*, **34**, 169 (1979).

(162) R. J. Santoro and I. Glassman, "A Review of Oxidation of Aromatic Compounds", *Combustion Science and Technology*, **19**, 161 (1979).

(163) J. N. White and W. C. Gardiner, Jr., "An Evaluation of Methane Combustion Mechanisms. 2. Comparison of Model Predictions with Experimental Data from Shock-Initiated Combustion of C_2H_2, C_2H_4, and C_2H_6", *J. Phys. Chem.*, **83**, 562 (1979).

(164) H. E. O'Neal and S. W. Benson, "A Method for Estimating the Arrhenius A Factors for Four- and Six-Center Unimolecular Reactions", *J. Phys. Chem.*, **71**, 2903 (1967).

APPENDIX A

PYROLYSIS

Pyrolysis is included here for two main reasons. One reason is that pyrolysis by itself can be used to either destroy organics or convert them to less complex compounds. The other reason is that pyrolysis reactions, even in the presence of excess oxygen, play a role in determining the overall rate and efficiency of oxidation processes and influence the distribution of final products.(103)

The general kinetics and mechanisms of hydrocarbon pyrolysis have been reviewed by Gordon(104) and Purnell and Quinn(105).

Pyrolysis Rate Data

A detailed discussion of the mechanism for methane has been presented by Chen et al.(106) A survey of the pyrolysis data available up to about 1970 has been published by Kahn and Crynes.(107) At atmospheric pressure methane pyrolysis appears to follow two parallel reactions(108)

$$2CH_4 \rightarrow C_2H_2 + 3H_2$$

$$CH_4 \rightarrow C + 2H_2$$

The maximum acetylene concentration in the reaction product increases with temperature. A simple mechanism for methane pyrolysis is based on the three reactions

$$CH_4 \xrightarrow{r_1} C + 2H_2$$

$$CH_4 \xrightarrow{r_2} \tfrac{1}{2} C_2H_2 + \tfrac{3}{2} H_2$$

$$C_2H_2 \xrightarrow{r_3} 2C + H_2$$

for the temperature range 1500 to 2000°C where the reaction rates are given by

$$r_1 = -\frac{1}{V_R}\frac{dn_{CH_4}}{dt} = k_1 P_{CH_4}$$

$$r_2 = -\frac{1}{V_R}\frac{dn_{CH_4}}{dt} = k_2 P_{CH_4}$$

$$r_3 = -\frac{1}{V_R}\frac{dn_{C_2H_2}}{dt} = k_3 \frac{P^2_{C_2H_2}}{1 + kP_{H_2}}$$

where V_R is the reactor volume in liters, P is partial pressure in atm, and the n's represent the gram moles of each species. Letting

$$x_1 = \frac{\text{g-mole of } CH_4 \text{ converted by } r_1}{\text{g-mole feed}}$$

$$x_2 = \frac{\text{g-mole of } CH_4 \text{ converted by } r_2}{\text{g-mole feed}}$$

$$x_3 = \frac{\text{g-mole of } C_2H_2 \text{ converted by } r_3}{\text{g-mole feed}}$$

The conversion relations can be expressed in terms of position within the reactor using the differential relationships

$$r_1\, dV_R = Q\, dx_1$$
$$r_2\, dV_R = Q\, dx_2$$
$$r_3\, dV_R = Q\, dx_3$$

where Q is the flow rate in gram moles/sec. The parameters for the rate constants are given in terms of

$$k_i = A_i\, e^{-E_i/RT}$$

as

$E_1 = 16{,}200$ cal/g-mole

$E_2 = 86{,}450$ cal/g-mole

$E_3 = 17{,}700$ cal/g-mole

$A_1 = 25.00$ g-mole/sec · liter · atm

$A_2 = 3.219 \times 10^{10}$ g-mole/sec · liter · atm

$A_3 = 2190$ g-mole/sec · liter · $(\text{atm})^2$

$k = 1.535\ \text{atm}^{-1}$

The reaction associated with r_1 can also be expressed in terms of the solid carbon by

$$r_c = 17.7\, c_{CH_4}\, e^{-16{,}200/RT}\ \text{g/cm}^2\text{-sec}$$

where c_{CH_4} is the methane concentration, g/cm^3.

Palmer et al.(109) have reported a first order rate constant for methane decomposition over the temperature range from 1000 to 1700°K:

$$\log_{10} k(\text{sec}^{-1}) = 13.0 - 18.6 \times 10^3/T(°K)$$

corresponding to an activation energy of 85 kcal. This rate constant is based on the equation

$$-\frac{dc_{CH_4}}{dt} = k c_{CH_4}$$

where the methane concentration is expressed in mole fraction.

Recent work(110) on high-temperature (1500 to 2000°C) pyrolysis of methane assuming the concentration of C_2H_6 is low at high temperatures has resulted in the mechanism described by the following differential equations

$$\frac{dn_{CH_4}}{dt} = -k_1\, n_{CH_4}$$

$$\frac{dn_{C_2H_4}}{dt} = \tfrac{1}{2} k_1\, n_{CH_4} - k_3\, n_{C_2H_4}$$

$$\frac{dn_{C_2H_2}}{dt} = k_3\, n_{C_2H_4} - k_4 \frac{n^2_{C_2H_2}}{V} \quad .$$

The reaction volume is given by

$$V = \frac{n_t RT}{P} = (2n^0_{CH_4} - n_{CH_4} - n_{C_2H_4}) \frac{RT}{P}$$

n_t is the total number of moles, $n^0_{CH_4}$ is the initial number of moles of methane, and P is the total pressure. The rate constants are

$$k_1 = 4.5 \times 10^{13}\, e^{-91,000/RT},\ \mathrm{sec}^{-1}$$

$$k_2 = 2.58 \times 10^{8}\, e^{-40,000/RT},\ \mathrm{sec}^{-1}$$

$$k_4 = 10^{11}\, e^{-44,370/RT},\ \mathrm{liter/mole\text{-}sec.}$$

For pure ethane pyrolysis(111), a first order homogeneous rate constant has been reported as

$$k = 10^{14.8}\, e^{-71,800/RT}\ \mathrm{sec}^{-1} \quad .$$

Pyrolysis can be quite sensitive to the presence of small amounts of oxygen. At very low conversions the homogeneous rate of pyrolysis is less with oxygen present than when oxygen is absent. A reversal occurs above 0.13 percent conversion after which oxygen increases the rate of pyrolysis. The main pyrolysis products are ethylene and methane. With pure ethane no surface effects are observed. In the presence of oxygen, a surface promoting effect is observed at very low conversions. At higher conversions, a surface inhibition occurs.

The homogeneous rate constant for ethylene pyrolysis is

$$k = 10^{11.0}\, e^{-65,400/RT}\ \mathrm{sec}^{-1} \quad .$$

High yields of acetylene are produced both in the presence or absence of oxygen. The presence of oxygen does, however, increase the reaction rate. Methane is the only other major product amounting to about 10 percent of the acetylene. Within an oxidized stainless steel tube the reaction rate is modified by the surface to

$$k = 10^{11.3}\, e^{-67,500/RT}\ \mathrm{sec}^{-1}$$

for a surface-to-volume ratio (S/V) of 1.4 cm^{-1}. Oxygen has a significant surface as shown in Figure A-1.

Propane(111) pyrolyzes to propylene, ethylene, and methane with propylene predominating in the absence of surfaces as shown in Figure A-2. The homogeneous rate

$$k = 10^{12.1}\, e^{-60,400/RT}\ \mathrm{sec}^{-1} \quad .$$

For a stainless steel reactor with $S/V = 0.7\ \mathrm{cm}^{-1}$, the rate is

$$k = 10^{12.3}\, e^{-60,200/RT}\ \mathrm{sec}^{-1}$$

and the corresponding product distribution is shown in Figure A-3.

Results by Crynes and Albright(112) indicate that the pyrolysis of propane is not a simple order reaction. Pyrolysis measurements performed in a tubular stainless-steel reactor at 700 and 750°C are presented in Figures A-4 and A-5, respectively. Data were correlated using both first-order and second-order kinetics based on the equations below for isothermal plug flow. For first-order kinetics:

$$k = \frac{Q}{V_R} \frac{RT}{P} [-x - 2 \ln (1 - x)] \quad ,$$

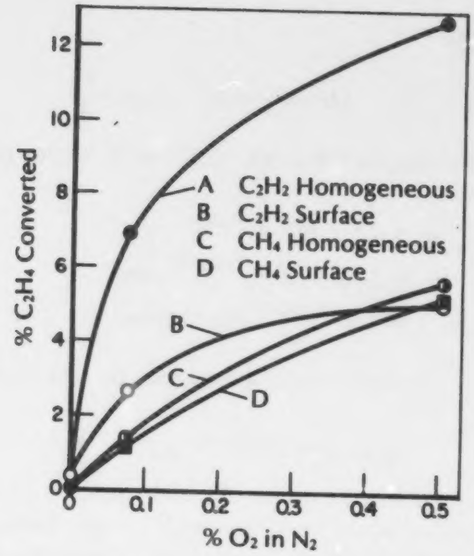

FIGURE A-1. EFFECT OF ADDED OXYGEN ON THE PYROLYSIS OF ETHYLENE. REACTION TIME: HOMOGENEOUS, 0.19 SEC; STAINLESS STEEL SURFACE, 0.18 sec. SURFACE-TO-VOLUME RATIO, 0.7 cm^{-1}. 0.4% O_2 IS ROUGHLY 1:1 O_2-TO-HYDROCARBON RATIO[111]

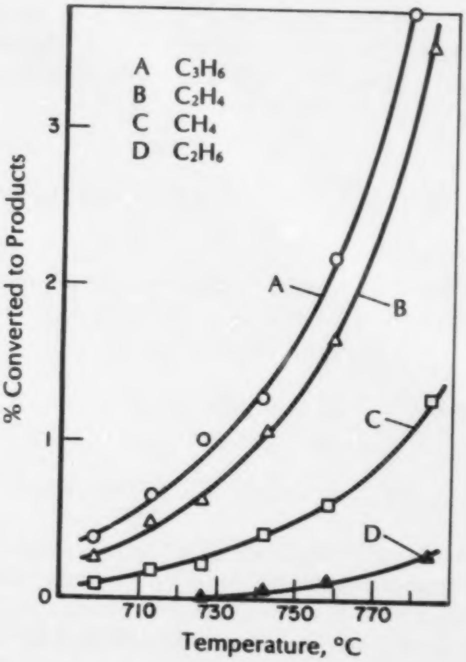

FIGURE A-2. PERCENT PROPANE CONVERTED TO PRODUCTS. HOMOGENEOUS. REACTION TIME ≃ 0.22 sec. VARIATION IN TEMPERATURE IN °C IS USED TO ATTAIN VARYING PRODUCT CONVERSIONS[111]

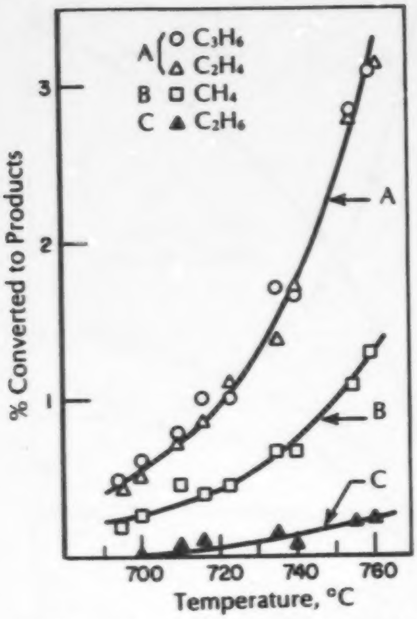

FIGURE A-3. PERCENT PROPANE CONVERTED TO PRODUCTS. CONVERSIONS VARIED WITH TEMPERATURE IN °C; OXIDIZED STAINLESS STEEL SURFACE; SURFACE-TO-VOLUME RATIO, 0.7 cm^{-1}; REACTION TIME ≃ 0.22 sec(111)

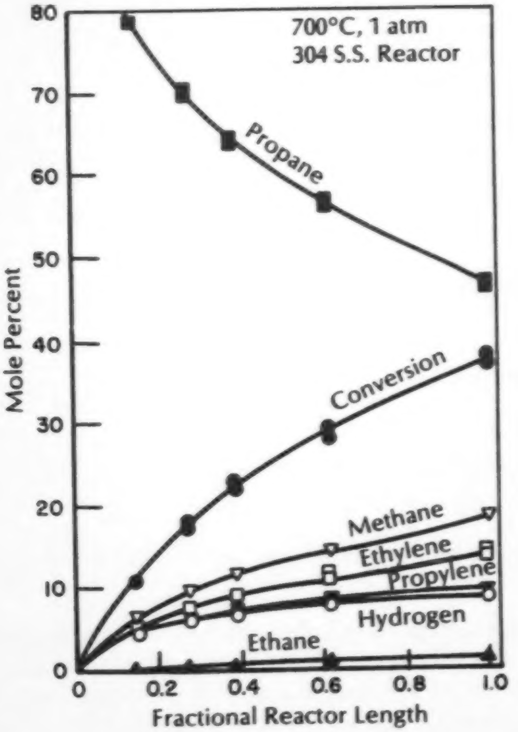

FIGURE A-4. PRODUCT DISTRIBUTION ALONG REACTOR LENGTH(112)

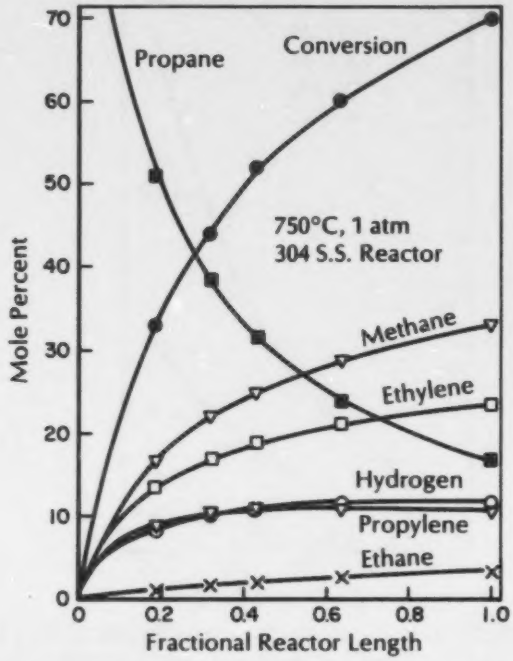

FIGURE A-5. PRODUCT DISTRIBUTION ALONG REACTOR LENGTH(112)

and for second-order kinetics

$$k = \frac{Q}{V_R}\left(\frac{RT}{P}\right)^2 \left[x + \frac{4x}{1-x} + 4 \ln (1-x)\right] \quad .$$

The above equations assume that 2 moles of product are produced per mole of propane pyrolyzed which was observed experimentally. In these equations, P is total pressure; Q, flow in moles/sec; V_R, the reactor volume; and x is the fractional conversion of propane in terms of moles reacted per moles of feed. Rate constants for both the first- and second-order kinetics are plotted in Figure A-6.

Rate data for the pyrolysis of propane and n-butane at atmospheric pressure are plotted in Figure A-7.

The homogeneous rate constant for the pyrolysis of isobutane(111) is

$$k = 10^{11.7}\, e^{-56,300/RT}\ \mathrm{sec}^{-1} \quad .$$

For a stainless steel tube with $S/V = 0.7\ \mathrm{cm}^{-1}$ the rate is given by

$$k = 10^{10.7}\, e^{-50,700/RT}\ \mathrm{sec}^{-1} \quad .$$

The product distributions for both the homogeneous and heterogeneous cases are shown in Figures A-8 and A-9.

Zdonik et al.(114,115) have compiled pyrolysis data on a number of organics. Data based on unimolecular disappearance kinetics for several light hydrocarbons are given in Table A-1 and Figure A-10. In general it has been found that the rate of disappearance of a reactant is independent of both pressure and the surface-to-volume ratio. Data for various classes of heavy hydrocarbons are given as a function of the number of carbon atoms in Figure A-11.

A listing of kinetic data for the pyrolysis of alcohols and mercaptans is given in Table A-2.

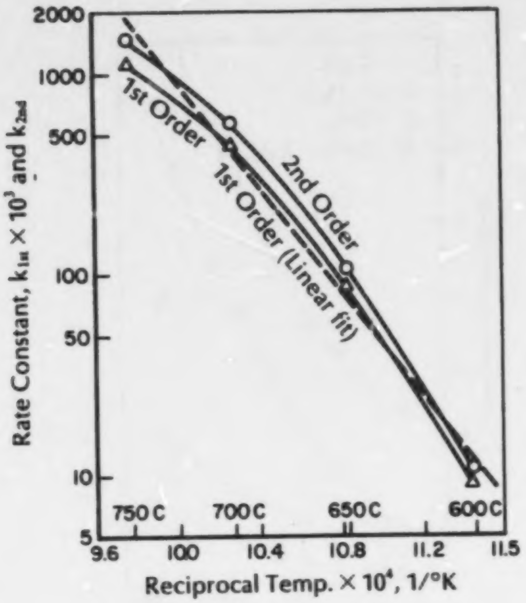

FIGURE A-6. ARRHENIUS PLOT FOR ASSUMED FIRST- AND SECOND-ORDER REACTION[112]

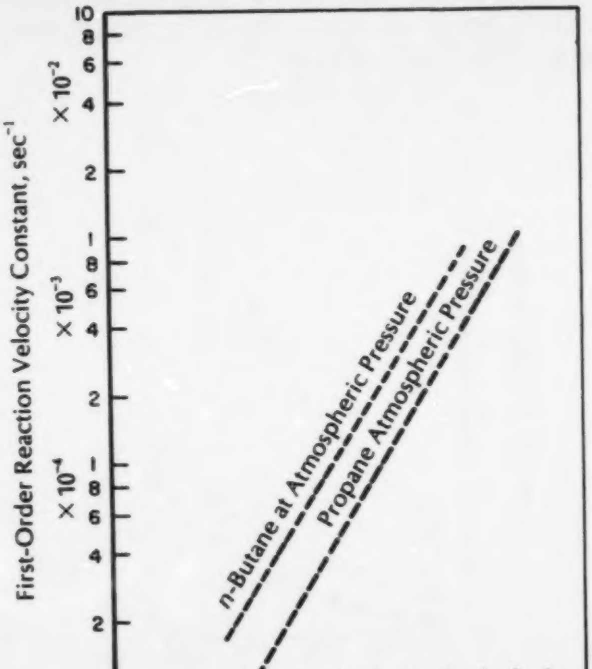

FIGURE A-7. COMPARISON OF DECOMPOSITION RATES FOR PROPANE AND BUTANE AT ATMOSPHERIC PRESSURE[113]

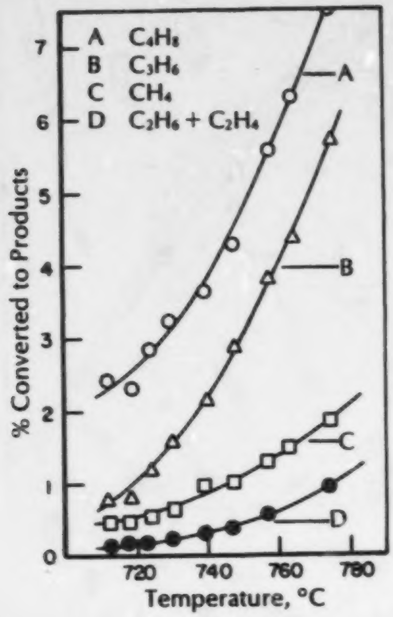

FIGURE A-8. PERCENT ISOBUTANE CONVERTED TO PRODUCTS. CONVERSIONS VARIED WITH TEMPERATURE IN °C. HOMOGENEOUS; REACTION TIME ≃ 0.22 sec(111)

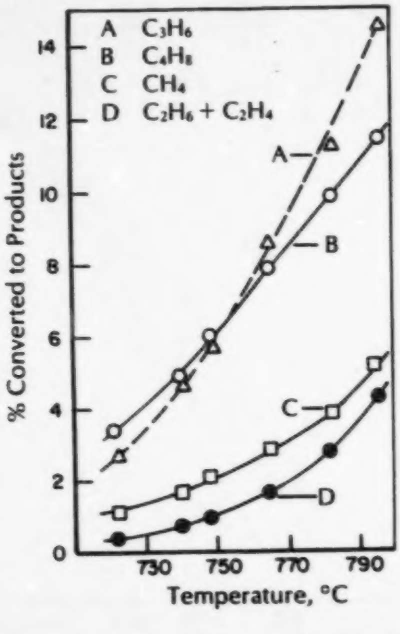

FIGURE A-9. PERCENT ISOBUTANE CONVERTED TO PRODUCTS. CONVERSIONS VARIED WITH TEMPERATURE IN °C; OXIDIZED STAINLESS STEEL SURFACE PRESENT; SURFACE-TO-VOLUME RATIO, 0.7 cm^{-1}; REACTION TIME ≃ 0.22 sec(111)

TABLE A-1. KINETIC RATE DATA FOR DISAPPEARANCE OF LIGHT HYDROCARBONS BY THERMAL PYROLYSIS(114)

Compound	log A	E_a, Btu/lb mole
Ethane	14.6737	130,133
Propylene	13.8334	120,976
Propane	12.6160	107,593
Isobutane	12.3173	103,138
n-Butane	12.2545	101,354
n-Pentane	12.2479	99,758

$$k = A\,e^{-E_a/RT},\ \text{sec}^{-1}$$

TABLE A-2. KINETIC PARAMETERS FOR THE PYROLYSIS OF SIMPLE ALCOHOLS AND MERCAPTANS(116)

Compound	Major Products	Temperature, °C	E_a	Log A
MeOH	H_2, $H_2C{=}O$, CO	669	68.00	
EtOH	CH_3CHO, CO, CH_4	525		
		576–624	57.40	10
n-PrOH	CH_4, CH_3CHO	570–622	49.95	17.6
i-PrOH	Me_2CO	524–615	34.00	8.4
n-BuOH	H_2CO, CO, CH_4	573–629	56.70	12.2
t-BuOH	$Me_2C{=}CH_2$, H_2O	487–620	54.50	11.51
t-BuOH	$Me_2C{=}CH_2$, H_2O	~500	65.50	14.68
t-BuOH	$Me_2C{=}CH_2$, H_2O	~750	61.60	13.4
t-BuOH	$Me_2C{=}CH_2$, H_2O	153		
t-AmylOH	$Me_2C{=}CHMe$, $CH_2{=}CMeCH_2CH_3$	~500	60.00	13.52
t-BuSH	$Me_2C{=}CH_2$, H_2S	~700	55.00	13.3
t-BuOEt	$Me_2C{=}CH_2$, EtOH	450	59.74	14.13
t-BuOMe	$Me_2C{=}CH_2$, MeOH	450	61.53	14.38
EtSH(a)	C_2H_4, H_2S	393	40.00	
	C_2H_4, H_2S	~500	55.00	
MeSH(a)	$CH_4 + H_2S$	~750	67.00	
$PhCH_2SH$(a)	$(PhCH_2)_2$, H_2S	600	53.00	

(a) Mercaptans also undergo a radical decomposition to R· and HS·.

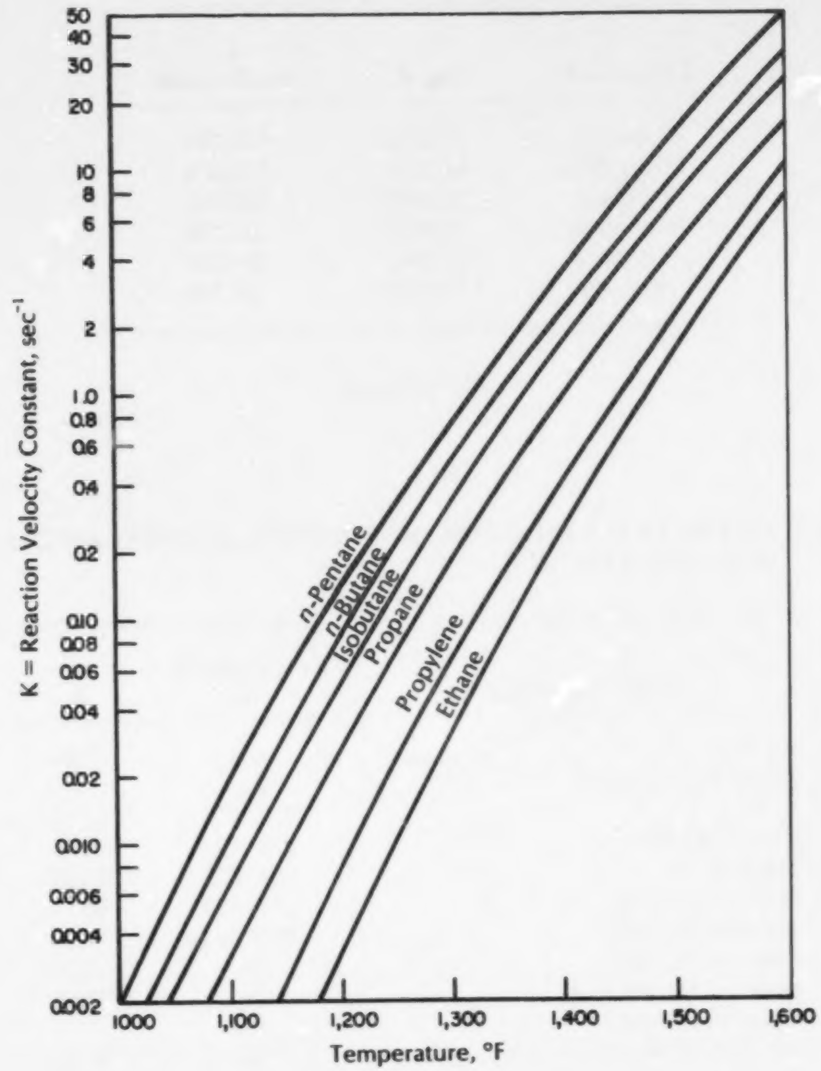

FIGURE A-10. KINETIC RATE DATA FOR DISAPPEARANCE OF LIGHT HYDROCARBONS BY THERMAL PYROLYSIS[114]

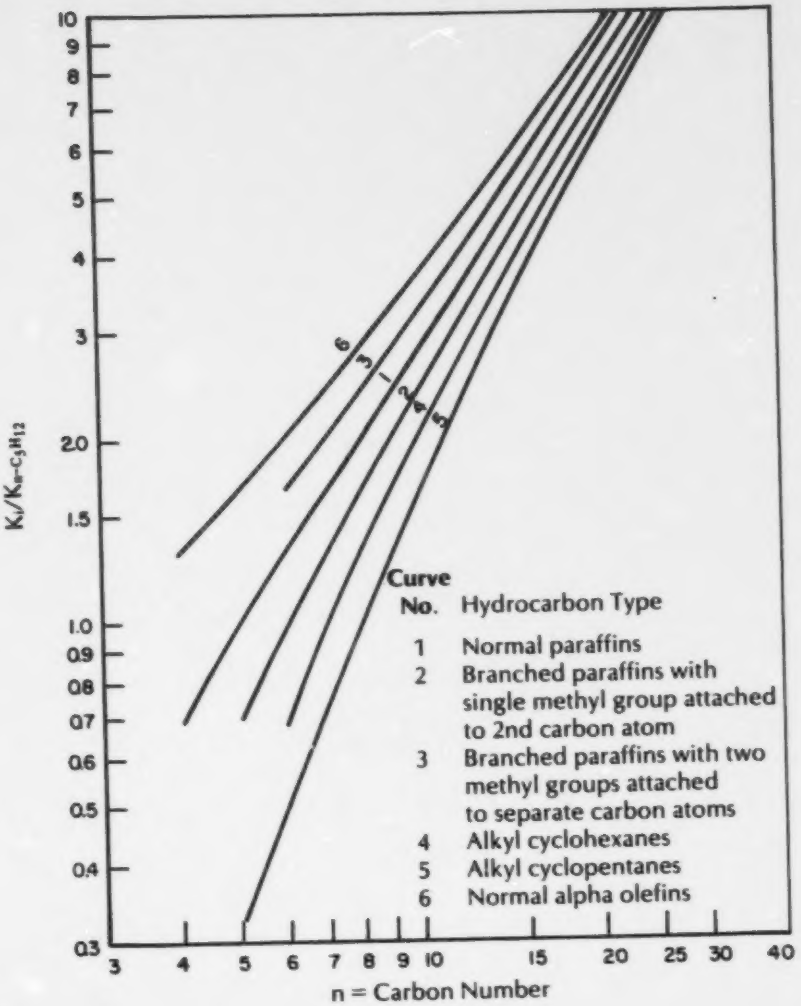

FIGURE A-11. REACTION VELOCITY CONSTANTS FOR HEAVY HYDROCARBONS RELATIVE TO n-C_5H_{12}[115]

APPENDIX B

POLLUTANT FORMATION REACTIONS

Primary pollutants are generally considered to be those which are emitted directly to the atmosphere while secondary pollutants are formed by subsequent chemical or photochemical reactions involving primary pollutants after they have been emitted and interact with the atmosphere. Unburned hydrocarbons, aldehydes, oxides of nitrogen, oxides of sulfur, and particulates are examples of primary pollutants. Examples of secondary pollutants are compounds like ozone and peroxyacetyl nitrate (PAN). Only primary pollutants are of concern in this study on afterburner chemistry.

Nitrogen Oxides (NO$_x$). In combustion systems NO appears to be the predominant oxide of nitrogen. Small amounts of NO_2 are often present and, occasionally, larger amounts of NO_2 are observed than expected. Some investigators attribute the high NO_2 to sampling effects.

NO in combustion systems can come from two sources: (1) thermal reactions involving atmospheric nitrogen and (2) reactions involving chemically-bound nitrogen. The latter source is often referred to as fuel-bound nitrogen.

The thermal source is only active at relatively high temperatures (>2400°F) and would probably not be an important source of NO in afterburner systems where the hydrocarbon oxidation section usually operates at temperatures below 2000°F. NO can be generated, though, within the auxiliary fuel flame zone, where the temperatures exceed 2500°F. In the fuel rich part of a flame, CN radicals can form which can be oxidized and contribute to NO formation.

In a premixed system the NO present can be estimated on the basis of the equilibrium reaction

$$N_2 + O_2 \rightarrow 2\,NO \quad .$$

Usually the kinetics of NO formation are analyzed in terms of the Zeldovich mechanism$^{(5)}$:

$$O + N_2 \rightarrow NO + N \qquad k = 1.4 \times 10^{14}\, e^{-78,500/RT}$$

$$N + O_2 \rightarrow NO + O \qquad k = 6.4 \times 10^{9}\, e^{-6,280/RT}$$

which is often modified to include the reaction

$$N + OH \rightarrow NO + H \qquad k = 2.8 \times 10^{13}$$

The O + N_2 reaction is the rate controlling step because of its high activation energy. For flame calculations, the O-atom concentration is often taken as its equilibrium value at the flame temperature. In hydrocarbon flames, especially fuel-rich flames, NO_M (called prompt NO) also may be formed within the flame zone by the reactions

$$CH + N_2 \rightarrow HCN + N$$

$$C_2 + N_2 \rightarrow 2\,CN \quad .$$

The N atoms then form NO through the modified Zeldovich mechanism, and the CN yields NO through reactions with O-atoms and O_2. An overshoot in the O-atom concentration within the flame zone could also account for the so-called "prompt" NO. Stable HCN which is found in highly fuel-rich flames, is thought to be controlled by the equilibrium reactions

$$CN + H_2 \rightarrow HCN + H$$

$$CN + H_2O \rightarrow HCN + OH \quad .$$

A mechanism proposed by Harris, Nasralla, and Williams(117) for NO formation in a high-temperature methane-air flame is presented in Table B-1. For fuel-lean CH_4-O_2-N_2 flames at temperatures above 2500°K the rate of NO formation can be expressed as

$$\frac{d\,[NO]}{dt} = \frac{2.44 \times 10^{-5}}{T(°K)}\, k_1\, [O]\, [N_2] \text{ ppm m/sec} \quad .$$

Since radical overshoot is small in these flames, [O] can be approximated by the equilibrium expression

$$[O] = \exp\,(n_1\phi + 0.00553\,T - 17.73)$$

where

$$n_1 = \frac{8.291 \times 10^4}{T} - \frac{10.363 \times 10^7}{T^2} - 18.71$$

and ϕ is the stoichiometric ratio and $k_1 = 9.1 \times 10^7\, e^{-38,000/T}$, m^3/mole.

TABLE B-1. REACTION MECHANISM AND RATE PARAMETERS FOR NO FORMATION(117)

Reaction	Rate Constant, $m^3/mol^{-1}\,sec^{-1}$	
	k_f	k_r
$O + N_2 = NO + N$	$7 \times 10^7 \exp(-37,997/T)$	1.55×10^7
$N + O_2 = NO + O$	$1.33 \times 10^3\, T \exp(-3563/T)$	$3.2 \times 10^3 T \exp(19,678/T)$
$N + OH = NO + H$	4.1×10^7	$4.1 \times 10^7/0.429 \exp(23,815/T)$
$N_2 + OH = N_2O + H$	$1.18 \times 10^6 \exp(-38,148/T)$	$3 \times 10^7 \exp(-5,420/T)$
$N_2 + O_2 = N_2O + O$	$(k_r)/1.05 \exp(42,008/T)$	$1.18 \times 10^8 \exp(-14,092/T)$
$O + N_2O = 2NO$	$1.42 \times 10^8 \exp(-14,092/T)$	$2.6 \times 10^6 \exp(-32,109/T)$

NO from compounds containing chemically-bound nitrogen, such as amines, can be formed at quite low temperatures compared to those required to generate thermal NO. Therefore, significant levels of NO_x could be produced when nitrogen containing organics are destroyed in afterburners. During combustion, compounds containing chemically-bound nitrogen decompose to form free radicals or intermediates (e.g., NH, NH_2, CN, HCN, NH_3, etc.) which serve as precursors for the formation of NO. The formation of NO from bound-nitrogen compounds is rapid and appears to be only slightly dependent on temperature. Under fuel-lean conditions where it is often desirable to operate to reduce hydrocarbon and CO emissions, bound-nitrogen compounds generally result in high NO production. The reason is that the reactions such as

$$NO + O \rightarrow N + O_2$$

$$NO + NO \rightarrow N_2O + O$$

$$NO + RH \rightarrow \text{product} \quad ,$$

which lead to the destruction of NO are quite slow. Under certain fuel-rich conditions CH and NH radicals can contribute to the reduction of NO. Several reactions involving pyrolysis fragments NH and CN which could lead to NO are listed below.(5) A general mechanism can be expressed as

$$\left.\begin{array}{c}\mathrm{NH}\\ \\ \mathrm{CN}\end{array}\right\} + \left\{\begin{array}{c}\mathrm{O_2}\\ \text{or}\\ 2\,\mathrm{O}\end{array}\right\} \rightarrow \begin{array}{c}\mathrm{NO + OH}\\ \\ \mathrm{CO + NO}\end{array}$$

A more detailed mechanism involving NH has been suggested to be

$$\mathrm{NH + O \rightarrow NO + H}$$

$$\mathrm{NH + O \rightarrow N + OH}$$

$$\mathrm{N + O_2 \rightarrow NO + O}$$

$$\mathrm{N + OH \rightarrow NO + H}$$

which are highly exothermic. A suggested CN mechanism is through the reactions

$$\mathrm{CN + O_2 \rightarrow OCN + O}$$

$$\mathrm{OCN + O \rightarrow CO + NO}$$

which are also highly exothermic. N-atoms, which lead to enhanced NO production in flame zones, can also be contributed by reactions such as

$$\mathrm{CH + N_2 \rightarrow HCN + N}$$

$$\mathrm{C_2 + N_2 \rightarrow 2\,CH}$$

$$\mathrm{C + N_2 \rightarrow CN + N} \quad .$$

A detailed analysis of NO generation from atmospheric and fuel nitrogen in hydrocarbon flames has been performed by Leonard, Plee, and Mellor.(118) A listing of the reactions used in their analysis is given in Table B-2.

NO_2 in flames is thought to be controlled through the formation reaction

$$\mathrm{NO + HO_2 \rightarrow NO_2 + OH}$$

and the destruction reaction

$$\mathrm{NO_2 + O \rightarrow NO + O_2} \quad .$$

A detailed mechanism suggested by Laurendeau(119) presented in Table B-3 can also account for both NO and NO_2 formation. The two-step mechanism:

$$\mathrm{NO + O + M \rightarrow NO_2 + M}$$

$$\mathrm{O + NO_2 \rightarrow NO + O_2}$$

rapidly converts NO to NO_2 in the presence of atomic oxygen. The mechanism is favored at high pressure and low temperatures from 600 to 1200°K. This mechanism may also explain the anomalously high levels of NO_2 sometimes observed.

Sulfur Oxides. In most combustion situations the final form of sulfur is SO_2 with only a few percent of SO_3. Under fuel-rich conditions, H_2S, COS, and elemental sulfur are also observed. Much of the kinetics of SO_2 formation are controlled by the SO radical with the three-body reaction

TABLE B-2. KINETIC MECHANISM FOR NITRIC OXIDE FORMATION(118)

Reaction No.	Reaction
1	$H + O_2 \leftrightarrow OH + O$
2	$O + H_2 \leftrightarrow OH + H$
3	$H_2 + OH \leftrightarrow H_2O + H$
4	$OH + OH \leftrightarrow H_2O + O$
5	$O + O + M \leftrightarrow O_2 + M$
6	$H + H + M \leftrightarrow H_2 + M$
7	$H + O + M \leftrightarrow OH + M$
8	$H + OH + M \leftrightarrow H_2O + M$
9	$N_2 + O \leftrightarrow NO + N$
10	$N + O_2 \leftrightarrow NO + O$
11	$N + OH \leftrightarrow NO + H$
12	$NH + O \leftrightarrow H + NO$
13	$NH + OH \leftrightarrow N + H_2O$
14	$NH + H \leftrightarrow N + H_2$
15	$NH + O \leftrightarrow N + OH$
16	$NH + NO \leftrightarrow N_2O + H$
17	$CN + NO \rightarrow CO + N_2$(a)
18	$CN + O_2 \rightarrow CO + NO$(a)
19	$CN + O \rightarrow CO + N$
20	$HCN + H \leftrightarrow CN + H_2$

(a) Nonelementary.

TABLE B-3. RATE CONSTANTS FOR N_2–O_2 REACTIONS(119)(a)

Reaction	Forward Rate Constant	Backward Rate Constant	Temperature Range, °K
(1) $O + N_2 \rightarrow NO + N$	$10^{14.158} \exp(-75.58/RT)$	$10^{13.491} \exp(-0.33/RT)$	300–1600
(2) $NO + O \rightarrow N + O_2$	$10^{9.162} T^{1.0} \exp(-38.34/RT)$	$10^{9.808} T^{1.0} \exp(-6.25/RT)$	300–2000
(3) $NO_2 + M \rightarrow NO + O + M$	$10^{16.041} \exp(-65.00/RT)$	$10^{10.593} T^{1.0} \exp(+9.54/RT)$	1400–2300
(4) $NO + O_2 \rightarrow O + NO_2$	$10^{12.484} \exp(-47.40/RT)$	$10^{13.000} \exp(-0.60/RT)$	280–550
(5) $NO + NO \rightarrow N_2O + O$	$10^{11.848} \exp(-65.00/RT)$	$10^{13.398} \exp(-26.90/RT)$	1400–2300
(6) $N_2O + M \rightarrow N_2 + O + M$	$10^{14.800} \exp(-56.80/RT)$	$10^{9.570} T^{1.0} \exp(-16.70/RT)$	1670–1920
(7) $NO_2 + NO_2 \rightarrow NO + NO + O_2$	$10^{12.602} \exp(-26.90/RT)$	$10^{6.576} T^{1.0} \exp(+0.84/RT)$	600–2000
(8) $O_2 + M \rightarrow O + O + M$	$10^{21.158} T^{-1.8} \exp(-118.0/RT)$	$10^{16.167} T^{-0.8} \exp(+3.40/RT)$	1500–5000

(a) Forward (f) direction of each reaction is endothermic; rate constants in units of moles/cc sec.

$$O + SO_2 + M \rightarrow SO_3 + M$$

being responsible for the SO_3 formation. For combustion at low excess air (<1 percent oxygen), SO_3 is generally less than 1 percent of the SO_2 level; at higher excess air, SO_3 may reach 2 or 3 percent of the SO_2 level.

Polycyclic Aromatic Hydrocarbons. During combustion processes, even with substantial amounts of oxygen, hydrocarbons can break down to produce unsaturated compounds such as olefins or polyacetylenes that can then polymerize to form large polycyclic aromatic hydrocarbons which are highly stable at flame temperatures.

Hydrogen Halides. Hydrogen chloride produced from incineration of chlorinated hydrocarbons is the most common hydrogen halide associated with afterburner systems. Generally when hydrogen halides are processed in afterburners the stack gases require special treatment. Either scrubbers or adsorbers are usually used to provide this special treatment. Recommended temperatures for the incineration of chlorinated hydrocarbons lie in the range from 1800 to 2700°F which is considerably higher than required for many afterburner applications.(120)

No overall or global rate data were located for halogenated organic compounds, but thermodynamics indicate that chlorine products are readily converted to HCl in combustion.

TABLE C-1. PHYSICAL AND COMBUSTION PROPERTIES OF SELECTED ORGANIC VAPORS IN AIR

Fuel	Mol. Wt.	Spec. Grav.	T_{Boil} (°F)	Heat of Vap. (Btu/lb)	Heat of Comb. (Btu/lb)	Stoichiometry		Flammability Limits (% Stoichio.)		Spont. Ign. Temp. (°F)	Fuel for Max. Flame Speed (% Stoichio.)	Relative Max. Flame Speed	Flame Temp. at Max. Fl. Speed (°R)	Ign. Energy (10^{-5} joule)		Quenching Dist. (in.)	
						% Vol.	f	Lean	Rich					Stoich.	Min	Stoich.	Min
Acetaldehyde	44.1	0.783	-70	245	–	0.0772	0.1280	–	–	–	–	–	–	37.6	–	0.09	–
Acetone	58.1	.792	134	224	–	.0497	.1054	[a]59	[a]233	1042	131	117	3820	115	–	.15	–
Acetylene	26.0	.621	[b]-119	–	20,734	.0772	.0755	[a]31		581	133	362	–	[c]3	–	.03	–
Acrolein	56.1	.841	127	–	–	.0564	.1163	[a]48	[a]752	532	≈100	144	–	[c]17.5	–	.06	–
Acrylonitrile	53.1	.797	173	–	–	.0528	.1028	[a]87	–	898	105	109	4430	[c]36	[d]16	.09	0.06
Allene (propadiene)	40.1	–	-30	–	19,921	.0497	.0728	–	–	–	121	189	4430	–	–	–	–
Ammonia	17.0	[c].817	-28	590	–	.2181	.1645	–	–	1204	–	–	–	–	–	–	–
Aniline	93.1	1.022	364	187	–	.0263	.0872	–	–	1100	–	–	–	–	–	–	–
Benzene	78.1	.885	176	169	17,446	.0271	.0755	43	336	1097	108	[f]104	4150	55	[d]22.5	.11	.07
,n-butyl-	134.2	.865	362	–	17,984	.0153	.0721	–	–	821	108	[f]84	4185	–	–	–	–
,sec-butyl-	134.2	.866	344	–	–	.0153	.0721	–	–	836	–	–	–	–	–	–	–
,tert-butyl-	134.2	.871	336	–	–	.0153	.0721	–	–	891	105	[f]85	4175	–	–	–	–
,1,2-diethyl-	134.2	.884	362	–	–	.0153	.0721	–	–	759	–	–	–	–	–	–	–
,1,3-diethyl-	134.2	.868	358	–	–	.0153	.0721	–	–	851	–	–	–	–	–	–	–
,1,4-diethyl-	134.2	.866	363	–	–	.0153	.0721	–	–	844	–	–	–	–	–	–	–
,1,2-dimethyl- (o-xylene)	106.2	.885	292	149	17,723	.0195	.0734	–	–	934	108	[f]80	4205	–	–	–	–
,1,3-dimethyl- (m-xylene)	106.2	.869	282	147	17,716	.0195	.0734	45	307	1045	–	–	–	–	–	–	–
,1,4-dimethyl- (p-xylene)	106.2	.866	281	146	17,719	.0195	.0734	–	–	1048	–	–	–	–	–	–	–
,ethyl-	106.2	.872	277	146	17,767	.0195	.0734	[a]50	–	860	–	–	–	–	–	–	–
,isobutyl-	134.2	.858	343	–	–	.0153	.0721	–	–	853	–	–	–	–	–	–	–
,isopropyl- (cumene)	120.2	.866	306	134	17,873	.0171	.0727	52	352	873	–	–	–	–	–	–	–
,1-methyl-2-ethyl-	120.2	.885	329	139	17,864	.0171	.0727	–	–	836	–	–	–	–	–	–	–
,1-methyl-3-ethyl-	120.2	.869	322	138	17,853	.0171	.0727	–	–	905	–	–	–	–	–	–	–
,1-methyl-4-ethyl-	120.2	.866	324	137	17,848	.0171	.0727	–	–	902	–	–	–	–	–	–	–
,1-methyl-3,5-diethyl-	148.2	.867	393	–	–	.0138	.0717	–	–	861	–	–	–	–	–	–	–
,nitro-	123.1	1.199	412	142	–	.0324	.1429	–	–	900	–	–	–	–	–	–	–
,propyl-	120.2	.867	319	137	17,887	.0171	.0727	–	–	853	–	–	–	–	–	–	–
,1,2,3-trimethyl- (hemimellitene)	120.2	.899	349	143	17,825	.0171	.0727	–	–	895	–	–	–	–	–	–	–
,1,2,4-trimethyl- (pseudocumene)	120.2	.880	337	140	17,809	.0171	.0727	–	–	970	109	[f]84	4180	–	–	–	–
,1,3,5-trimethyl- (mesitylene)	120.2	.870	328	140	17,802	.0171	.0727	–	–	1039	–	–	–	–	–	–	–
,vinyl- (styrene)	104.1	.911	293	–	17,598	.0205	.0755	–	–	914	–	–	–	–	–	–	–
Benzyl alcohol	108.1	1.050	401	–	–	.0240	.0923	–	–	802	–	–	–	–	–	–	–
Biphenyl	154.2	1.180	490	–	–	.0141	.0772	–	–	1071	–	–	–	–	–	–	–
,2-butyl-	210.3	–	–	–	–	.0101	.0745	–	–	811	–	–	–	–	–	–	–
,2-ethyl-	182.3	–	–	–	–	.0118	.0755	–	–	840	–	–	–	–	–	–	–
,2-methyl-	168.2	1.010	500	–	–	.0129	.0763	–	–	936	–	–	–	–	–	–	–
,2-propyl-	196.3	–	–	–	–	.0109	.0750	–	–	845	–	–	–	–	–	–	–
1,2-Butadiene (methylallene)	54.1	[g].658	52	–	19,567	.0366	.0714	–	–	–	117	149	4355	–	–	–	–
1,3-Butadiene (divinyl, vinylethylene)	54.1	[g].627	24	–	19,153	.0366	.0714	[a]53	[a]340	784	119	140	4275	[c]23.5	12.5	.07	.05
,2,3-dimethyl-	82.1	.731	156	–	–	.0240	.0701	–	–	–	119	112	4170	–	–	–	–
,2-methyl- (isoprene)	68.1	.686	93	–	19,003	.0290	.0706	–	–	824	118	119	4220	–	–	–	–
n-Butane	58.1	[g].584	31	166	19,655	.0312	.0649	54	330	807	113	97	4060	76	26	.12	.07
,2-cyclopropyl-	98.2	–	–	–	–	.0195	.0678	–	–	–	129	102	–	–	–	–	–
,2,2-dimethyl-	86.2	.654	122	131	19,299	.0216	.0659	55	351	824	113	92	4055	164	[d]25	.18	.07
,2,3-dimethyl-	86.2	.666	136	136	19,338	.0216	.0659	55	372	790	113	93	4055	–	–	–	–
,1,1-diphenyl-	210.3	–	–	–	–	.0101	.0745	–	–	863	–	–	–	–	–	–	–
,2-methyl- (isopentane)	72.1	.625	82	146	19,451	.0255	.0654	50	359	800	114	94	4055	[c]96	[d]21	.14	.07
,2,2,3-trimethyl-	100.2	.695	178	124	19,241	.0187	.0661	58	358	849	116	92	4035	100	–	.14	–
Butanone (methylethyl ketone)	72.1	.805	175	191	–	.0366	.0951	–	–	–	100	92	–	53	28	.10	.08
1-Butene	56.1	[g].601	21	168	19,475	.0337	.0678	53	353	830	116	111	4175	–	–	–	–
,2-cyclopropyl-	96.2	–	–	–	–	.0205	.0698	–	–	–	115	109	4215	–	–	–	–
,2,3-dimethyl-	84.2	.683	132	–	19,159	.0227	.0678	–	–	697	131	101	3970	–	–	–	–
,2-ethyl-	84.2	.694	148	–	19,198	.0227	.0678	–	–	615	117	101	4110	–	–	–	–
,2-methyl-	70.1	.656	88	–	19,252	.0271	.0678	–	–	–	115	100	4135	–	–	–	–
,3-methyl- (α-isoamylene)	70.1	.633	68	–	19,297	.0271	.0678	–	–	706	115	106	4150	–	–	–	–
,2,3,3-trimethyl-	98.2	.710	172	–	19,092	.0195	.0678	–	–	721	–	–	–	–	–	–	–
trans-2-Butene	56.1	[g].610	34	174	19,389	.0337	.0678	[a]52	[a]307	–	–	–	–	–	–	–	–
2,3-dimethyl-2-butene	84.2	.713	164	–	19,135	.0227	.0678	–	–	764	115	95	4115	–	–	–	–
2-methyl-2-butene	70.1	.668	101	–	19,214	.0271	.0678	–	–		–	–	–	–	–	–	–
3-Buten-1-yne (vinylacetylene)	52.1	.687	41	–	–	.0402	.0755	–	–	–	109	193	4520	8.22	–	.04	–
n-Butyl chloride	92.6	.884	172	–	–	.0324	.1075	–	–	–	–	–	–	[c]124	–	.15	–
1-Butyne	54.1	[g].650	47	–	19,590	.0366	.0714		–	–	120	149	4345	–	–	–	–
,3,3-dimethyl-	82.1	–	–	–	–	.0240	.0701		–		121	122	4210	–	–	–	–
2-Butyne	54.1	.697	81	–	19,440	.0366	.0714	–	–	–	120	132	4320	–	–	–	–
d-Camphor	152.2	.990	[b]399	–	–	.0153	.0818	–	–	871	–	–	–	–	–	–	–
Carbon disulfide	76.1	1.263	115	151	–	.0652	.1841	[a]18	[a]1120	248	≈102	127	–	1.5	–	.02	–
Carbon monoxide	28.0	–	-310	91	–	.2950	.4064	[a]34	[a]676	1128	≈170	[h]100	–	–	–	–	–
Cyanogen	52.0	.866	-5	186	–	.0947	.1887	–	–	1562	–	–	–	–	–	–	–
Cyclobutane	56.1	.703	55	–	–	.0337	.0678	–	–	–	115	145	4155	–	–	–	–
,ethyl-	84.2	–	–			.0227	.0678	[a]55	[a]376	–	115	115	4125	–	–	–	–
,isopropyl-	98.2	–	–	–		.0195	.0678	–	–	–	135	100	3900	–	–	–	–
,methyl-	70.1	.693	97			.0271	.0678	–	–	–	118	114	–	–	–	–	–
,methylene-	68.1	–	–			.0290	.0706	–	–	–	123	132	–	–	–	–	–

TABLE C-1. (Continued)

Fuel	Mol. Wt.	Spec. Grav.	T_{Boil} (°F)	Heat of Vap. (Btu/lb)	Heat of Comb. (Btu/lb)	Stoichiometry		Flammability Limits (% Stoichio.)		Spont. Ign. Temp. (°F)	Fuel for Max. Flame Speed (% Stoichio.)	Relative Max. Flame Speed	Flame Temp. at Max. Fl. Speed (°R)	Ign. Energy (10^{-5} joule)		Quenching Dist. (in.)	
						% Vol.	f	Lean	Rich					Stoich.	Min	Stoich.	Min
Cyclohexane	84.2	.783	177	154	18,846	.0227	.0678	48	401	518	117	99	4050	138	[d]22.3	.16	.07
,ethyl-	112.2	.792	269	133	18,816	.0171	.0678	[a]54	[a]420	507	-	-	-		-	-	-
,methyl-	98.2	.774	214	139	18,797	.0195	.0678	45	359	509	125	96	3935	-	[d]27	-	.07
,1-methyl-2-*tert*-butyl-	154.3	-	-	-	-	.0125	.0678	-	-	597	-	-	-			-	-
Cyclohexene	82.1	.810	181	-	-	.0240	.0701	-	-	-	-	103		[c]86		.13	-
Cyclopentadiene	66.1	.805	109	-	-	.0312	.0738	-	-	-	100	101	-	67		.11	-
Cyclopentane	70.1	.751	121	167	19,001	.0271	.0678	-	-	725	117	96	4075	[c]83	-	.13	-
,methyl-	84.2	.754	161	148	18,930	.0227	.0678	43	368	614	122	92	4010	-	-	-	-
,*n*-propyl-	112.2	.781	268	-	18,907	.0171	.0678	-	-	545	-	-	-			-	-
Cyclopentene	68.1	.772	112	-	-	.0290	.0706	-	-	-	121	104	-			-	-
Cyclopropane	42.1	[e].720	-30	-	-	.0444	.0678	[a]58	[a]276	928	113	122	4190	[c]24	[c]23	.07	.07
,*cis*-1,2-dimethyl-	70.1	-	-	-	-	.0271	.0678	-	-	-	116	119	4170	-	-	-	-
,*trans*-1,2-dimethyl-	70.1	-	-	-	-	.0271	.0678	-	-	-	118	119	4160	-	-	-	-
,ethyl-	70.1	-	-	-	-	.0271	.0678	-	-	-	125	122	4125	-	-	-	-
,methyl-	56.1	[i].691	41	-	-	.0337	.0678	-	-	-	116	126	4170	-	-	-	-
,1,1,2-trimethyl-	84.2	-	-	-	-	.0227	.0678	-	-	-	115	112	4155	-	-	-	-
***trans*-Decalin (decahydronaphthalene)**	138.2	.874	369	-	-	.0142	.0692	-	-	521-	109	[f]79	4000	-	-	-	-
***n*-Decane**	142.3	.734	345	119	19,175	.0133	.0666	45	356	449	105	[f]94	4115		-	-	-
1-Decene	140.3	.745	339	-	19,094	.0138	.0678	36	392	471	112	[f]96	4135	-	-	-	-
Diethyl ether	74.1	.714	94	151	-	.0337	.0896	[a]55	[a]2640	366	115	102	4055	49	[d]28	.10	.08
Dihydropyran	84.1	-	-	-	-	.0312	.0939	-	-	-	-	-	-	[c]56	-	.11	-
Diisopropyl ether	102.2	.726	154	-	-	.0227	.0824	-	-	-	-	-	-	114		.15	-
Dimethoxymethane	76.1	.856	111	-	-	.0497	.1381	-	-	-	-	-	-	42	-	.09	-
Dimethyl ether	46.1	-	-11	-	-	.0652	.1115	[a]50	[a]330	662	119	117	4010	[c]45	-	.09	-
Dimethyl sulfide	62.1	.846	100	-	-	.0444	.1001	-	-	-	-	-	-	[c]76	-	.12	-
Di-*tert*-butyl peroxide	146.2	-		-	-	.0179	.0923	-	-	-	-	-	-	[c]65	-	.11	-
Divinyl ether	70.1	.774	102	-	-	.0402	.1017	-	-	680	-	-	-	-	-	-	-
Ethane	30.1	-	-128	210	20,416	.0564	.0624	50	272	882	112	103	4040	[c]42	[d]24	.09	.07
,1,1-diphenyl-	182.3	1.006	522	-	-	.0118	.0756	-	-	909	-	-	-	-	-		-
Ethene	28.1	-	-155	208	20,276	.0652	.0678	41	>610	914	115	175	4275	9.6	-	.05	-
Ethyl acetate	88.1	.901	171	-	-	.0402	.1279	[a]61	[a]236	907	≈100	83	-	142	48	.17	.10
Ethyl alcohol	46.1	.789	173	368	-	.0652	.1115	-	-	738	-	-	-	-	-		-
Ethylamine	45.1	.706	62	263	-	.0528	.0873	-	-	-	-	-	-	240		.21	-
Ethylene oxide	44.1	1.965	51	250	-	.0772	.1280	-	-	804	125	234	4340	10.5	6.2	.05	.04
Ethylenimine	43.1	.832	132	-	-	.0605	.0962	-	-	-	100	101		48	-	.10	-
Furan	68.1	0.936	90	172	-	0.0444	0.1098	-	-	-	-	-		22.5	-	0.07	
,tetrahydro-	72.1	-	149	-	-	.0366	.0951	-	-	-	-	-	-	54		.11	-
,thio- (thiophene)	84.1	1.064	183	-	-	.0337	.1017	-	-	-	-	-	-	[c]60	-	.11	-
***n*-Heptane**	100.2	.688	209	136	19,314	.0187	.0661	53	450	477-	122	99	3985	[c]115	[d]24	.15	0.07
,3,3-dimethyl-	128.3	.730	279	118	-	.0147	.0665	-	-	626	-	-		-	-	-	-
1-Heptene	98.2	.702	201	-	19,202	.0195	.0678	-	-	505	-	-	-	-	-	-	-
1-Heptyne	96.2	.738	212	-	19,262	.0205	.0698	-	-	-	-	-	-	[c]93.1	-	.13	-
Hexadecane	226.4	.777	548	98	19,052	.0085	.0671	-	-	446	108	[f]95	4115	-		-	-
1-Hexadecene	224.4	.785	544	-	19,000	.0086	.0679	-	-	464	-	-	-	-	-	-	-
1,5-Hexadiene	82.1	.697	139	-	-	.0240	.0701	-	-	-	118	113	-	-	-	-	-
***n*-Hexane**	86.2	.664	156	144	19,391	.0216	.0659	51	400	501-	117	99	4030	95	23	.14	.07
,2,3-dimethyl-	114.2	.717	240	126	19,236	.0165	.0663	-	-	820	-	-	-	-	-	-	-
1-Hexene	84.2	.678	146	-	19,262	.0227	.0679	52	393	521	118	108	4115	-	-	-	-
1-Hexyne	82.1	.721	161	-	19,334	.0240	.0701	-	-	-	124	124	4200	-	-		-
3-Hexyne	82.1	.726	-	-	-	.0240	.0701	-	-	-	-	116	4150	-	-	-	-
Hydrogen	2.0	-	-423	194	51,571	.2950	.0290	-	-	1060	≈170	679	-	2.0	1.8	.025	.024
Hydrogen sulfide	34.1	-	-79	237	-	.1224	.1650	-	-	554	-	-	-	[c]7.7	-	.04	-
Isopropyl alcohol	60.1	.785	180	286	-	.0444	.0969	-	-	852	100	89	-	65	-	.11	-
Isopropylamine	59.1	.690	93	-	-	.0383	.0817	-	-	-	114	68	4030	200	-	.19	-
Isopropyl chloride	78.5	.859	96	-	-	.0422	.1199	-	-	-	-	-	-	155	-	.17	
Isopropyl mercaptan	76.2	.836	154	-	-	.0337	.0922	-	-	-	-	-	-	[c]87	-	.13	-
***dl*-Limonene**	136.2	.842	351	125	-	.0147	.0706	-	-	505	-	-	-	-	-		-
Methane	16.0	-	-259	219	21,502	.0947	.0581	46	164	1170	106	87	4025	33	29	.10	.08
,diphenyl-	168.2	1.001	503	-	-	.0129	.0763	-	-	962	107	[f]77	4280		-	-	-
Methyl alcohol	32.0	.793	148	473	-	.1224	.1548	[j]48	[j]408	878	≈101	122		21.5	[d]14	.07	.06
Methyl formate	60.1	.975	89	203	-	.0947	.2181	-	-	-	-	-	-	[c]62	-	.11	-
Naphthalene, 1-ethyl-	156.2	1.012	498	-	-	.0138	.0755	-	-	898	-	-	-		-	-	
,1-methyl-	142.2	1.025	472	-	-	.0153	.0764	-	-	1017		-			-		-
***n*-Nonane**	128.3	.722	303	124	19,211	.0147	.0665	47	434	453	-	-			-	-	-
,2-methyl-	142.3	.732	332	-	-	.0133	.0666	-	-	418	-	-		-			-
***n*-Octane**	114.2	.707	258	129	19,256	.0165	.0663	51	425	464-		-			-		-
,2,3-dimethyl-	142.3	.742	327	-	-	.0133	.0666	-		447		-	-				
,4-ethyl-	142.3	.744	334	-	-	.0133	.0666	-		458							
,2-methyl-	128.3	.718	290	123	-	.0147	.0665			440							
,3-methyl-	128.3	.725	292	123	-	.0147	.0665		-	442							-
,4-methyl-	128.3	.724	288	123	-	.0147	.0665	-		450							-
1-Octene	112.2	.719	250	-	19,157	.0171	.0678	46	384	493					-		

TABLE C-1. (Continued)

Fuel	Mol. Wt.	Spec. Grav.	T_{Boil} (°F)	Heat of Vap. (Btu/lb)	Heat of Comb. (Btu/lb)	Stoichiometry		Flammability Limits (% Stoichio.)		Spont. Ign. Temp. (°F)	Fuel for Max. Flame Speed (% Stoichio.)	Relative Max. Flame Speed	Flame Temp. at Max. Fl. Speed (°R)	Ign. Energy (10^{-5} joule)		Quenching Dist. (in.)	
						% Vol.	f	Lean	Rich					Stoich.	Min	Stoich.	Min
1,2-Pentadiene (ethylallene)	68.1	.698	113	–	19,444	.0290	.0706	–	–	–	119	133	4285	–	–	–	–
cis-1,3-Pentadiene	68.1	.696	111	–	19,018	.0290	.0706	–	–	–	120	119	4205	–	–	–	–
trans-1,3-Pentadiene (piperylene)	68.1	.681	108	–	19,016	.0290	.0706	–	–	–	119	117	4230	–	–	–	–
,2-methyl-(*cis* or *trans*)	82.1	.724	169	–	–	.0240	.0701	–	–	–	115	100	4220	–	–	–	–
1,4-Pentadiene	68.1	.666	79	–	19,190	.0290	.0706	–	–	–	115	119	4270	–	–	–	–
2,3-Pentadiene	68.1	.700	119	–	19,399	.0290	.0706	–	–	–	119	130	4280	–	–	–	–
n-Pentane	72.1	.631	97	154	19,499	.0255	.0654	54	359	544	115	99	4050	[c]82	[d]22	.13	.07
,2,2-dimethyl-	100.2	.678	175	125	19,235	.0187	.0661	–	–	–	119	89	4040	–	–	–	–
,2,3-dimethyl-	100.2	.699	194	130	19,265	.0187	.0661	69	437	640	119	94	3995	–	–	–	–
,2,4-dimethyl-	100.2	.677	177	127	19,253	.0187	.0661	–	–	–	117	92	4025	–	–	–	–
n-Pentane, 2,4-dimethyl-3-ethyl-	128.3	.742	278	119	–	.0147	.0665	–	–	734	–	–	–	–	–	–	–
,3,3-dimethyl-	100.2	.698	187	127	19,255	.0187	.0661	–	–	–	–	–	–	–	–	–	–
,2-methyl-	86.2	.658	140	139	19,356	.0216	.0659	60	372	585	115	94	4050	–	–	–	–
,3-methyl-	86.2	.669	146	140	19,369	.0216	.0659	–	–	580	116	94	4040	–	–	–	–
,2,2,3,3-tetramethyl-	128.3	.761	284	118	–	.0147	.0665	[a]54	[a]344	845	–	–	–	–	–	–	–
,2,3,3,4-tetramethyl-	128.3	.759	287	117	–	.0147	.0665	–	–	818	–	–	–	–	–	–	–
,2,2,3-trimethyl-	114.2	.720	230	121	19,212	.0165	.0663	–	–	816	–	–	–	–	–	–	–
,2,2,4-trimethyl- (isooctane)	114.2	.696	211	117	19,197	.0165	.0663	48	360	837-	117	89	4020	[c]29	28	.08	.07
,2,3,3-trimethyl-	114.2	.730	239	123	19,226	.0165	.0663	–	–	806	–	–	–	–	–	–	–
1-Pentene	70.1	.646	86	–	19,346	.0271	.0678	[j]47	[j]370	569-	114	109	4165	–	–	–	–
,2-methyl-	84.2	.687	141	–	19,185	.0227	.0678	–	–	582	124	102	4025	–	–	–	–
,4-methyl-	84.2	.669	129	–	19,225	.0227	.0678	–	–	580	117	104	4130	–	–	–	–
,2,3,4-trimethyl-	112.2	.733	226	–	–	.0171	.0678	–	–	495	–	–	–	–	–	–	–
,2,4,4-trimethyl- (diisobutylene)	112.2	.719	215	–	–	.0171	.0678	–	–	788	–	–	–	[c]175	–	.18	–
cis-2-Pentene	70.1	.661	99	–	19,308	.0271	.0678	[j]49	[j]345	–	124	111	4035	[c]82	[d]18	.13	.06
,2,4,4-trimethyl-	112.2	.726	221	–	–	.0171	.0678	–	–	587	–	–	–	–	–	–	–
,3,4,4-trimethyl-(*cis* or *trans*)	112.2	.743	234	–	–	.0171	.0678	–	–	626	–	–	–	–	–	–	–
trans-2-Pentene	70.1	.653	97	–	19,280	.0271	.0678	–	–	–	–	–	–	–	–	–	–
1-Pentyne	68.1	.695	104	–	19,436	.0290	.0706	–	–	–	122	136	4265	–	–	–	–
,4-methyl-	82.1	–	–	–	–	.0240	.0701	–	–	–	120	115	4220	–	–	–	–
2-Pentyne	68.1	.716	133	–	19,338	.0290	.0706	–	–	–	115	132	4280	–	–	–	–
,4-methyl-	82.1	–	–	–	–	.0240	.0701	–	–	–	125	117	4160	–	–	–	–
α-Pinene	136.2	.858	309	–	–	.0147	.0706	–	–	506	–	–	–	–	–	–	–
Propadiene (see Allene)																	
Propane	44.1	[g].508	-44	183	19,929	.0402	.0640	51	283	940-	114	100	4050	30.5	–	.08	.07
,2-cyclopropyl-	84.2	–	–	–	–	.0227	.0678	–	–	–	118	109	–	–	–	–	–
,1-deutero-	45.1	–	–	–	–	.0402	.0655	–	–	–	110	86	–	–	–	–	–
,1-deutero-2-methyl-	59.1	–	–	–	–	.0312	.0660	–	–	–	110	86	–	–	–	–	–
,2-deutero-2-methyl-	59.1	–	–	–	–	.0312	.0660	–	–	–	110	86	–	–	–	–	–
,2,2-dimethyl- (neopentane)	72.1	.597	49	136	–	.0255	.0654	54	283	853	–	85	4060	[c]157	–	.17	–
,1,1-diphenyl-	196.3	–	–	–	–	.0109	.0750	–	–	870	–	–	–	–	–	–	–
,2-methyl- (isobutane)	58.1	[g].563	11	158	19,593	.0312	.0649	60	321	890-	110	90	4065	–	–	–	–
Propene	42.1	[g].522	-54	188	19,683	.0444	.0678	48	272	1036-	114	112	4210	28.2	–	.08	–
,2-cyclopropyl-	82.1	–	–	–	–	.0240	.0701	–	–	–	119	115	–	–	–	–	–
,2-methyl-	56.1	[g].600	20	169	19,346	.0337	.0678	–	–	–	114	96	–	–	–	–	–
Propionaldehyde	58.1	.807	120	–	–	.0497	.1054	–	–	–	131	126	3855	49	–	.10	–
n-Propyl alcohol	60.1	.804	207	295	–	.0444	.0969	–	–	812	–	–	–	–	–	–	–
n-Propyl chloride	78.5	.890	117	–	–	.0422	.1199	–	–	–	–	–	–	108	–	.15	–
Propylene oxide (1,2-epoxypropane)	58.1	.831	95	–	–	.0497	.1054	47	–	–	128	179	4170	19	[d]14	.07	.06
1-Propyne	40.1	–	-10	–	19,849	.0497	.0728	–	–	–	119	179	4450	–	–	.06	.05
Spiropentane	68.1	–	–	–	–	.0290	.0706	–	–	–	120	154	–	–	–	–	–
1-Tetradecene	196.4	.775	484	–	19,022	.0099	.0678	–	–	463	–	–	–	–	–	–	–
Tetrahydropyran	86.1	.854	179	–	–	.0290	.0893	–	–	–	≈90	105	–	121	[d]22	.15	.07
Tetralin (tetrahydronaphthalene)	132.2	.971	405	–	–	.0158	.0738	–	–	794	101	[f]84	4175	–	–	–	–
Toluene (methylbenzene)	92.1	.872	231	156	17,601	.0227	.0743	43	322	1054-	105	[f]90	4220	–	–	–	–
Triethylamine	101.2	.723	193		–	.0210	.0753	–	–	–	–	–	–	115	–	.15	–
Turpentine (mainly β-pinene)	–	–	–	–	–	–	–	–	–	486	–	–	–	–	–	–	–
Vinyl acetate	86.1	.932	162	–	–	.0444	.1388	–	–	–	–	–	–	[c]120	–	.15	–
Gasoline, 73-octane	–	–	–	–	–	–	–	–	–	570	–	–	–	–	–	–	–
Gasoline, 100-octane	–	–	–	–	–	–	–	–	–	800-950	106	[j]88	–	–	–	–	–
Jet fuel, grade JP-1[k]	150	.81		–	[l]18,500	.013	.068	–	–	[j]480	107	[j]86	–	–	–	–	–
Jet fuel, grade JP-3[k]	112	.76	–	–	[l]18,700	.017	.068	–	–	–	–	–	–	–	–	–	–
Jet fuel, grade JP-4[k]	126	.78	–	–	[l]18,700	.015	.068	–	–	[i]502	107	[j]89			–	–	–
Jet fuel, grade JP-5[k]	170	.83	–	–	[l]18,500	.011	.069	–	–	468	–	–	–		–	–	–

[a] Tube open at lower end.

[b] Sublimes.

[c] Flanged electrodes.

[c2] Unflanged electrodes.

[d] 0.0225-inch stainless-steel electrodes, spark duration, 1 millisec.

[e] Measured at -110°F.

[f] Measured at elevated temperatures by Bunsen-burner schlieren total-area method and extrapolated to room temperature.

[g] Saturation pressure.

[h] Dry air, 0.97 percent hydrogen in carbon monoxide.

[i] Measured at -4°F.

[j] Unpublished NACA data.

[k] Properties are given for average quality of jet fuels.

[l] Lower heating value; i.e., liquid to gas.

TABLE C-2. ELECTRON AFFINITIES[129]

Species	Electron Affinity, eV
F	3.40
Cl	3.61
Br	3.36
I	3.06
H	0.75
Na	0.54
O	1.47
OH	1.83
SH	2.30
NO	0.9
CH_3	~0.2
C_2H_5	~0.4
CH_3O	~1.40
HO_2	~1.07
CF_3	~1.0
CCl_3	~0.5

TABLE C-3. THE CONTRIBUTIONS OF THE DIFFERENT END GROUPS TO THE ACTIVATION ENERGIES[129]

Atom or Group	X (kcal/mol^{-1})	F (kcal/mol^{-1})$^{1/2}$
H	4.7	3.00
F	−3.8	0.35
Cl	−2.3	0.57
Br	−4.8	0.32
I	−5.7	0.15
O	2.0	2.15
Na	2.6	2.30
OH	−0.2	1.30
SH	−1.7	0.84
NH_2	−1.6	1.30
HO_2	1.1	1.70
CHO	0.3	1.55
CH_3	6.2	3.50
CF_3	4.1	2.95
C_2H_5	4.2	2.85

TABLE C-4. PROCEDURE FOR CALCULATING HARD-SPHERE COLLISION PARAMETERS[8]

Step	Operation
1	Calculate the average inverse temperature $\overline{T} = T_1T_2/(T_1 + T_2)$ for the temperature range under consideration
2	Find ϵ/k for each molecule from Table C-5
3	Form $T^* = \overline{T}k/\epsilon$
4	Find $\Omega^{(2,2)*}$ for each molecule by interpolation in Table C-6
5	Calculate σ_A from value of σ in Table C-5 using $\sigma_A = \sigma^2\Omega^{(2,2)*}$
6	The collision cross section for a pair of A and B molecules is given by $\sigma_{AB} = \frac{1}{2}(\sigma_A + \sigma_B)$

TABLE C-5. PARAMETERS FOR LENNARD-JONES POTENTIAL[139-141]

Gas	σ, A	ϵ/k, °K	Gas	σ, A	ϵ/k, °K	Gas	σ, A	ϵ/k, °K
Al	2.655	2750	C_2H_2	4.033	232	Hg	2.969	750
AlO	3.204	542	$C_2H_2CHCH_3$	4.678	299	I_2	5.160	474
Al_2	2.940	2750	C_2H_4	4.163	225	Kr	3.655	179
Air	3.711	79	C_2H_5Cl	4.90	300	Li	2.850	1899
Ar	3.542	93	$C_2H_5OC_2H_5$	5.678	313.8	LiO	3.334	450
Br_2	4.27	520	C_2H_5OH	4.530	363	Li_2	3.200	1899
C	3.385	31	C_2H_6	4.443	216	Li_2O	3.561	1827
$C(CH_3)_4$	6.464	193.4	C_2N_2	4.361	349	Mg	2.926	1614
CCl_2	4.692	213	n-C_3H_7OH	4.549	576.7	N	3.298	71
CCl_2F_2	5.25	253	C_3H_8	5.118	237	NH_3	2.900	558
CCl_4	5.947	323	n-C_4H_{10}	4.687	531	NO	3.492	117
CH	3.370	69	iso-C_4H_{10}	5.278	330	N_2	3.798	71
CHBrClF	5.13	345	n-C_5H_{12}	5.784	341	N_2O	3.828	232
$CHCl_3$	5.389	340	C_6H_6	5.27	440	Na	3.567	1375
CH_2Cl_2	4.759	406	C_6H_{12}	6.182	297	NaCl	4.186	1989
CH_2CNCH_3	4.68	299	n-C_6H_{14}	5.949	399	NaOH	3.804	1962
CH_3CCH	4.761	252	n-C_7H_{16}	8.88	282	Na_2	4.156	1375
CH_3Cl	3.375	855	n-C_8H_{18}	7.45	320	Ne	2,820	33
CH_3COCH_3	4.600	560.2	n-C_9H_{20}	8.45	240	O	3.050	107
CH_3COOCH_3	4.936	469.8	c-hexane	6.09	324	OH	3.147	80
$CH_3COOC_2H_5$	5.205	521.3	Cl	3.613	131	O_2	3.467	107
CH_3OCH_3	4.31	395	Cl_2	4.217	316	S	3.839	847
CH_3OH	3.626	482	H	2.708	37	SO	3.993	301
CH_4	3.758	149	HCN	3.630	569	SO_2	4.112	335
CN	3.856	75	HCl	3.339	345	Si	2.910	3036
CO	3.690	92	H_2	2.827	60	SiO	3.374	569
CO_2	3.941	195	H_2O	3.737	32	SiO_2	3.706	2954
COS	4.13	355	H_2O_2	4.196	289	UF_6	5.967	237
CS_2	4.483	467	H_2S	3.623	301	Xe	4.047	231
C_2	3.913	79	He	2.551	10	Zn	2.284	1393

TABLE C-6. LENNARD-JONES POTENTIAL TRANSPORT INTEGRAL $\Omega^{(2,2)*(138)}$

T^*	$\Omega^{(2,2)*}$	T^*	$\Omega^{(2,2)*}$
0.30	2.785	2.7	1.069
0.35	2.628	2.8	1.058
0.40	2.492	2.9	1.048
0.45	2.368	3.0	1.039
0.50	2.257	3.1	1.030
0.55	2.156	3.2	1.022
0.60	2.065	3.3	1.014
0.65	1.982	3.4	1.007
0.70	1.908	3.5	0.9999
0.75	1.841	3.6	0.9932
0.80	1.780	3.7	0.9870
0.85	1.725	3.8	0.9811
0.90	1.675	3.9	0.9755
0.95	1.629	4.0	0.9700
1.00	1.587	4.1	0.9649
1.05	1.549	4.2	0.9600
1.10	1.514	4.3	0.9553
1.15	1.482	4.4	0.9507
1.20	1.452	4.5	0.9464
1.25	1.424	4.6	0.9422
1.30	1.399	4.7	0.9382
1.35	1.375	4.8	0.9343
1.40	1.353	4.9	0.9305
1.45	1.333	5	0.9269
1.50	1.314	6	0.8963
1.55	1.296	7	0.8727
1.60	1.279	8	0.8538
1.65	1.264	9	0.8379
1.70	1.248	10	0.8242
1.75	1.234	20	0.7432
1.80	1.221	30	0.7005
1.85	1.209	40	0.6718
1.90	1.197	50	0.6504
1.95	1.186	60	0.6335
2.00	1.175	70	0.6194
2.10	1.156	80	0.6076
2.20	1.138	90	0.5973
2.30	1.122	100	0.5882
2.40	1.107	200	0.5320
2.50	1.093	300	0.5016
2.60	1.081	400	0.4811

TABLE C-7. VALUES OF α FOR CALCULATING ACTIVATION ENERGIES FROM BOND STRENGTHS(155)

	$E_{A\ exp.}$	$E_{A\ calc.}$
Unimolecular Decomposition, Two-Center Activated Complex; α = 0.95		
$CH_3{\cdot}CH_2{\cdot}CH_2{\cdot} \rightarrow C_3H_6 + H{\cdot}$	38.0	37.7
$(CH_3)_3{\cdot}C{\cdot} \rightarrow (CH_3)_2C{:}CH_2 + H{\cdot}$	40.0	40.6
$CH_3{\cdot}CH_2{\cdot}CH_2{\cdot} \rightarrow CH_3{\cdot} + C_2H_4$	20.0	20.8
${\cdot}CH_2OCH_3 \rightarrow CH_3{\cdot} + CH_2O{\cdot}$	19.0	14.2
Unimolecular Decomposition, Four-Center Activated Complex (Closed); α = 01]75		
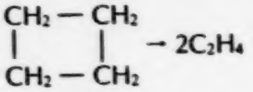	61.0	62.9
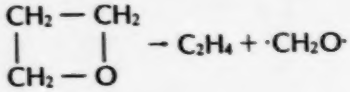	60.0	54.5
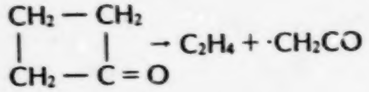	52.0	57.6
Unimolecular Decomposition, Four-Center Activated Complex (Open); α = 0.73		
$CH_3{\cdot}CH_2{\cdot}CH_2Cl \rightarrow HCl + C_3H_6$	55.0	46.9
$(CH_3)_3{\cdot}CCl \rightarrow HCl + (CH_3)_2C{:}CH_2$	41.4	45.9
$CH_3{\cdot}CH_2{\cdot}CH_2Br \rightarrow HBr + C_3H_6$	47.7	45.4
Cyclohexyl bromide → Cyclohexene + HBr	46.1	44.3
$Bu^tOH \rightarrow H_2O + C_4H_8$	54.5	58.9
Unimolecular Decomposition, Six-Center Activated Complex (Closed); α = 0.72		
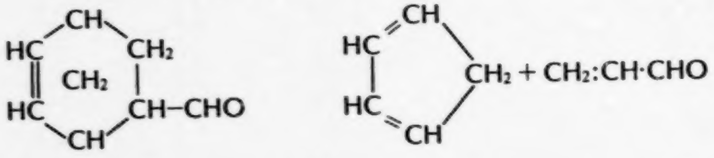 CH HC CH₂ CH₂ HC CH–CHO CH CH HC CH₂ + CH₂:CH·CHO HC CH	33.6	34.0
Unimolecular Decomposition, Six-Center Activated Complex (Open); α = 0.76		
$H{\cdot}CO{\cdot}O{\cdot}CH_2{\cdot}CH_3 \rightarrow H{\cdot}CO{\cdot}OH + C_2H_4$	44.1	45.3

TABLE C-7. (Continued)

		$E_{A\ exp.}$	$E_{A\ calc.}$
Transfer Reactions, Three-Center Activated Complex; $\alpha = 0.96$			
$H\cdot + D_2 \rightarrow HD + H\cdot$		6.5	5.1
$H\cdot + C_6H_6 \rightarrow H_2 + C_6H_5\cdot$		7.0	7.9
$Cl\cdot + H_2 \rightarrow HCl + H\cdot$		5.5	4.2
$Br\cdot + H_2 \rightarrow H\cdot + HBr$		17.6	19.3
$Br\cdot + C_2H_6 \rightarrow HBr + C_2H_5\cdot$		13.9	14.1
$CH_3\cdot + H_2 \rightarrow H\cdot + CH_4$		9.9	7.2
$CH_3\cdot + CH_2{:}CH_2 \rightarrow CH_2{:}CH\cdot + CH_4$		10.0	5.0
$CF_3\cdot + H_2 \rightarrow H\cdot + CF_3H$		9.5	10.0
$CF_3\cdot + C_2H_6 \rightarrow C_2H_5\cdot + CF_3H$		7.5	4.9
$C_2H_5\cdot + H_2 \rightarrow H\cdot + C_2H_6$		11.5	9.1
$C_3F_7\cdot + CH_4 \rightarrow CH_3\cdot + C_3F_7H$		9.5	9.8
Transfer Reactions, Four-Center Activated Complex; $\alpha = 0.71$			
$HI + HI \rightarrow H_2 + I_2$		44.0	44.8
Transfer reactions, Three-Center Activated Complex (Exothermic Reactions); $\alpha = 0.0109$, $\Delta H = +0.943$			
$H\cdot + CH_4 \rightarrow H_2 + CH_3\cdot$	0.908	11–13	9.3
$H\cdot + CH_3\cdot CH_2\cdot CH_2\cdot CH_3 \rightarrow H_2 + C_4H_9\cdot$	0.854	8.9	6.9
$H\cdot + (CH_3)_3\cdot C\cdot CH_3 \rightarrow H_2 + C_5H_{11}\cdot$	0.866	9.2	7.6
$H\cdot + \text{cyclo-}C_4H_8 \rightarrow H_2 + \text{cyclo-}C_4H_7\cdot$	0.831	8.2	8.2
$D\cdot + D_2 \rightarrow D_2 + D\cdot$	0.943	6.0	6.0
$D\cdot + CH_3\cdot CH_2\cdot CH_2\cdot CH_3 \rightarrow DH + C_4H_9\cdot$	0.845	7.1	7.1
$D\cdot + (CH_3)_2CO \rightarrow DH + CH_3\cdot CO\cdot CH_2\cdot$	0.845	8.0	7.1
$D\cdot + \text{cyclo-}C_4H_8 \rightarrow DH + \text{cyclo-}C_4H_7\cdot$	0.824	7.7	7.6
$Cl\cdot + CH_4 \rightarrow HCl + CH_3\cdot$	0.909	6.2	6.3
$Cl\cdot + CH_3Cl \rightarrow HCl + CH_2Cl$	0.844	3.4	7.0
$Br\cdot + C_6H_5\cdot CH_3 \rightarrow HBr + C_6H_5\cdot CH_2\cdot$	0.873	7.2	4.7
$O + N_2O \rightarrow 2\cdot NO$	0.764	15.5	19.0
$NO + O_3 \rightarrow NO_2 + O_2$	0.801	2.5	1.3
$Na + C_2H_5Cl \rightarrow NaCl + C_2H_5\cdot$	0.736	10.2	6.9

TABLE C-7. (Continued)

	$\alpha_{calc.}$	$E_{A\ exp.}$	$E_{A\ calc.}$
Transfer Reactions, Three-Center Activated Complex (Exothermic Reactions); $\alpha = 0.0109$, $\Delta H = +0.943$			
$CH_3\cdot + CH_3\cdot CH_2\cdot CH_2\cdot CH_3 \rightarrow CH_4 + C_4H_9\cdot$	0.888	8·6	6.2
$CH_3\cdot + CH_3\cdot CH(CH_3)\cdot CH(CH_3)\cdot CH_3 \rightarrow CH_4 + C_6H_{13}\cdot$	0.867	7.4	6.3
$CH_3\cdot + \text{cyclo-}C_5H_{10} \rightarrow CH_4 + \text{cyclo-}C_5H_9\cdot$	0.878	8.3	6.2
$CH_3\cdot + CH_3C\cdot C(CH_3){:}CH_2 \rightarrow CH_4 + C_4H_7$	0.681	7.3	7.9
$CH_3\cdot + C_6H_5\cdot CH_3 \rightarrow CH_4 + C_6H_5\cdot CH_2\cdot$	0.714	8.3	7.6
$CH_3\cdot + CH_2\cdot CH(OH)\cdot CH_3 \rightarrow C_3H_6\cdot OH + CH_4$	0.801	7.3	6.9
$CH_3\cdot + CH_3\cdot CHO \rightarrow CH_3CO + CH_4$	0.823	7.5	6.7
$CH_3\cdot + (C_2H_5)_2\cdot CO \rightarrow C_2H_5\cdot CO\cdot C_2H_4 + CH_4$	0.867	7.0	6.3
$CH_3\cdot + CH_3Cl \rightarrow \cdot CH_2Cl + CH_4$	0.878	9.4	6.2
$CD_3 + CH_3\cdot CH_2\cdot CH_2\cdot CH_3 \rightarrow C_4H_9\cdot + CD_3H$	0.845	9.3	7.4
$CF_3\cdot + CH_3\cdot CH_2\cdot CH_2\cdot CH_3 \rightarrow C_4H_9\cdot + CF_3H$	0.921	5.1	5.7
$CF_3\cdot + C_6H_5\cdot CH_3 \rightarrow C_6H_5\cdot CH_2\cdot + CF_3H$	0.867	6.0	5.9
$C_2H_5\cdot + CH_3\cdot CH_2\cdot CO\cdot CH_2\cdot CH_3 \rightarrow C_2H_5\cdot CO\cdot C_2H_4\cdot + C_2H_6$	0.888	7.4	6.0

TABLE C-8. DISSOCIATION ENERGIES, D, OF SOME MOLECULES AND RADICALS

Molecule	D, eV	D, kcal/mole	Molecule	D, eV	D, kcal/mole
C_2	4.9 ± 0.3	173	NO_2	3.114_9 (N–O)	72
CN	8.1 ± 0.3	187	NO_2	4.505_6 (NO_2)	104
CO	11.11	256	HI	3.06 ± 0.01	71
Cl_2	2.476	57	Hg_2	0.060 ± 0.003	1.4
F_2	1.6 ± 0.35	37	N_2	9.762	225
H_2	4.4776	103	NO	6.49 ± 0.05	150
H_2^+	0.649	15	Na_2	0.75 ± 0.03	17.3
HCl	4.431	102	NaCl	4.24 ± 0.05	98
HBr	3.75 ± 0.02	86	O_2	5.084	117
HF	5.8 ± 0.2	134	OH	4.45 ± 0.2	103
H_2O	5.113_6	118	S_2	4.4 ± 0.1	101
H_2S	3.26	75	SH	3.85 ± 0.2	89
HCN	9.69 (C–N)	223	O_3	1.0_4	23
HCN	5.6_5 (C–N)	130	SO_2	5.61_3	129
N_2O	4.930_3 (N–N)	114	NH_3	4.3_8	101
N_2O	1.6771_1 (N–O)	39	CH_4	4.40_6	101
CO_2	5.453	126	C_2H_4	7.2_6 ± 0.3 (C–C)	167
OCS	3.71	86	N_2O_4	0..5937 (N–N)	13.7
NH	3.73	85.9	HO_2	(H–O_2)	47

TABLE C-9. DISSOCIATION ENERGIES OF BONDS(145)

Compound	Bond	Q, kcal	Compound	Bond	Q, kcal
CCl_3Br	C–Br	49.0	$CHCl_3$	C–H	88.9 ± 3
CBr_4	C–Br	49.0	CCl_3F	C–F	102 ± 7
$CHBr_3$	C–Br	55.5	CCl_4	C–Cl	67.9
$CHCl_2Br$	C–Br	53.5	CH_3SH	C–S	70
CH_2Br_2	C–Br	62.5	C_2H_2SH	C–S	69
CH_3Br	C–Br	67.5	*tert*-C_4H_9SH	C–S	65
CF_3Br	C–Br	64.0	CH_3SCH_3	C–S	73
$(C_4H_5)_3C{-}C(C_6H_5)_3$	C–C	11.0	$C_2H_5SC_2H_5$	C–S	69
$C_6H_5CH_2{-}CH_2CH_3$	C–C	57.5	CH_3ONO	O–N	36.4
$C_6H_5CH_2{-}CH_3$	C–C	63.2	C_2H_5ONO	O–N	37.7
$C_6H_5CH_2{-}CH_2CH_2CH_3$	C–C	65.0	C_3H_7ONO	O–N	37.7
$C_6H_5CH_2{-}H$	C–H	77.5	*iso*-C_3H_7ONO	O–N	37.0
$CH_3CO{-}COCH_3$	C–C	60	*n*-C_4H_9ONO	O–N	37.0
$C_6H_5CH_2{-}CH_2C_6H_5$	C–C	47	*iso*-C_3H_7Cl	C–Cl	73.3
$C_6H_5CH_2{-}Br$	C–Br	50.0	*iso*-C_3H_7Br	C–Br	58.8
$CH_2{=}CH{-}CH_2Br$	C–Br	47.5	*iso*-C_3H_7I	C–I	42.4
$C_6H_5CH_2NH_2$	C–N	59.0	$CH{\equiv}C{-}CH_2Br$	C–Br	57.9
$H_2N{-}NH_2$	N–N	60.0	$CH{\equiv}C{-}CH_2I$	C–I	45.7
$(CH_3)_3CO{-}OC(CH_3)_3$	O–O	36.0	*p*-Fluorobromobenzene	C–Br	70.4
C_6H_5COBr	C–Br	57.0	*p*-Chlorobromobenzene	C–Br	70.3
β-$C_{10}H_7Br$	C–Br	70.0	*m*-Chlorobromobenzene	C–Br	69.9
α-$C_{10}H_7Br$	C–Br	70.9	o-Chlorobromobenzene	C–Br	69.7
C_6H_5Br	C–Br	70.9	*p*-Dibromobenzene	C–Br	70.6
9-Bromophenanthrene	C–Br	67.7	o-Dibromobenzene	C–Br	69.1
9-Bromoanthracene	C–Br	65.6	*p*-Bromotoluene	C–Br	70.7
n-C_3H_7SH	C–S	71.4	*m*-Bromotoluene	C–Br	70.7
H_2S	S–H	92.2	*o*-Bromotoluene	C–Br	70.1
CH_4	C–H	101.4	*p*-Bromodiphenyl	C–Br	70.7
CH_3	C–H	85.3	*m*-Bromodiphenyl	C–Br	70.1
CH_2	C–H	89.9	*o*-Bromodiphenyl	C–Br	68.2
CH	C–H	80	*p*-Bromophenyl cyanide	C–Br	70.6
CF_4	C–F	123 ± 2	*m*-Bromophenyl cyanide	C–Br	70.1
CF_4	C–F	116	*o*-Bromophenyl cyanide	C–Br	70.3
CF_3H	C–H	103 ± 4	*p*-Bromophenol	C–Br	67.0
CF_3Cl	C–Cl	83 ± 3	*o*-Bromophenol	C–Br	67.1
CF_3I	C–I	57 ± 4	3-Bromopyridine	C–Br	75.9
CF_3CH_3	C–C	90	2-Bromopyridine	C–Br	71.5
CF_3CF_3	C–C	97	2-Bromothiophene	C–Br	68.5

TABLE C-9. (Continued)

Compound	Bond	Q_{C-H} kcal	Q_{C-Cl}, kcal
CH_3Br	C–H	95.2	–
CH_2Br_2	C–H	87.7	–
$CHBr_3$	C–H	80.2	–
CH_3Cl	C–H; C–Cl	97.4	83.5
CH_2Cl_2	C–H; C–Cl	93.2	78.5
$CHCl_3$	C–H; C–Cl	89	73.5
CCl_4	C–Cl	–	68.4
$C_6H_5-C_6H_5$	C–C	94.5	–
$C_6H_5-CH_3$	C–C	87.5	–
C_6H_6	C–H	99	–
$C_6H_5-CH_2CH_2CH_3$	C–C	84.6	–

TABLE C-10. DISSOCIATION ENERGIES OF BONDS IN KCAL(145)

R' \ R''	H	CH_3	C_2H_5	$CH_2{=}CH$	$CH{\equiv}C$	n-C_3H_7	iso-C_3H_7	$CH_2{=}CH{-}CH_2$	n-C_4H_9	tert-C_4H_9	C_6H_5
CH_3	101	83	82	90*	110*	79	74.5*	60	78	74*	91*
C_2H_5	98	82	82	90	109*	79	75*	60.5	78	73*	91*
$CH_2{=}CH$	104*	90*	90*	101*	–	87*	85*	68.5*	86*	81*	101*
$CH{\equiv}C$	121*	110*	109*	–	–	106*	103*	–	–	–	119*
n-C_3H_7	95	79	79	87*	106*	76	72*	57.5	75	70*	88*
iso-C_3H_7	89*	74.5*	75*	85*	109*	72*	66.5*	54.5*	71*	65*	83*
$CH_2{=}CH{-}CH_2$	77	60	60.5	68.5*	–	57.5	54.5*	38	56.5	–	–
n-C_4H_9	94	78	78	86*	–	75	71*	56.5	74	69*	87*
$(CH_3)_3C$	85*	74*	73*	81*	–	70*	65*	–	69*	60*	78*
$CH_2{=}C(CH_3)CH_2$	76*	60*	60*	–	–	–	–	–	–	–	–
C_6H_5	104*	91*	91*	101*	119*	88*	83*	–	87*	78*	103*
$C_6H_5CH_2$	77.5	63	62	–	–	59	54.5*	–	57.5	–	76.5*
o-$CH_3C_6H_4CH_2$	74	58	58	–	–	–	–	–	–	–	–
m-$CH_3C_6H_4CH_2$	77.5	62	62.5	–	–	–	–	–	–	–	–
p-$CH_3C_6H_4CH_2$	75	60	60	–	–	–	–	–	–	–	–

R' \ R''	H	$C_6H_5CH_2$	Cl	Br	I	OH	NH_2	CN	CHO	$COCH_3$	NO_2
CH_3	101	63	80	66-67	54-55	90	79	105	71-75	77*	57
C_2H_5	98	62	80	65	51-52	90	78	–	71*	77*	52
n-C_3H_7	95	59	77	–	50	92	77	–	71*	77*	–
iso-C_3H_7	89*	54.5*	–	–	46	~90	–	–	–	73*	–
n-C_4H_9	94	57.5*	–	–	–	–	–	–	–	–	–
$(CH_3)_3C$	85*	–	75*	61*	~45*	91*	76*	–	–	–	–
$CH_2{=}CH$	104*	–	86*	–	55*	–	–	121*	84*	–	–
$CH_2{=}CH{-}CH_2$	77	–	58	48	35-37	71	64*	92*	50*	–	–
CHO	79*	–	–	–	–	96*	89*	–	–	59*	–
CH_3CO	85*	–	82*	67*	51*	102*	98*	–	59*	60	–
C_6H_5	104*	76.5*	88*	–	57*	107*	94*	124*	83*	–	–
$C_6H_5CH_2$	77.5	47	–	50.5	39*	73*	59	95*	–	63	–

*Determined indirectly and may be questionable.